Sponsored by:

IEEE Celebrating 125 Years of Engineering the Future

IES

SICE

de rem facemmo ali 1990 POLITECNICO DI BARI

ISIE 2010 Bari ITALY

IEEE International Symposium on Industrial Electronics

4-7 July 2010

TUTORIAL

Power Electronics for PV Power Systems Integration

Presented by

Remus Teodorescu, Aalborg University
Pedro Rodriguez, UPC Barcelona
Marco Liserre, Politecnico di Bari

Synopsis

Future PV power converters should ensure smart and efficient integration of PV energy into existing electrical networks. To achieve this goal, new essential issues should be addressed by engineers and researchers. This tutorial, divided into 3 parts.

First part is devoted to PV inverter topologies with focus on the new trend on transformerless ones and control structure of PV inverters, goes deeper into issues related to efficiency and leakage current. The most relevant topologies used in PV inverters are presented in this lecture. These topologies will be classified into H-bridge based topologies and neutral point clamped (NPC) based topologies. A general overview of the PV inverter control structure will be given.

Second block deals with the grid monitoring task in PV inverters, characterizing the grid state in point of connection. This block also tackles grid synchronization and provides essential clues about design of single-phase PLL systems including frequency-adaptive structures. The effectiveness of conventional grid synchronization techniques under unbalanced and distorted conditions will be evaluated and advanced solutions will be presented and discussed

The third block introduces the islanding phenomenon and makes a review of different passive and active anti-islanding detection methods for photovoltaic utility-interactive power systems. A review of the grid requirements for PV grid

integration in different countries will be given together with a discussion about the process of harmonization.

The tutorial is divided in the following parts:

Topologies and control of PV inverters – Remus Teodorescu – 45 min

Monitoring and synchronization of PV inverters- Pedro Rodriguez- 45 min

Break – 15 min

Anti-islanding techniques for PV inverters – Marco Liserre- 45 min

Panel Discussion – 30 min

This tutorial is intended to electrical and control engineers and researchers dealing with grid power converters and interested in go deeply into essential issues related to the integration of PV and also other renewable energy into electricity networks.

About the Speakers

Remus Teodorescu received the Dipl.Ing. degree in electrical engineering from Polytechnical University of Bucharest, Romania in 1989, and PhD. degree in power electronics from University of Galati, Romania, in 1994. In 1998, he joined Aalborg University, Institute of Energy Technology, power electronics section where he currently works as full professor

He has more than 100 papers published, 1 book and 3 patents (pending). He is the co-recipient of the Technical Committee Prize Paper Awards at IEEE IAS Annual Meeting 1998, and Third-ABB Prize Paper Award at IEEE Optim 2002. He is a Senior Member of IEEE, Associate Editor for IEEE Power Electronics Letters and chair of IEEE Danish joint IES/PELS/IAS chapter. His areas of interests are: design and control of power converters used in renewable energy systems, distributed generation mainly wind power and photovoltaics, computer simulations, digital control implementation. Remus Teodorescu is the founder and coordinator of the Green Power Laboratory at Aalborg University focusing on the development and testing of grid converters for renewable energy systems.

email: ret@iet.aau.dk

Pedro Rodriguez received the MSc and PhD degree in Electrical Engineering from the Technical University of Catalonia (UPC), Spain in 1994 and 2004, respectively. In 1990, he joined the Electrical Engineering Department, at the UPC, where he is currently an associate professor teaching power electronics and circuit analysis as well as supervising PhD students. Since 1998, he focused his interest on Power Electronics applied to Power Quality Conditioning and Distributed Energy Systems Integration. Currently, he is leading the Renewable Electrcial Energy Systems (REES) research group at the UPC. He stayed as a researcher in the Center for Power Electronics

Systems (CPES) at Virginia Polytechnic Institute and State University, USA, and in the Institute of Energy Technology (IET) at Aalborg University, Denmark, respectively in 2005 and 2006. He has participated in 6 research project dealing with power electronics applied to renewable energies integration and power quality improvement. He has 3 patents about active filtering and authored more than 50 technical papers published in international journals and conferences. Pedro Rodriguez has organized special sessions about power electronics for renewable energies in different international conferences and currently is the general chairman of the IEEE IES Student Forum.

email: prodriguez@ee.upc.edu

Marco Liserre, received the MSc and PhD degree in Electrical Engineering from the Polytechnic of Bari, respectively in 1998 and 2002. From January 2004 he is an assistant professor in the same university teaching courses of power electronics, industrial electronics and electrical machines.

Recently his research interests are focused on industrial electronics applications to distributed power generation systems based on renewable energies. He has co-authored some 100 technical papers, 20 of them in international peer-reviewed journals and 3 chapters of a book.

He has been a visiting Professor at Aalborg University (Denmark) and he has been giving lectures in different universities including three tutorials in international conferences.

Marco Liserre is member of the Industrial Electronics Society, Power Electronics Society and Industry Applications Society. He has served them as reviewer both for conferences and journals. Within the IES he has been active as responsible of student activities, AdCom member, editor of the newsletter, responsible of region 8 membership activities, and chairman of the subcommittee “Power Electronics Applications in Power Systems and Renewable Energies” of the committee “Power Electronics” chaired by Prof. Greg Asher. He has been involved in IEEE conferences organization in different capacities. He is an Associate Editor of the IEEE Transactions on Industrial Electronics. He is Editor-in-Chief of the IEEE Industrial Electronics Magazine.

email: liserre@poliba.it

PV INVERTERS STRUCTURES, TOPOLOGIES AND CONTROL

Remus Teodorescu
Aalborg University
ret@ @iet.aau.dk
www.iet.aau.dk

Outlines

- Structures
- Topologies
- Modulation
- Control

4535

Structures

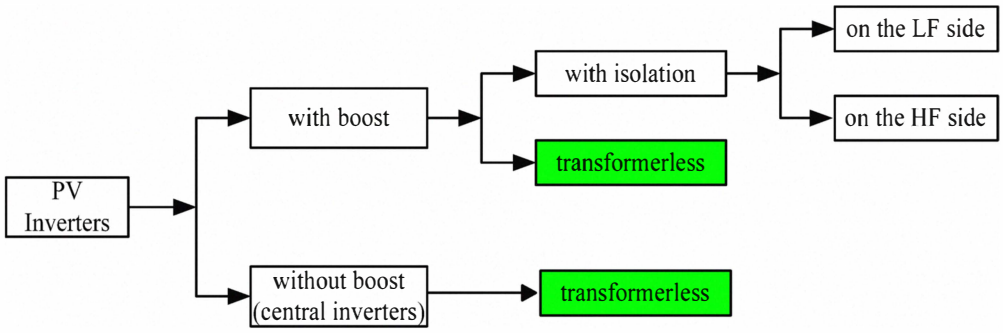

- PV DCvoltage typically low for string inverters → boost needed for low power
- For high power (>100 kW) central PV inverters w/o boost, typical three-phase FB topologies with LV-MV trafo)
- Galvanic isolation necessary in some countries
- LF/HF transformer (cost-volume issue)
- A large variety of topologies
- The optimal topology is not matured yet as for drives
- **Transformerless** topologies having higher efficiency are emerging and the grid regulations are changing in order to allow them

Structures

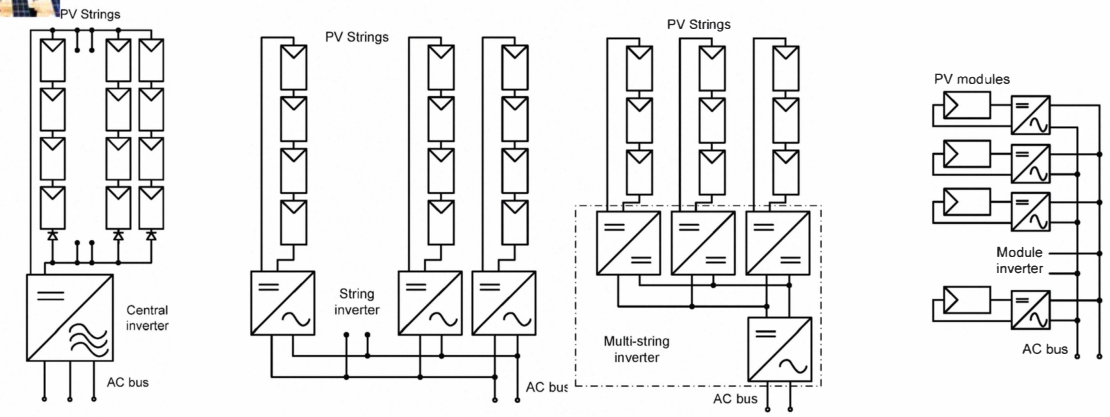

Central inverters

- 10-250kW, three-phase, several strings in parallel
- high efficiency, low cost, low reliability, not optimal MPPT
- used for power plants

String (Multi)inverters

- 1.5-5 kW, typical residential application
- each string has its own inverter enabling better MPPT
- the strings can have different orientations
- three-phase inverters for power<5kW

Module inverters

- 50-180W, each panel has its own inverter enabling optimal MPPT
- lower efficiency, difficult maintenance
- higher cost/kWp

4536

High efficiency Mini-central PV inverters (8-15 kW) are also emerging for modular configuration in medium and high power PV systems

Structures: Transformer-Based

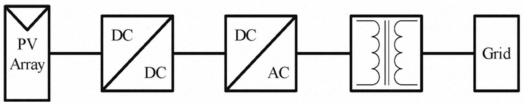

On low frequency (LF) side

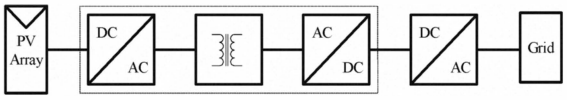

On high frequency (HF) side

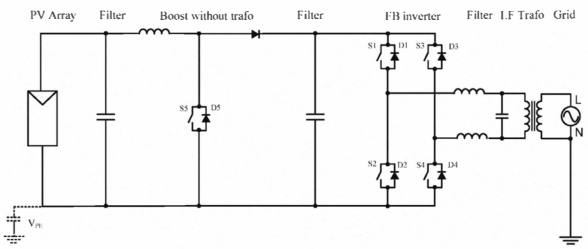

Boosting inverter with LF trafo based on boost converter

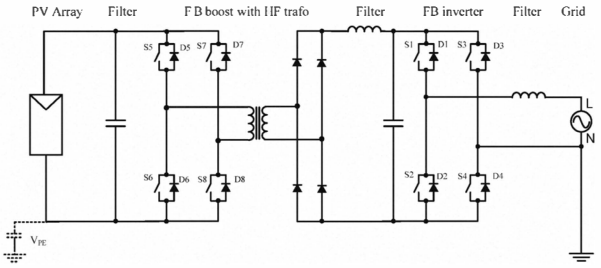

Boosting inverter with HF trafo based on FB boost converter [2]

Both technologies are on the market! Efficiency 93-95%

Structures: Transformer-Less

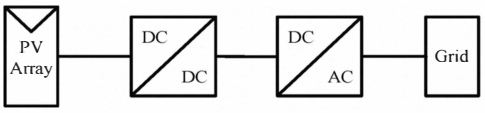

•FB inverter + boost

• Typical configuration [1]

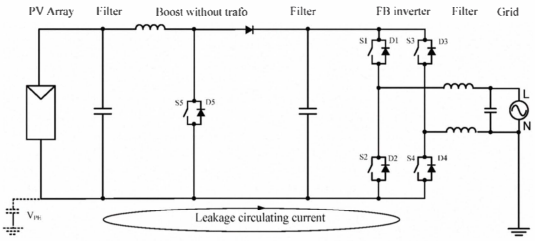

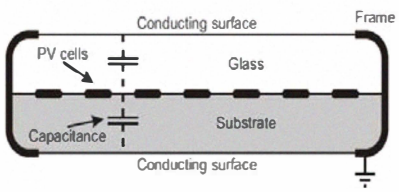

- High efficiency (>95%)
- Leakage current problem
- Safety issue

•Time sharing configuration[3]

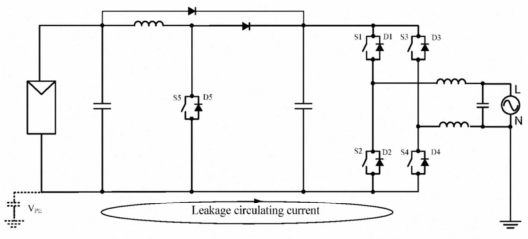

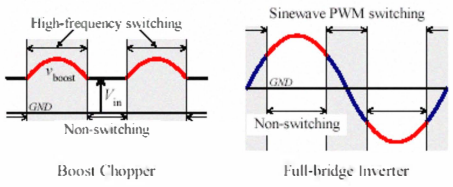

4537

- Efficiency > 96%
- Extra diode to bypass boost when $V_{pv} > V_g$
- Boost with rectified sinus reference

Structures: Transformer-Less

Parasitic capacitance of the PV array

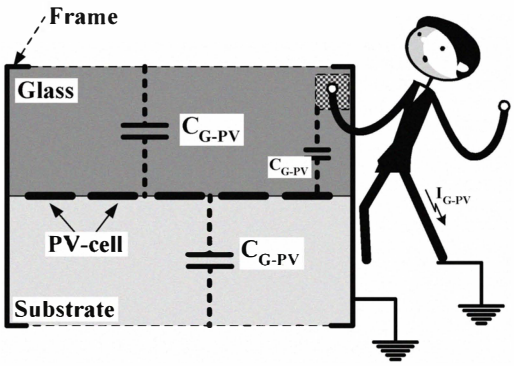

- PV panel array has huge surface
- Parasitic capacitance formed between
- grounded frame and PV cells
- Its value depends on the:
  - Surface of the PV array and grounded frame
  - Distance of PV cell to the module
  - Atmospheric conditions
  - Dust and humidity, which can increase the electrical conductivity
  - of the panel's surface

Structures: Transformer-Less

Leakage current

- Charging and discharging this capacitance leads to ground leakage currents (unsafe for human interaction; damage PV panels)
- Amplitude of leakage current depends on
  - Value of parasitic capacitance
  - Amplitude and frequency of imposed voltage
- RCM (Residual Current Monitoring) unit for monitoring leakage ground currents

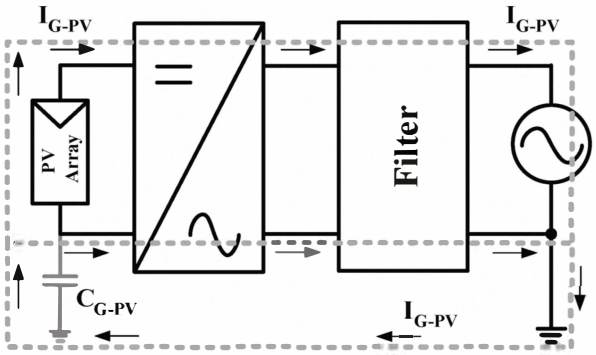

4538

Structures: Transformer-Less

	Soleil FVG 36-125	Kyocera KS10	BPSolar MSX120
Surface of PV panel	204 x 352mm²	1197 x 535mm²	1108 x 991mm²
Power at MPP (STC)	80W	10W	120W
$C_{G\text{-}PV}$(1 panel)	130pF	57pF	21pF
$C_{G\text{-}PV}$(1panel) wet	1,38nF @ 10kHz	2,39nF @ 10kHz	3nF @ 10kHz
$C_{G\text{-}PV}$(2panels)	247pF	101pF	not available
$C_{G\text{-}PV}$(1panel+ palm)	140pF	150pF	200pF
$C_{G\text{-}PV}$ (1panel+palm) wet	185pF @ 10kHz	230pF @ 10kHz	200pF @ 10kHz
$C_{G\text{-}PV}$(1panel+ copper plate)	160pF	140pF	150pF
$C_{G\text{-}PV}$(1panel+ copper plate) wet	210pF @ 10kHz	212pF @ 10kHz	257pF @ 10kHz

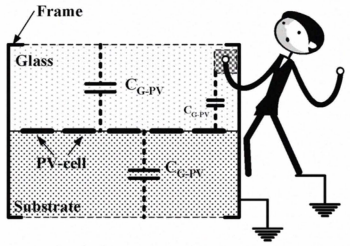

V_{AB}, V_{PE} and I_{PE} for FB-UP

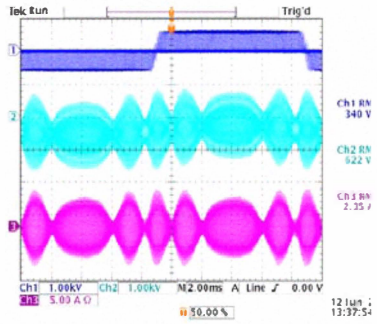

Spectrum of voltage to earth

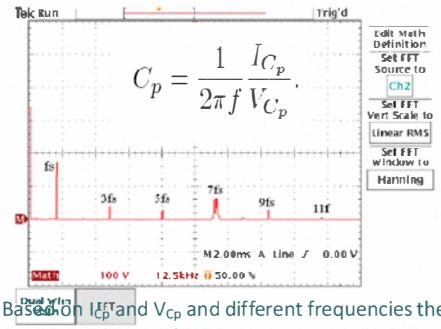

Spectrum of leakage current

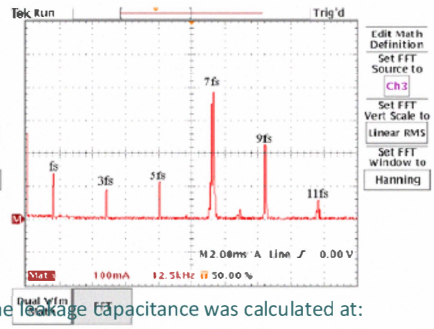

Based on I_{Cp} and V_{Cp} and different frequencies the leakage capacitance was calculated at: Cp=13.6nF (7.06nF/kWp). Cp is useful in high-frequency analysis and in damping resonances

Structures: comparison

With transformer

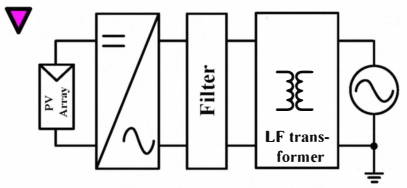

*

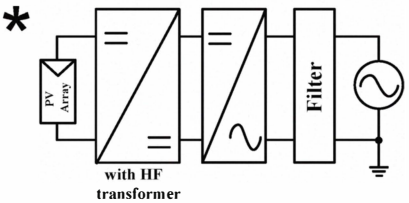

○

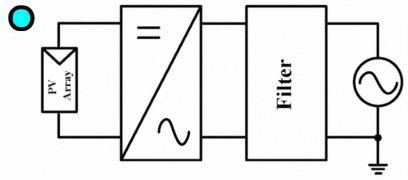

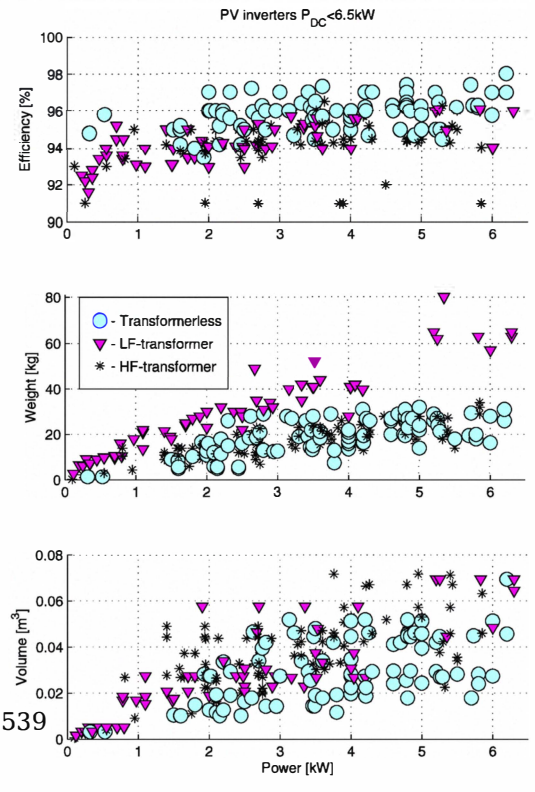

4539

Structures: PV Modules

- High Performance compared to a traditional PV System
- Modularity
- Simplicity
- Intelligence
- Reliability

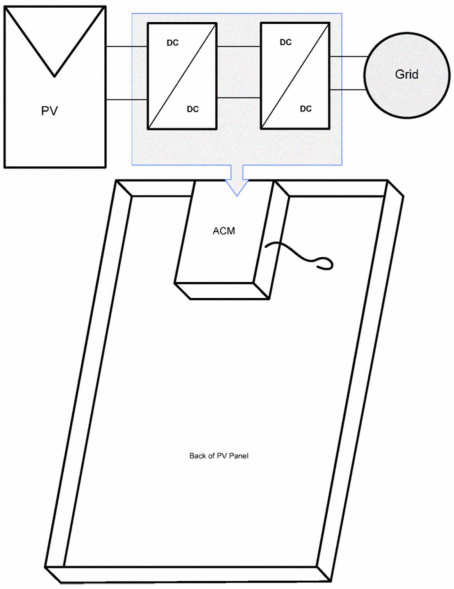

Structures: PV Modules

The advantages of PV modules compared to traditional PV systems are:

- Each module works independently
- High modularity allowing easy system expansion
- Use of standard AC installation material, which reduces costs of installation material and system design.
- Low conduction losses and cable costs.
- No mismatch losses at system level as each AC module operates in its own Maximum Power Point (MPP).
- No need for string diodes.
- No need for bypass diodes.
- Low lightning induced surge voltages, because of the compact DC system layout.

4540

Structures: PV Modules

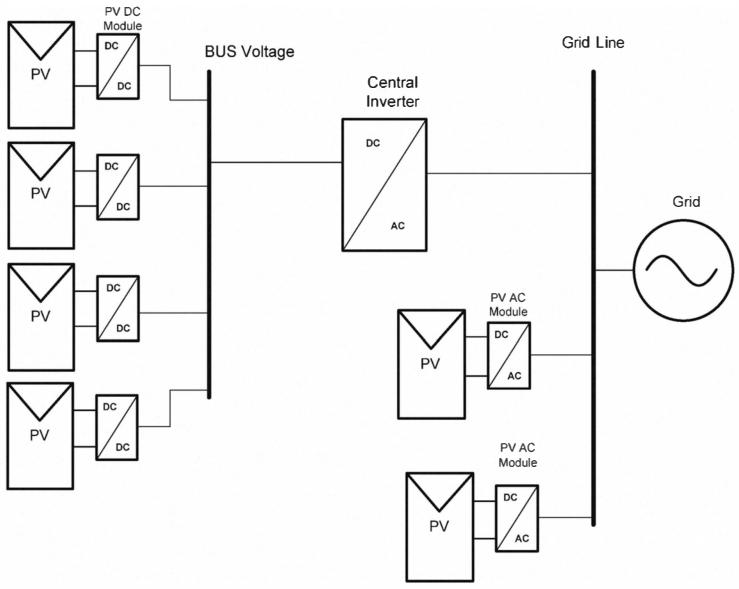

- DC/DC Converter box for each module plus Central Inverter for grid Connection
- DC/AC Converter for each module directly connected with the grid

Structures: PV-DC Modules Double Stage

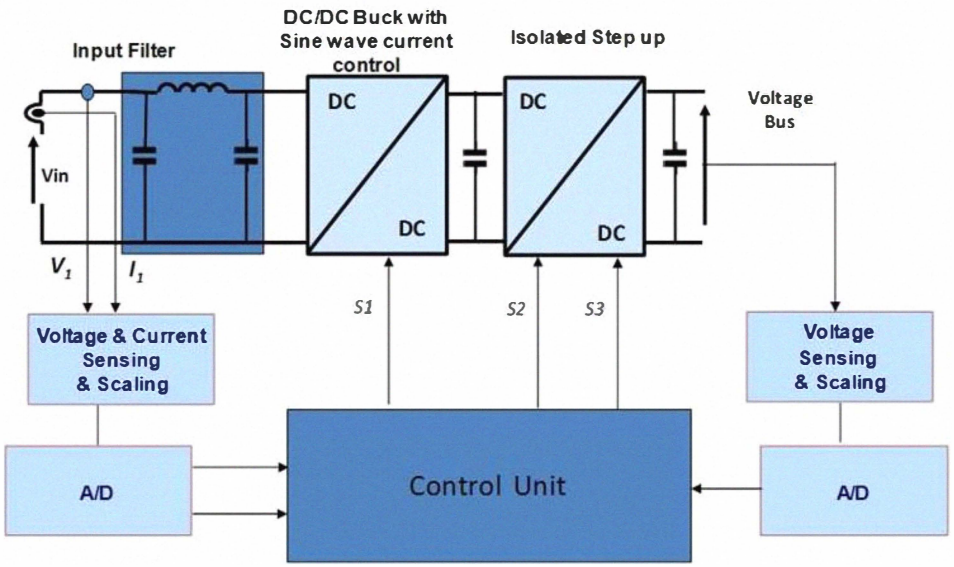

Advantages:

- Wide MPPT range
- Simple Control
- Low number of sensors required
- Small Inverter bus capacitor

Drawbacks:

- Number of power devices
- Input Ripple Current

4541

Structures: PV-DC Modules Single Stage

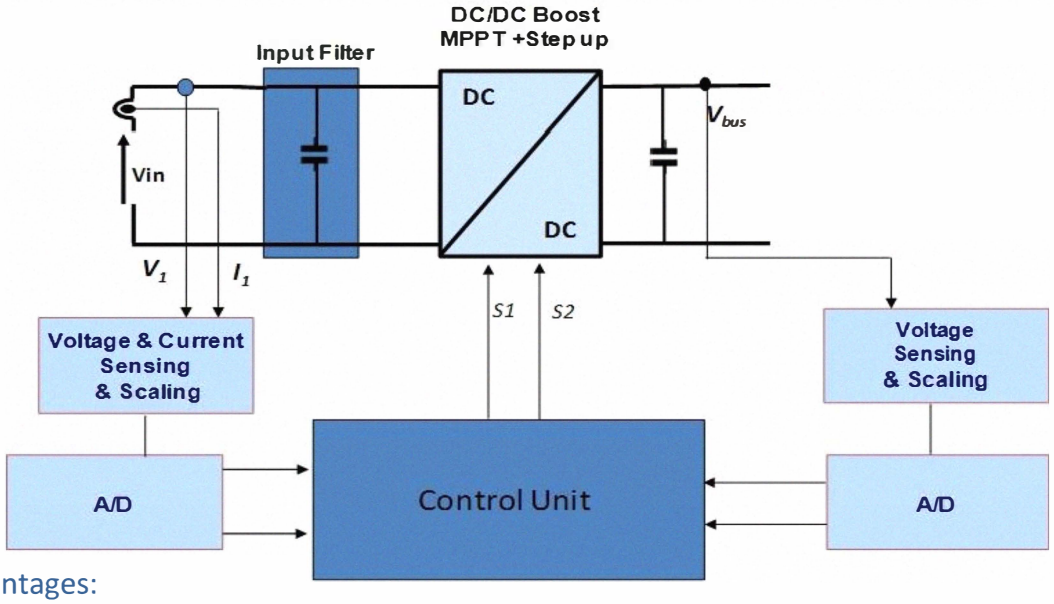

Advantages:

- Low ripple current
- Low component count
- High Efficiency
- No Electrolytic Caps

Drawbacks:

- More complex control

Structures: PV-AC Modules

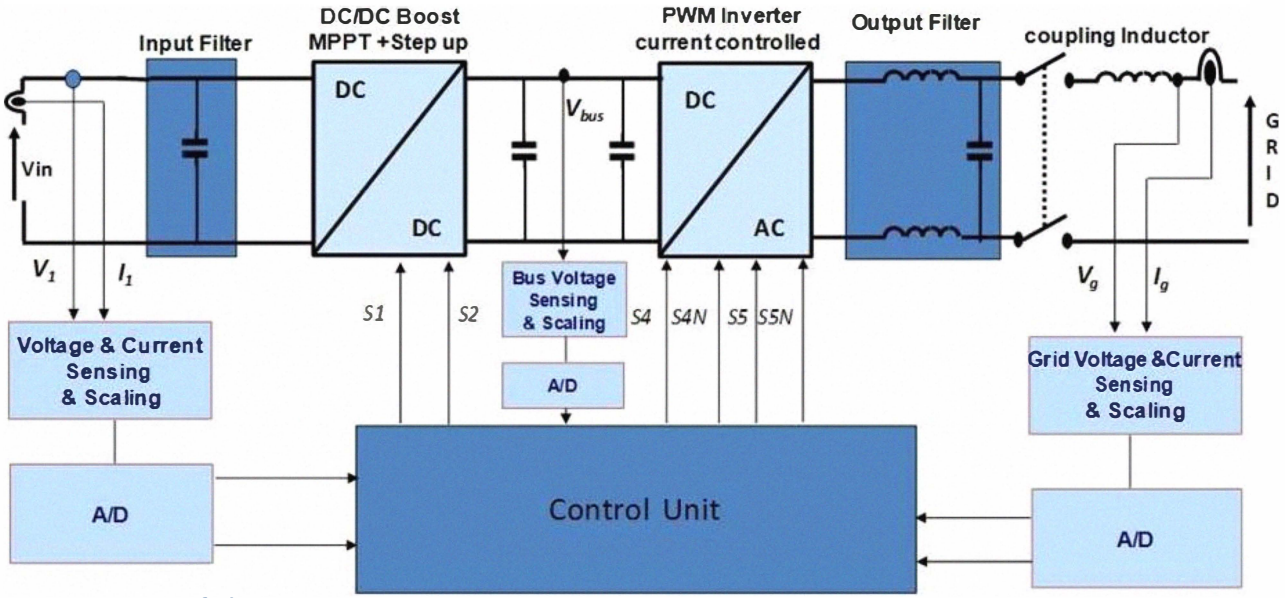

Advantages:

- Low ripple current
- Low component count
- High Efficiency
- No Electrolytic Caps

Drawbacks:

- Number of sensors required
- More complex control

4542

Topologies PV Modules

PV-DC Modules Double Stage

- Buck Converter plus Push-Pull

PV-DC Modules SIngle Stage

- Interleaved Boost with/without Charge pump System or Flyback

PV-Modules DC/AC

- Flyback plus Full-Bridge or Flyback (Current COntrol) plus Full Bridge (Low Switching Frequancy operation)

Structures: Central Inverters

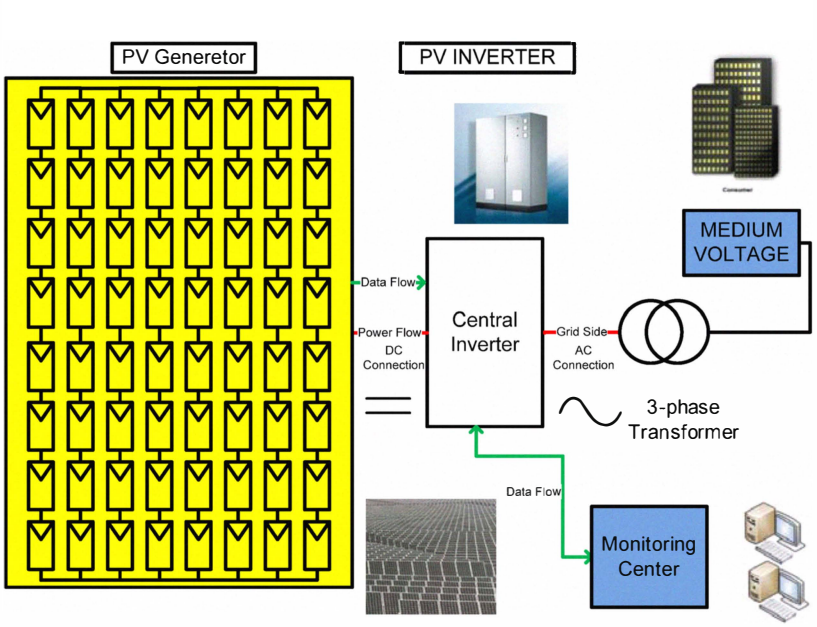

- High Performance for Large PV Plant, High Level Monitoring , High Level Intelligence, Reliability,
- High Efficiency (up 97%), Competitive prize/performance ratio.
- Typical structure – String inverter, 3-phase FB proven technology with transformer to MV and connection to Distribution System

4543

Sample of Big Plant Topology

Example of Central inverter Schematic (ABB)

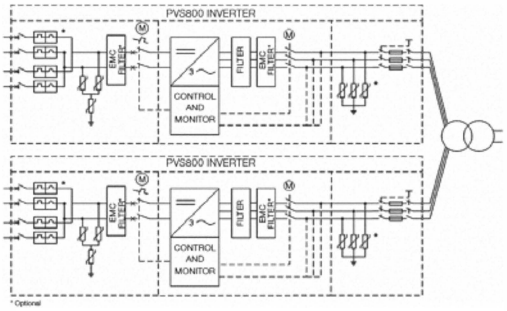

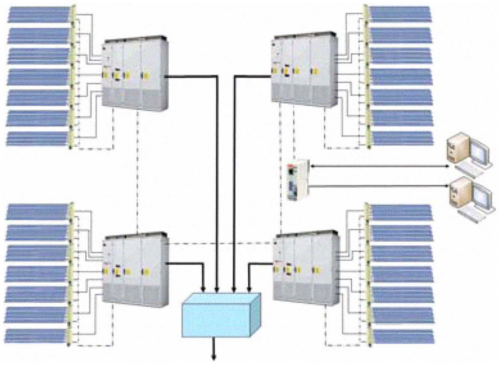

- 100-500 kW,
- 450-750Vdc input
- 400Vac out
- efficiency > 97.5%
- Long life-time
- Modular design
- PF Compensation

Sample of Big Plant Topology

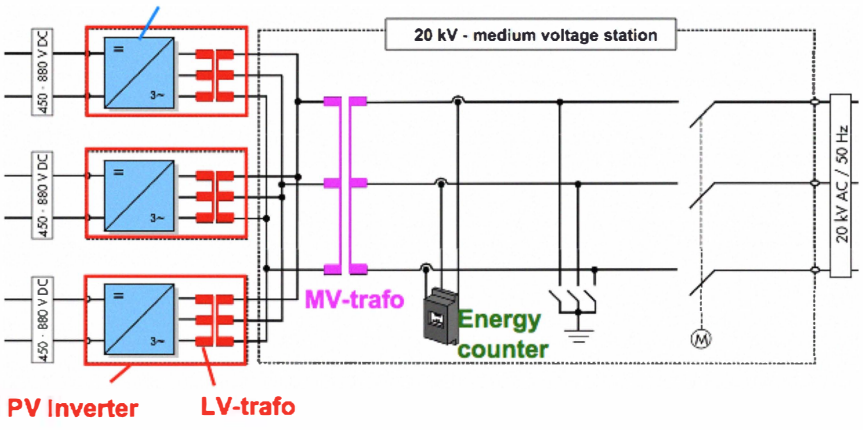

Standard approch for 1MW PV Plant (SMA)

- 3 Inverter units 330 kW each with an integrated LV-Trafo
- Connection to standard public Low voltage grid (400V) PV
- Inverter separated for Medium Voltage station including– MV-trafo 400 V/20kV and energy counte

4544

Central-Inverters In the market

Aero Sharp, Aros (Sirio), Conergy, Control Techniques, EEI - Equipaggiamenti Elettronici Industriali Srl, Eurener, Green Power, Helios System, Hyunday Heavy, Integral Drive Systems AG, Ingeteam, Jema, Kaco, Layer, Leonics, Lti, Padcon, Pairan, Power One, PV Powered, Refu, Elettronica Santerno, SatCon, Schneider Electric, Siel, Siemens, Siliken, SMA, Sputnik, Voltwerk, Zigor

Large PV-Plants

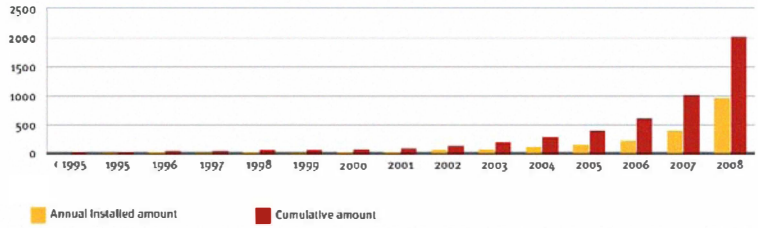

MWp	COUNTRY	LOCATION	REGION/PROVINCE	DESCRIPTION
60	Spain	Olmedilla de Alarcón	Castilla-La Mancha	Parque fotovoltaico Olmedilla de Alarcón
47	Spain	Puertollano *	Castilla-La Mancha	Parque solar Puertollano
46	Portugal	Moura **	Alentejo	Moura photovoltaic power plant
40	Germany	Brandis ***	Saxony	Solarpark Waldpolenz
34.19	Spain	Arnedo	La Rioja	Planta solar Arnedo
30	Spain	Osa de la Vega ****	Castilla-La Mancha	Huerta solar Osa de la Vega
30	Spain	Trujillo	Extremadura	Solar Park La Magascona/La Magasquilla
30	Spain	Merida	Extremadura	Parque fotovoltaico SPEX
28	Spain	Casas de los Pinos	Castilla-La Mancha	Planta fotovoltaica Casas de los Pinos
26	Spain	Fuente Álamo	Murcia	Parque fotovoltaico Fuente Álamo
24	Korea	Sinan	Southern Jeolla	Sinan power plant
23.2	Spain	Lucainena de las Torres	Andalusia	Planta fotovoltaica de Lucainena de las Torres
23.1	Spain	Abertura	Extremadura	Parque fotovoltaico Abertura Solar
23	Spain	Jumilla	Murcia	Parque solar Hoya de Los Vincentes
22.1	Spain	Almaraz	Extremadura	Huerta solar Almaraz
21.2	Spain	Villarrobledo	Castilla-La Mancha	Parque solar El Calaveron
20.28	Spain	El Coronil	Andalusia	Parque solar El Coronil I+II
20	Spain	Calasparra	Murcia	Planta solar fotovoltaico Calasparra I+II+III
20	Spain	Benelxama	Valencia	Planta solar Benelxama

4545

Structures - Conclusions

- Transformerless multistring PV inverters feature in comparison with Transformer Based PV inverters:
  - Higher efficiency
  - Lower volume and weight

- Today more than 70% of the PV inverters sold on the market are transformerless achieving 98% max conversion efficiency and 97.7% "european" (weighted) efficiency [Photon Magazine]

- PV Modules are emerging on the market with more manufacturers.
- Central inverters are preferred in multi MW range PV power plants

*Source [Burger, B., Schmidt,H. "25 YEARS TRANFORMLESS INVERTERS" – Proceedings of PVSEC 2007]

RECAP-Bridge Modulation- SPWM

$$\text{Amplitude modulation ratio}: M = \frac{\hat{V}_{control}}{\hat{V}_{tri}}$$

$$\text{Frequency modulation ratio}: m = \frac{f_S}{f_1}$$

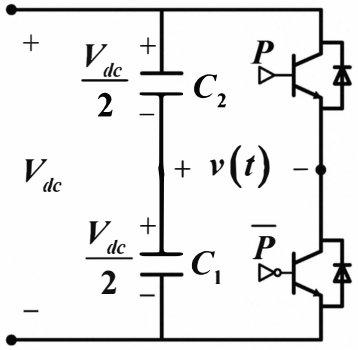

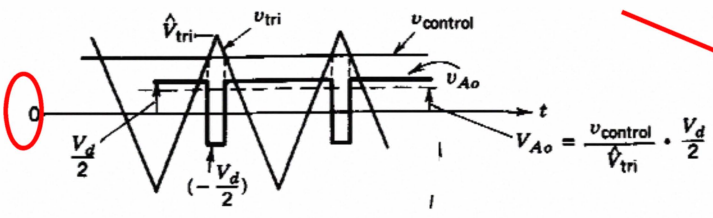

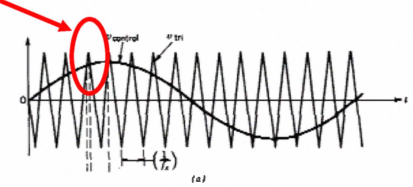

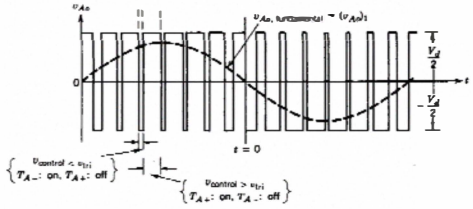

Output voltage averaged over one switching period:

$$V_{Ao} = \overline{v}_{Ao} = \frac{v_{control}}{\hat{V}_{tri}} \frac{V_d}{2} \quad ; \quad v_{control} \leq \hat{V}_{tri}$$

Topologies: FB Modulation

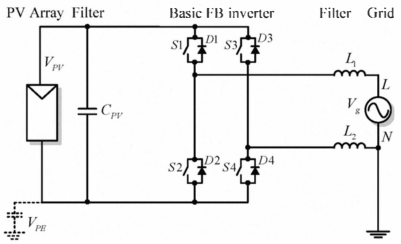

Bipolar PWM
S1 + S4 and S2 + S3 are switched complementary at high frequency.

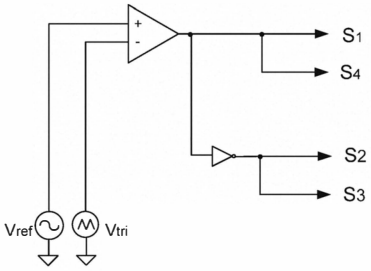

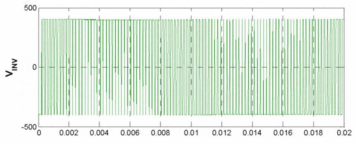

Unipolar PWM
Leg A and B are switched with high frequency with mirrored sinusoidal ref.

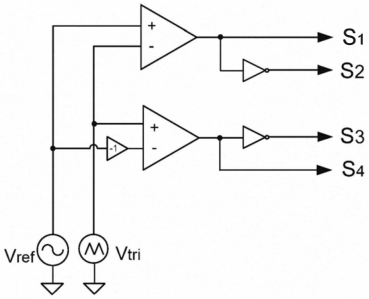

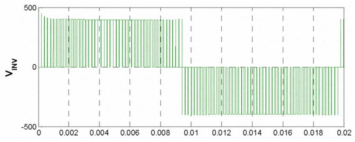

Hybrid PWM
Leg A is switched with grid low frequency and Leg B is switched with high freq

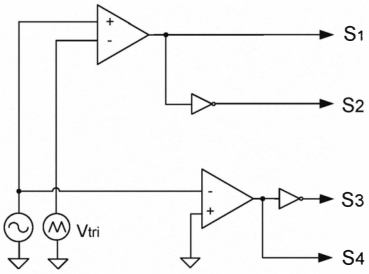

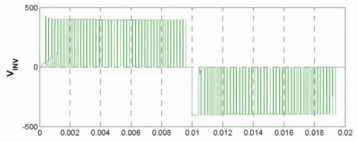

Topologies: FB Bipolar PWM

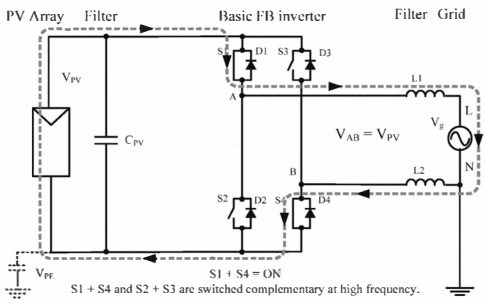

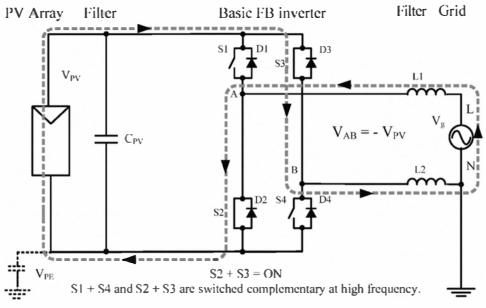

- S1 + S4 and S2 + S3 are switched complementary at high frequency (PWM)
- No 0 output voltage possible
- The switching ripple in the current equals **1x** switching frequency → large filtering
- Voltage across filter is bipolar → **high core losses**
- **No common mode voltage** → V_{PE} free for high frequency →low leakage current
- Max efficiency 96.5% due to reactive power exchange L1(2)<-> Cpv during freewheeling and that 2 switched are simultaneously switched every switching
- **This topology is not suited to transformerless PV inverter due to low efficiency!**

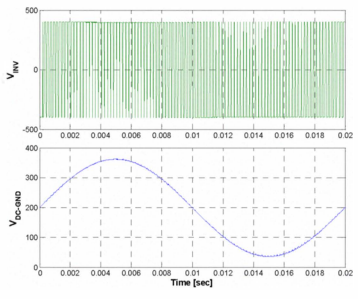

Topologies: FB Unipolar PWM

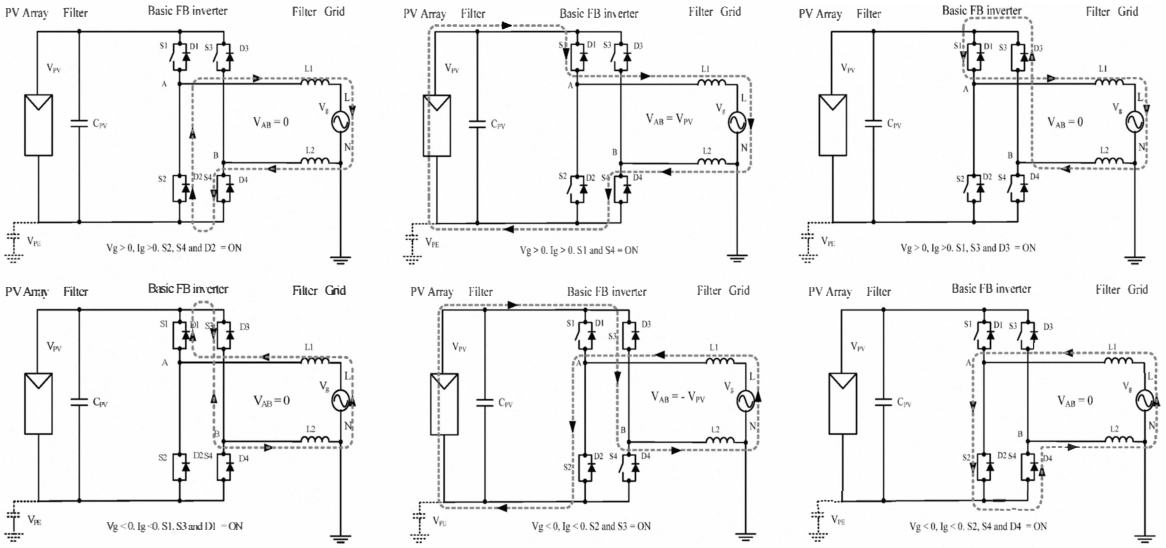

- Leg A and B are switched with high frequency with mirrored sinusoidal reference
- Two 0 output voltage states possible: S1 and S2 = ON and S3 and S4 = ON
- The switching ripple in the current equals **2x** switching frequency → lower filtering
- Voltage across filter is unipolar → **low core losses**
- V_{PE} has switching frequency components → **high leakage current and EMI**
- Max efficiency 98% due to **no** reactive power exchange L1(2)<-> Cpv during freewheeling
- **This topology is not suited for TL PV inverter due to high leakage!**

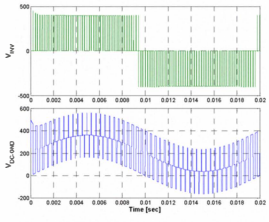

Topologies: FB Hybrid PWM

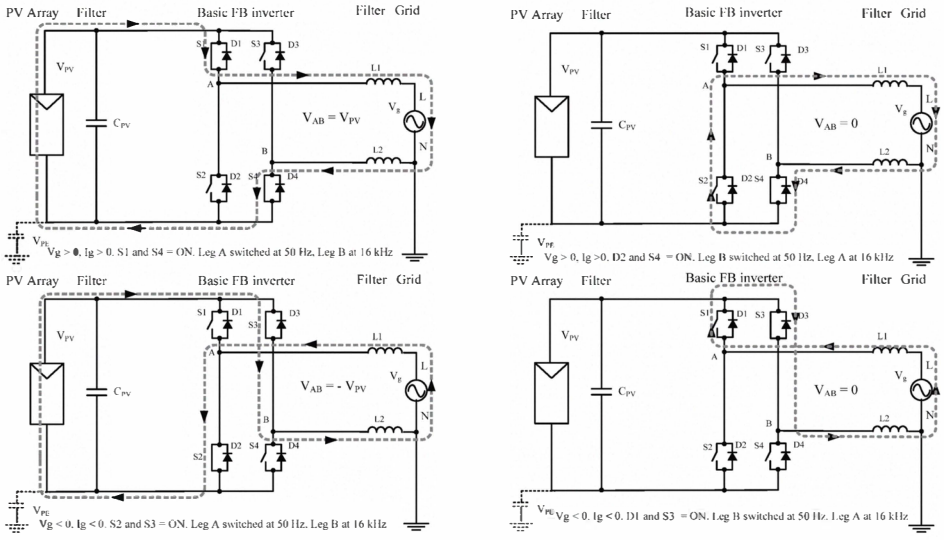

- Leg A is switched with high frequency PWM and Leg B is switched with grid low frequency
- Two 0 output voltage states possible: D1 and S3= ON and D2 and S4 = ON
- The switching ripple in the current equals **1x** switching frequency → high filtering
- Voltage across filter is unipolar → **low core losses**
- V_{PE} has square wave variation at grid frequency → **high leakage current and EMI**
- High efficiency 98% due to **no** reactive power exchange L1(2)<-> Cpv during freewheeling and due to **lower frequency switching in one leg.**
- **This topology is not suited for transformerless PV inverter due to high leakage!**

4548

Source [Ray-Shyang Lai; Ngo, K.D.T., "A PWM method for reduction of switching loss in a full-bridge inverter," Power Electronics, IEEE Transactions on , vol.10, no.3, pp.326-332, May 1995]

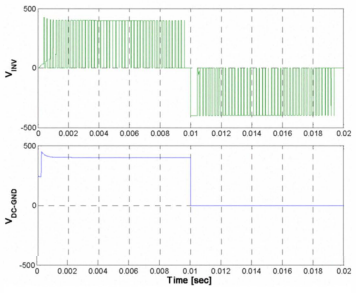

Topologies : H5 (SMA) Modulation

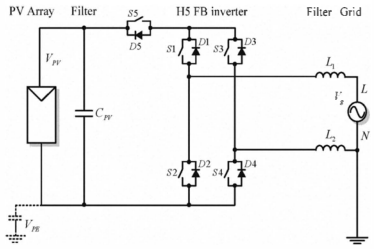

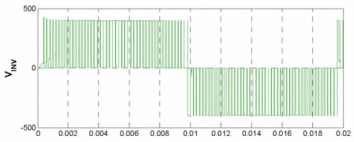

S5 and S4 (S3) are switched with high frequency
A1 (S2) are switched with low grid freq

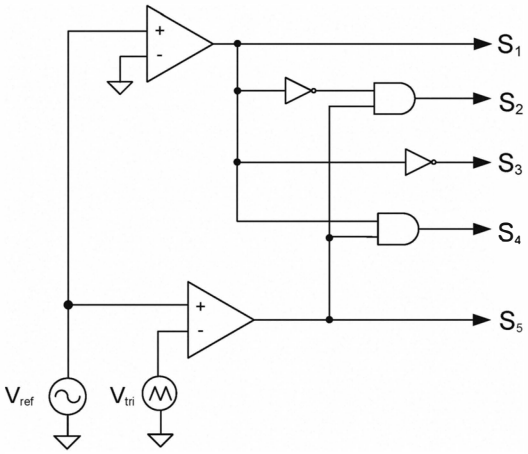

Source [Victor M.et al.- US Patent Application, Pub.No.: US 2005/0286281 A1, Pub. Date: 29.Dec.2005]

Topologies: H5 (SMA)

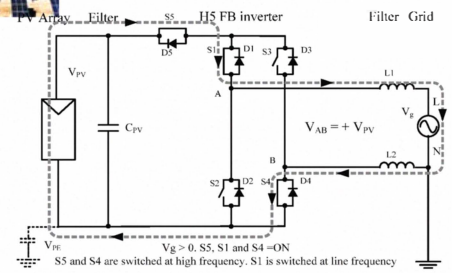

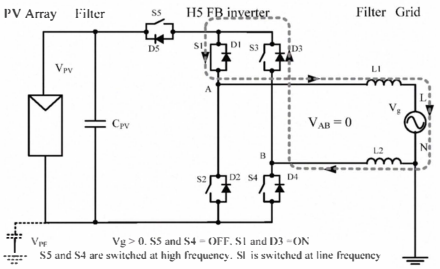

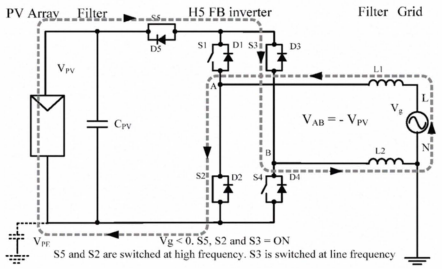

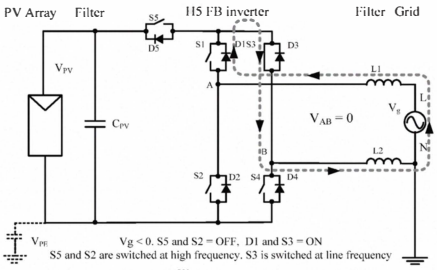

- Extra switch in the dc link to decouple the PV generator from grid during 0 voltage
- Two 0 output voltage states possible: S5 = OFF, S1 = ON and S5 = OFF, S3 = ON
- The switching ripple in the current equals **1x** switching frequency → high filtering
- Voltage across filter is unipolar → **low core losses**
- V_{PE} is sinusoidal with grid frequency component → **low leakage current and EMI**
- High max. efficiency **98%** due to **no** reactive power exchange as reported by Photon Magazine for SMA SunnyBoy 4000/5000 TL single-phase

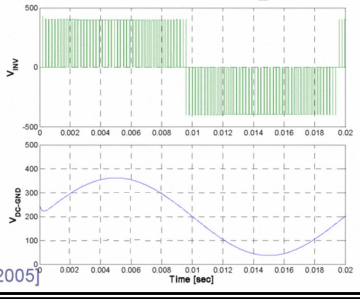

Source [Victor M.et al.- US Patent Application, Pub.No.: US 2005/0286281 A1, Pub. Date: 29.Dec.2005]

Topologies - HERIC Modulation

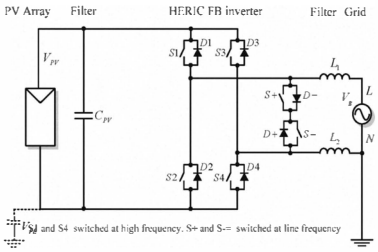

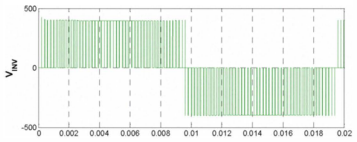

S+ and S- are switched with grid freq
S1&S4 (S&S3) are switched with high freq

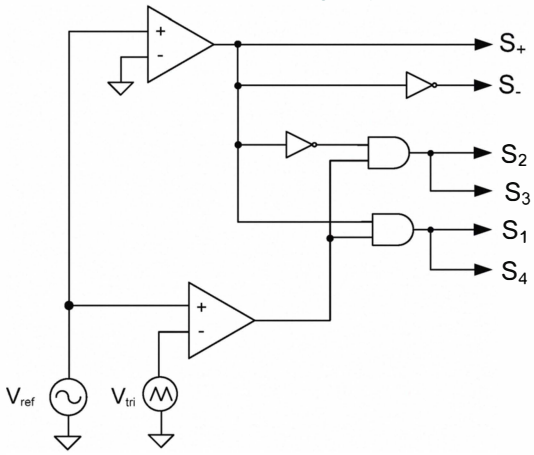

Source [Schmid H. et al. US Patent No: 7046534, issued 16 May 2006]

Topologies- HERIC

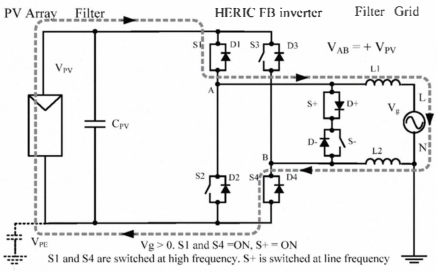

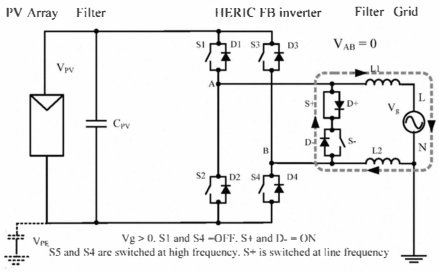

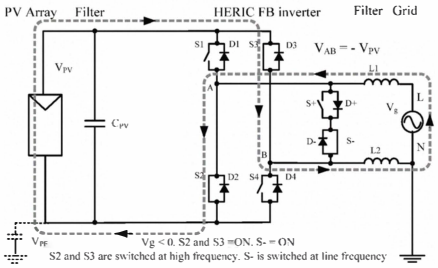

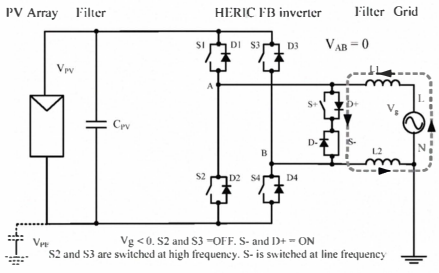

- Two 0 output voltage states possible: S+ and D- = ON and S- and D+ = ON
- The switching ripple in the current equals **1x** switching frequency → high filtering
- Voltage across filter is unipolar → **low core losses**
- V_{PE} is sinusoidal has grid frequency component → **low leakage current and EMI**
- High efficiency **98%** due to **no** reactive power exchange as reported in Photon Magazine for Sunways AT series 2.7 – 5 kW single-phase

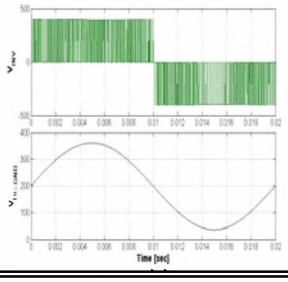

Source [Schmid H. et al. US Patent No: 7046534, issued 16 May 2006]

Topologies- FBDC Bypass (H6)

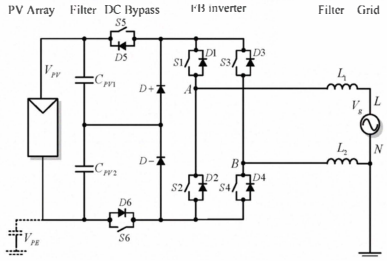

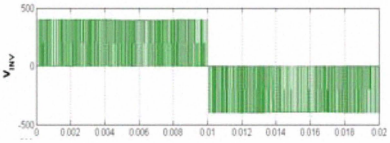

S5 and S6 are switched at high frequency, S1 and S4 at line frequency

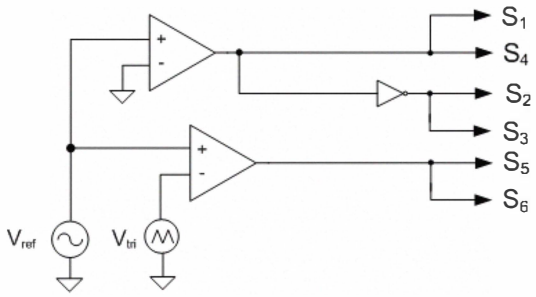

Source [Gonzalez S R, et.al.- International Patent Application, Pub No. WO2008015298, Pub. Date: 2 July 2007]

Topologies- FBDC Bypass (H6)

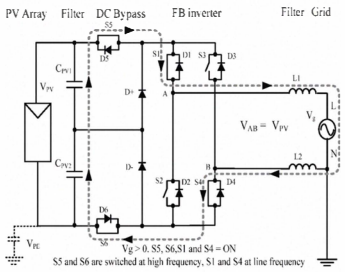

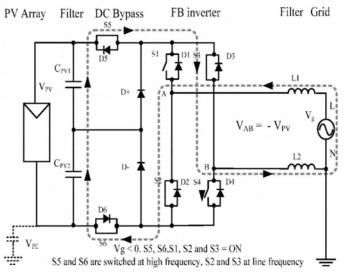

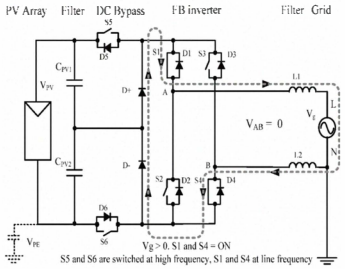

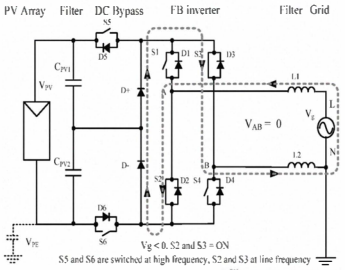

- Two extra switches switching with high frequency and 2 diodes bypassing the dc bus. The 4 switches in FB switch at low fsw
- Two 0 output voltage states possible by "natural clamping# of D+ and D-
- The switching ripple in the current equals **1x** switching frequency → high filtering
- Voltage across filter is unipolar → **low core losses**
- V_{PE} is sinusoidal and has grid frequency component → **low leakage and EMI**
- High max efficiency **96.5%** due to **no** reactive power exchange as reported by Photon Magazine for Ingeteam Ingecon Sun TL series (2.5/3.3/6 kW, single-phase)

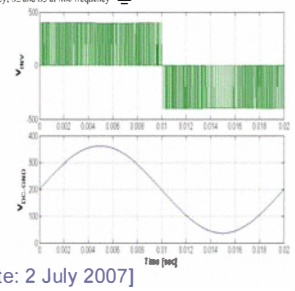

Source [Gonzalez S R, et.al.- International Patent Application, Pub No. WO2008015298, Pub. Date: 2 July 2007]

Topologies- ZVFBR Modulation

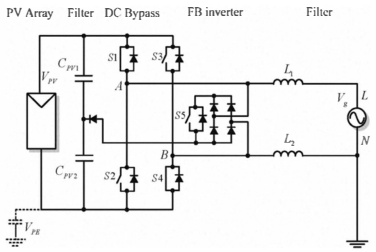

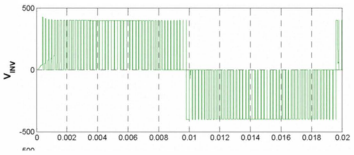

S5 is switched with grid freq
S1&S4 (S&S3) are switched with high freq

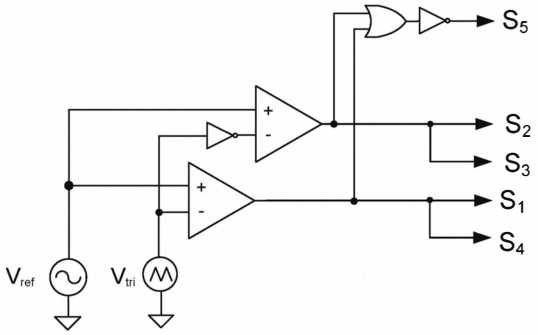

Source [T. Kerekes, R. Teodorescu, P. Rodriquez, G. Vazquez and E. Aldabas, A new high-efficiency single-phase transformerless PV inverter topology; IEEE Transactions on Industrial Electronics]

Topologies- ZVFBR (AAU+UPC)

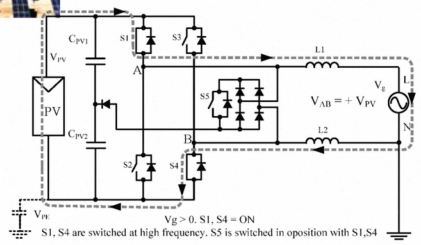

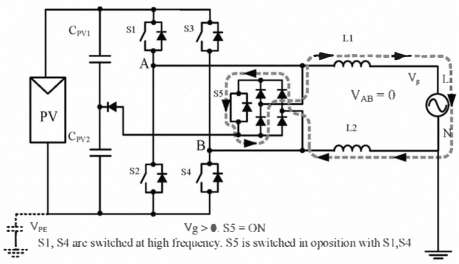

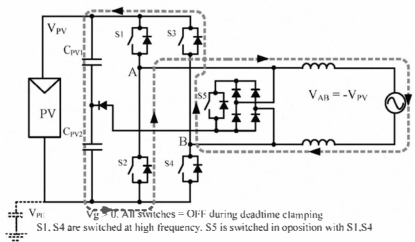

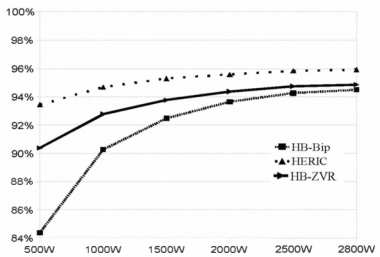

- Derived from HERIC but the bidirectional grid-short-circuiting switch is implemented using a diode bridge and 1 switch
- Zero voltage is achieved by turning the FB off and turning T5 on -> higher losses as HERIC due to high switching frequency of T5
- The switching ripple in the current equals **1x** switching frequency → high filtering
- Voltage across filter is bipolar due to deadtime clamping → **higher core losses**
- V_{PE} is constant → **low leakage current and EMI**
- High efficiency due to **no** reactive power exchange during zero voltage

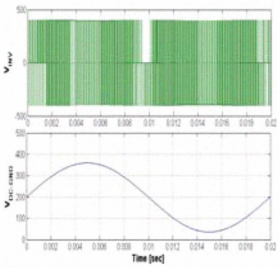

4552

Source [T. Kerekes, R. Teodorescu, P. Rodriquez, G. Vazquez and E. Aldabas, A ne transformerless PV inverter topology; IEEE Transactions on Industrial Electronics]

Topologies- UltraEta - REFU

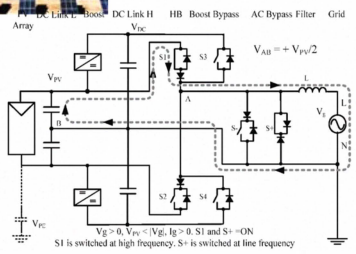

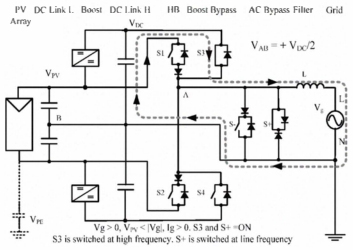

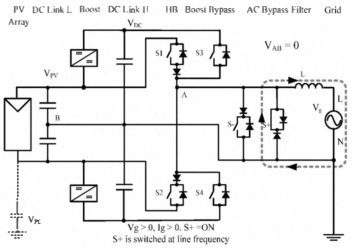

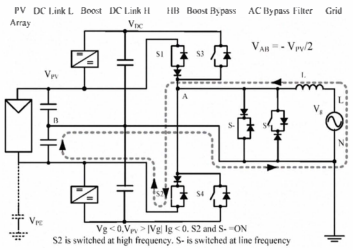

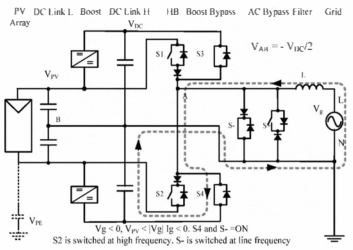

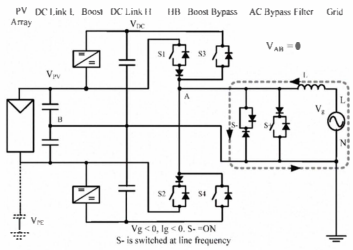

- Three-level output. Requires double PV voltage input in comparison with FB but it include time-shared boost
- Zero voltage is achieved by short-circuiting the grid using the bidirectional switch
- The switching ripple in the current equals **1x** switching frequency → high filtering
- Voltage across filter is unipolar → **low core losses**
- V_{PE} w/o high freq component → **low leakage current and EMI . No L in neutral!**
- High max efficiency **98%** due to **no** reactive power exchange, as reported by Photon Magazine for Refu Solar RefuSol (11/15 kW, three-phase)

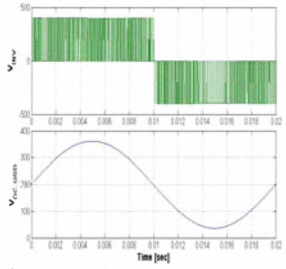

Source [Hantschel J. German Patent Application, Pub. No. DE102006010694 A11, Pub Date: 20 Sep 2007]

Topologies- NPC (Danfoss Solar)

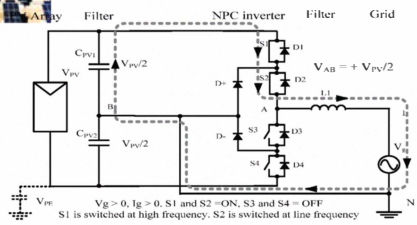

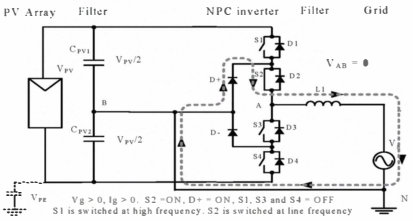

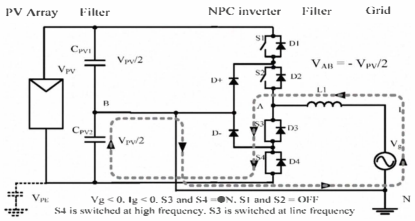

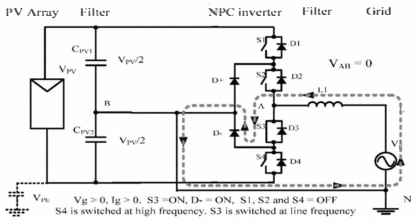

- Three-level output. Requires double PV voltage input in comparison with FB. Typically needs boost.
- Two 0 output voltage states possible: S2 and D+ = ON and S3 and D- = ON. For zero voltage during Vg>0, Ig<0, S1 and S3 switch in opposition and S2 and S4 for Vg<0, Ig>0
- The switching ripple in the current equals **1x** switching frequency → high filtering
- Voltage across filter is unipolar → **low core losses**
- V_{PE} is equal –Vpv/2 w/o high freq comp → **low leakage and EMI . No L in N!**
- High max efficiency **98%** due to **no** reactive power exchange, as reported by Danfoss Solar TripleLynx series (10/12.5/15 kW)

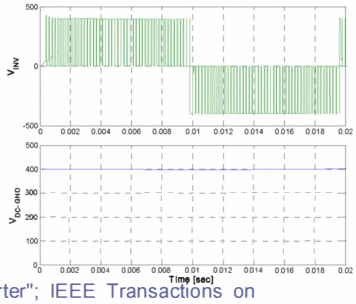

Source [A. Nabae, I. Takahashi, and H. Akagi; "A New Neutral-Point-Clamped PWM Inverter"; IEEE Transactions on Industry Applications, vol. IA-17, no. 5, 1981, pp. 518-523]

Topologies- CONERGY

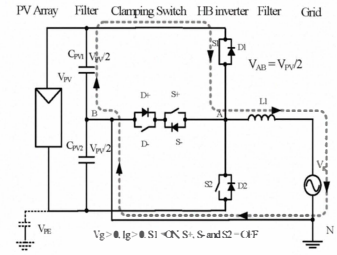

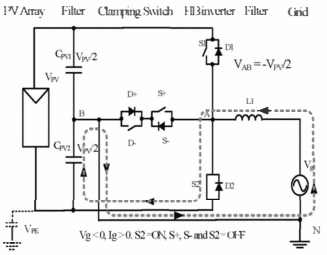

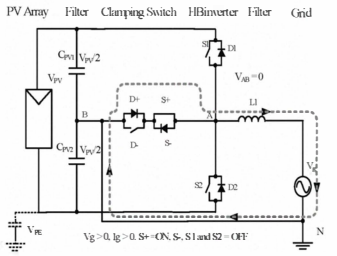

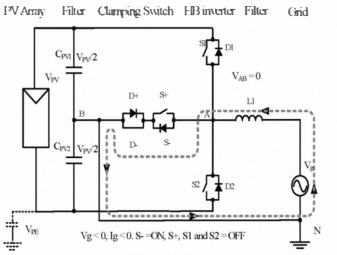

- Only 4 switches needed with 2 of them (S+ and S-) rated only Vpv/4
- Three-level output. Requires double PV voltage input in comparison with FB. Typically needs boost.
- Two 0 voltage states using the bidirectional clamping switch (S+ and S-)
- The switching ripple in the current equals **1x** switching freq → high filtering
- Voltage across filter is unipolar → **low core losses**
- V_{PE} is equal –Vpv/2 w/o high freq comp → **low leakage and EMI . No L in N!**
- High max efficiency **96.1%** due to **no** reactive power exchange, as reported by Conergy IPG series (2-5 kW single-phase)

Source [Knaup P – International Patent Application, Pub No. WO 2007/048420 A1, Pub. Date: 3

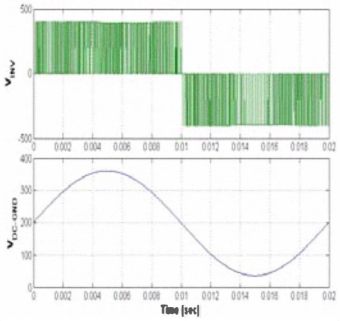

Topologies TL Comparison

Topologies derived from FB

• Actually both HERIC, H5, REFU and FB-DCBP topologies are converting the 2 level FB (or HB) inverter in a 3 level one.

• This increases the efficiency as both the switches and the output inductor are subject to half of the input voltage stress.

• The zero voltage state is achieved by shorting the grid using higher or lower switches of the bridge (H5) or by using additional ac bypass (HERIC or REFU) or dc bypass (FB-DCBP).

• H5 and HERIC are isolating the PV panels from the grid during zero voltage while REFU and FB-DCBP is clamping the neutral to the mid-point of the dc link.

• Both REFU and HERIC use ac by-pass but REFU uses 2 switches in anti- parallel and HERIC uses 2 switches in series (back to back). Thus the conduction losses in the ac-bypass are lower for the REFU topology.

• REFU and H5 have slightly higher efficiencies as they have only one switch switching with high-frequency while HERIC and FB_DCBP have two.

• FB-ZVR derives from HERIC but uses a different implementation of the bidirectional switch using a diode bridge and one switch. Constant Vpe but moderate high efficiency (lower than HERIC but higher than FB-UP). Can also work with non-unitary PF.

Topologies derived from NPC

•The classical NPC and its "variant" Conergy-NPC are both three-level topologies featuring the advantages of unipolar voltage across the filter, high efficiency due to disconnection of PV panels during zero-voltage state and practical no leakage due to grounded DC link mid-point.

• Due to higher complexity in comparison with FB-derived topology, these structures are typically used in three-phase PV inverters with ratings over 10 kW (mini-central).

Topologies Conclusion

❑The "race" for higher efficiency PV inverters has resulted in a large variety of "novel" transformerless topologies derived from H-Bridge with higher efficiency and lower CM/EMI (H5, HERIC)

❑ Equivalent high-efficiency can be achieved with 3-level topologies (ex NPC)

❑Today more than 70% of the PV inverters sold on the market are transformerless achieving 98% max conversion efficiency and 97.7% "european" (weighted) efficiency

❑ Further improvements in the efficiency can be achieved by using SiC MosFets. ISE Fraunhofer-Freiburg reported recently* 99% efficiency (25% reduction in switching + conduction losses)

❑ For 3-phase systems the trend is to use 3 independent controlled single-phase inverters like 3xH5 or 3xHERIC but 3FB-SC and 3NPC (not proprietary) are also present on the market. 3NPC achieve higher efficiency 98%

❑The general trend in PV topologies is "More Switches for Lower Losses"

*Source [Burger, B., Schmidt,H. "25 YEARS TRANFORMLESS INVERTERS" – Proceedings of PVSEC 2007]

Control Structure Overview

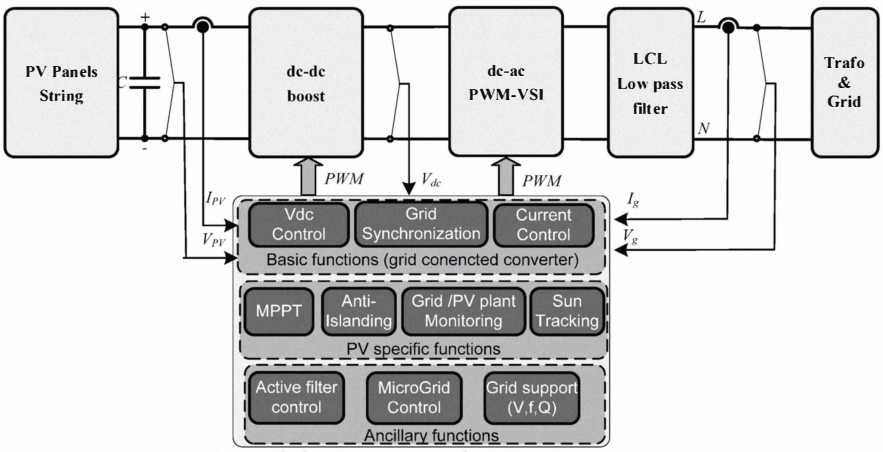

Basic functions – common for all grid-connected inverters

- Grid current control
  - THD limits imposed by standards
  - Stability in case of grid impedance variations
  - Ride-through grid voltage disturbances (not required yet!)
- DC voltage control
  - Adaptation to grid voltage variations
  - Ride-through grid voltage disturbances (optional yet)
- Grid synchronization
  - Required for grid connection or re-connection after trip.

PV specific functions – common for PV inverters

- Maximum Power Point Tracking – MPPT
  - Very high MPPT efficiency in steady state (typical > 99%)
  - Fast tracking during rapid irradiation changes (dynamical MPPT efficiency)
  - Stable operation at very low irradiation levels
- Anti-Islanding – AI as required by standards (VDE0126, IEEE1574, etc)
- Grid Monitoring
  - Operation at unity power factor as required by standards
  - Fast Voltage/frequency detection
- Plant Monitoring
  - Diagnostic of PV panel array
  - Partial shading detection
- Sun Tracking (mechanical MPPT)
  - 1-2 axis motion controler tracking of Sun

Ancillary Support – (future?)

- Voltage Control
- Fault Ride-through
- Power Quality
  - harmonics
  - unbalance

Control Structure for Dual-Stage

Typical control structure for dual-stage PV inverter

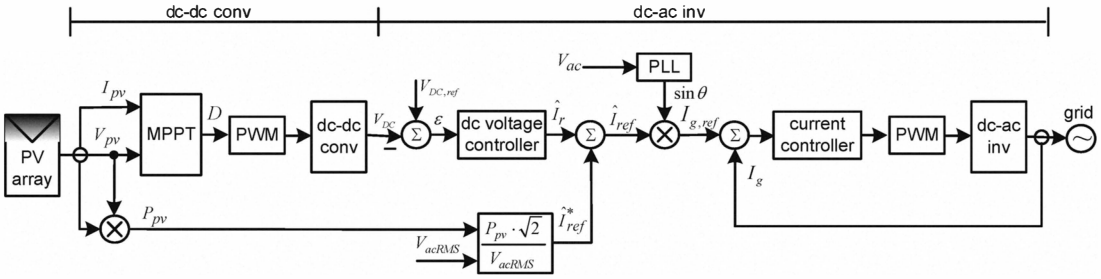

- The MPPT is implemented in the dc-dc boost converter.
- The output of the MPPT is the duty-cycle function. As the dc-link voltage V_{DC} is controlled in the dc-ac inverter the change of the duty-cycle will change voltage at the output of the PV panels, V_{PV} as:

$$V_{DC} = K\frac{V_{PV}}{1-D}$$

- The dc-ac inverter is a typical current controlled voltage source inverter (VSI) with PWM and dc-voltage controller.
- The power feed-forward requires communication between the two stages and improves the dynamics of MPPT

Control Structure for Single-Stage

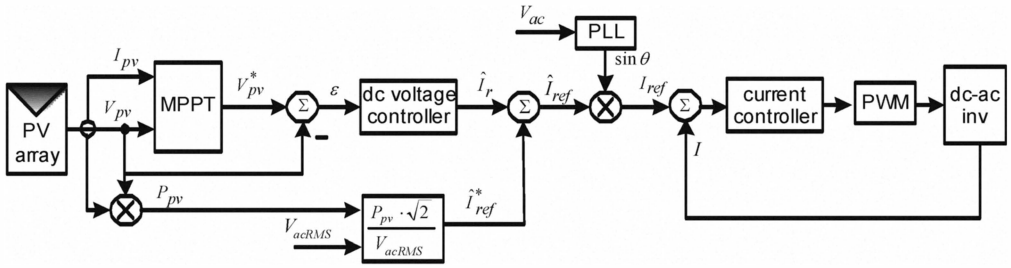

- In these topologies -which are becoming more and more popular in countries with low grid voltage (120V) like Japan and thus the voltage from the PV array is high enough- the MPPT is implemented in the dc-ac inverter
- Also in topologies with boost transformer on AC side (SMA)
- The output of the MPPT is the dc-voltage reference. The output of the dc-voltage controller is the grid current reference amplitude. The power feed-forward improves the dynamic response as MPPT runs at a slow sampling frequencies (typ. 1 Hz).
- A PLL is used to synchronize the current reference with the grid voltage

4556

Control Implementation

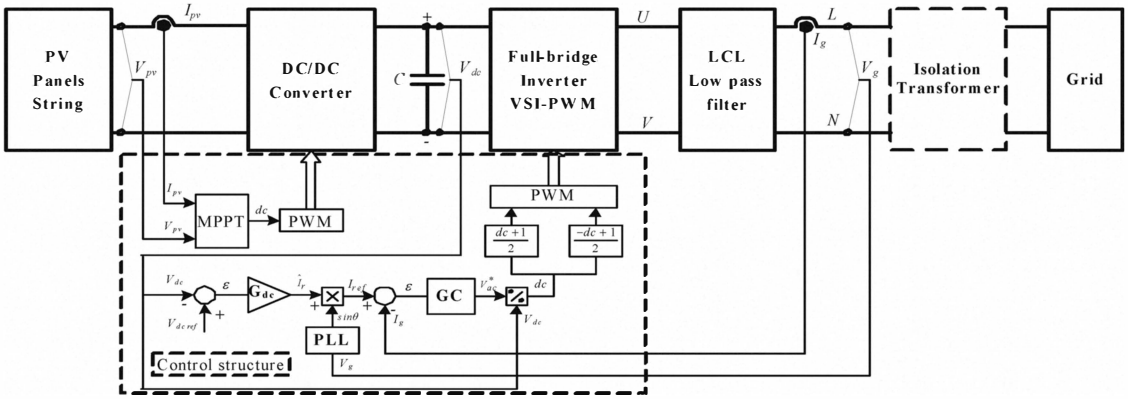

- The current controller Gc can be of PI or PR (Proportional Resonant) type
- Other non-linear controllers like hysteresis or predictive control can be used for current control
- The dc voltage controller can be P type due to the integration effect of the typical large capacitor

PI current control

- Typically PI controllers are used for the current loop in grid inverters
- Technical optimum design (damping 0.707 overshoot 5%)
- Implementation in synchronous frame (dq)

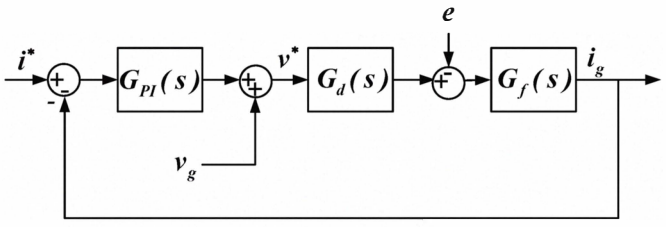

$$G_{PI}(s) = K_P + \frac{K_I}{s}$$

$$G_d(s) = \frac{1}{1+1.5T_s s}$$

$$G_f(s) = \frac{i(s)}{v(s)} = \frac{1}{R+Ls}$$

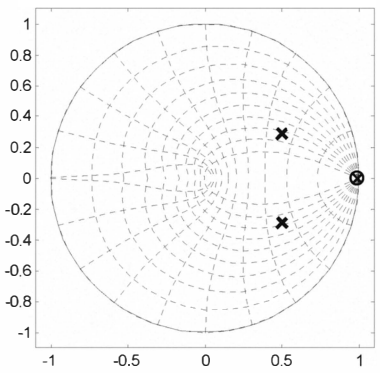

4557

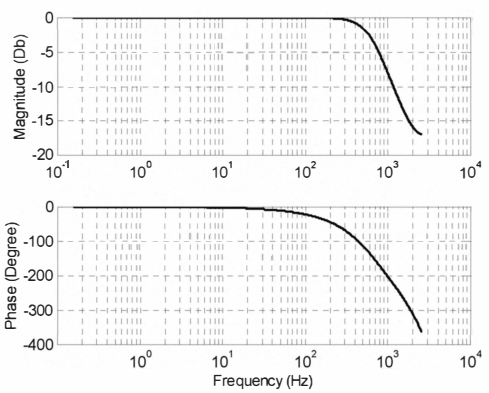

Shortcomings of PI controller

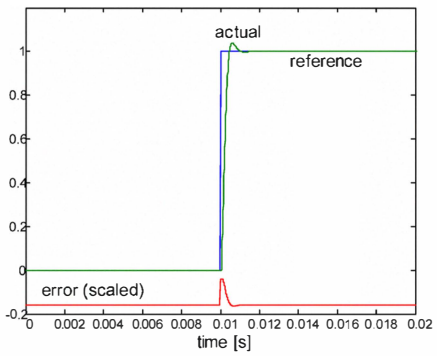

steady-state magnitude and phase error
limited disturbance rejection capability

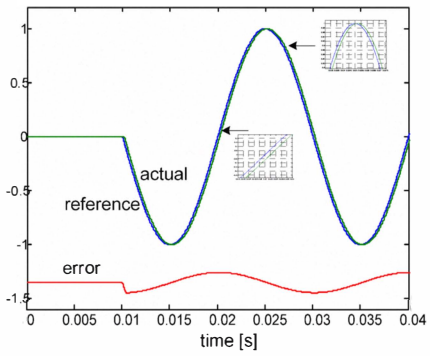

- When the current controlled inverter is connected to the grid, the phase error results in a power factor decrement and the limited disturbance rejection capability leads to the need of **grid feed-forward compensation**.
- However the imperfect compensation action of the feed-forward control due to the **background distortion** results in high harmonic distortion of the current and consequently non-compliance with international power quality standards.

Use of a PI controllers in single-phase systems

- an independent Q control is achieved
- a phase delay block create the virtual quadrature component that allows
- to emulate a two-phase system
- the v_b component of the command voltage is ignored for the calculation of the duty-cycle.

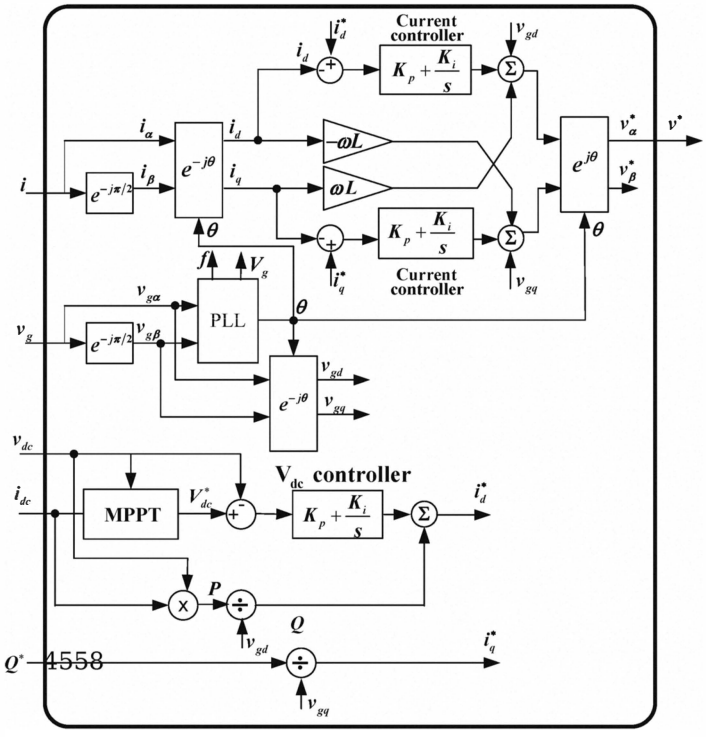

Resonant control

- Resonant control is based on the use of Generalized Integrator (GI)
- A double integrator achieves infinite gain at a certain frequency, called resonance frequency, and almost no attenuation outside this frequency

$$GI = \frac{s}{s^2 + \omega^2}$$

- The GI will lead to zero stationary error and improved and selective disturbance rejection as compared with PI controller

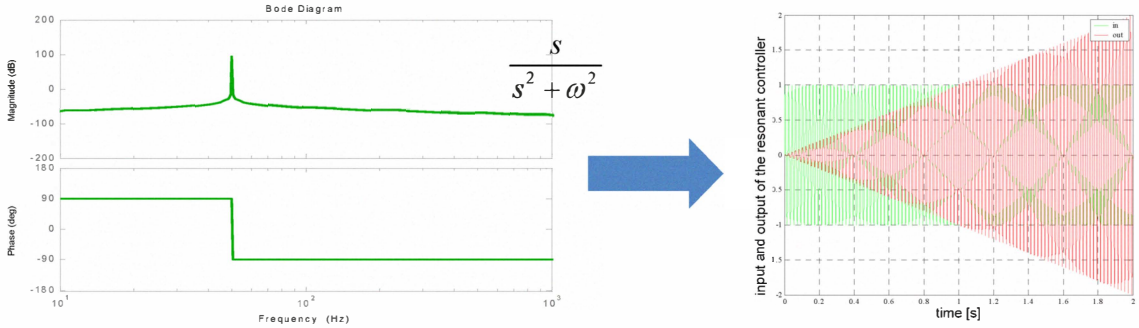

Resonant control

- The stability of the system should be taken into consideration
- The phase margin (PM) decreases as the resonant frequency approach to the crossover frequency

$$k_P + k_I \frac{s}{s^2 + \omega^2}$$

$$\left(k_P + k_I \frac{s}{s^2 + \omega^2}\right)\left(\frac{1}{R + Ls}\right)$$

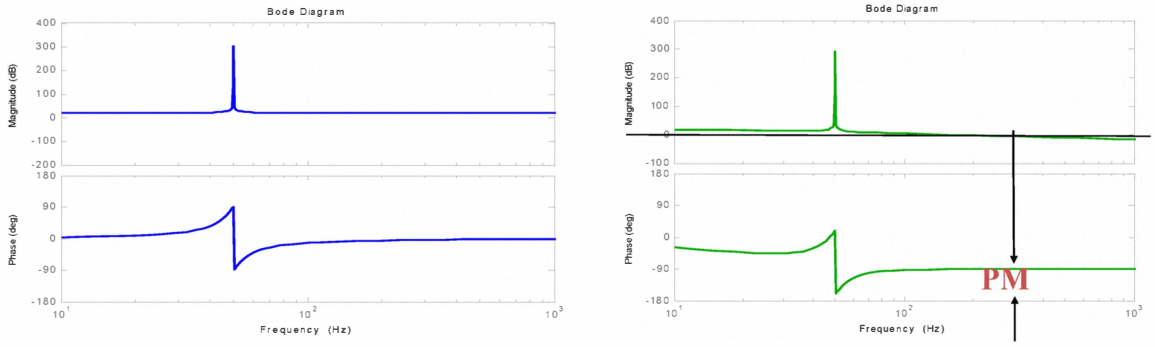

4559

Tuning of resonant control

• The gain *Kp* is found by ensuring the desired bandwidth using either rlocus Matlab function or SISOTOOL

•The integral constant *Ki* acts to eliminate the steady-state phase error.

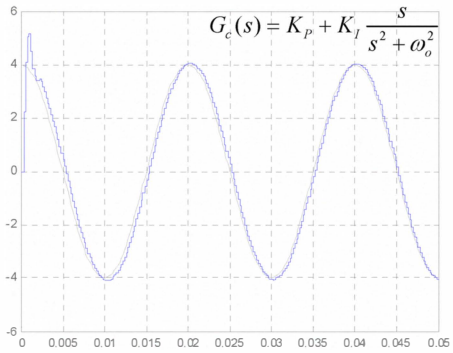

Ki = 100

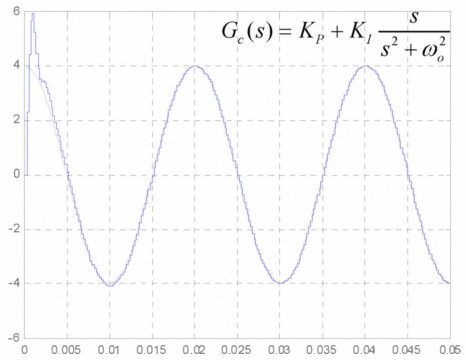

Ki = 500

- A higher *Ki* will "catch" the reference faster but with higher overshoot
- Another aspect is that *Ki* determines the bandwidth centered at the resonance frequency, in this case the grid frequency, where the attenuation is positive. Usually, the grid frequency is stiff and is only allowed to vary in a narrow range, typically ± 1%.

Harmonic compensation with resonant control

Besides single frequency compensation (obtained with the generalized integrator tuned at the grid frequency), selective harmonic compensation can also be achieved by cascading several resonant blocks tuned to resonate at the desired low-order harmonic frequencies to be compensated.

As an example, the transfer functions of a non-ideal harmonic compensator (HC) designed to compensate for the 3rd, 5th and 7th harmonics is reported

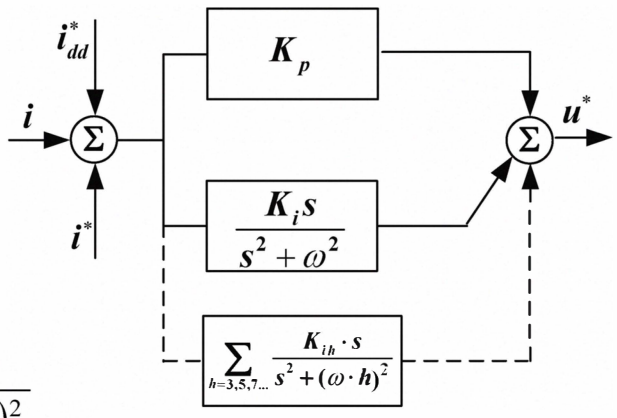

$$G_h(s) = \sum_{h=3,5,7} \frac{2K_{ih}\omega_c s}{s^2 + 2\omega_c s + (h\omega)^2}$$ 4560

Harmonic compensation with resonant control

Open-loop PR current control system with and without harmonic compensator

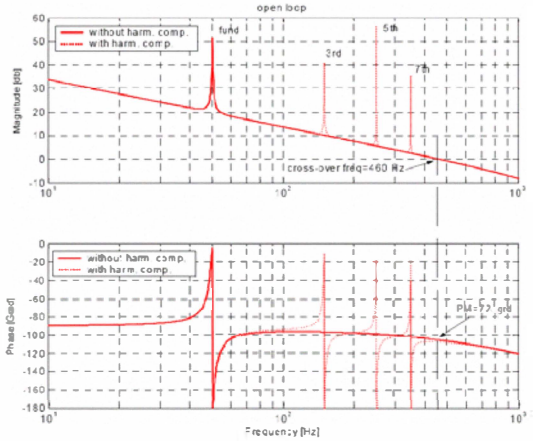

Closed loop PR current control system with and without harmonic compensator

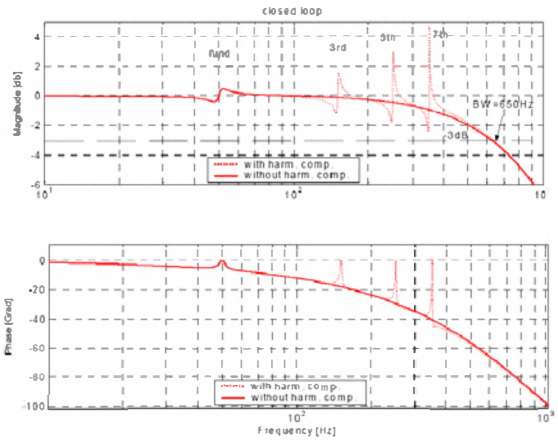

- Having added the harmonic compensator, the open-loop and closed-loop bode graphs changes as it can be observed with dashed line. The change consists in the appearance of gain peaks at the harmonic frequencies, but what is interesting to notice is that the **dynamics** of the controller, in terms of **bandwidth** and **stability margin remains unaltered**.

PI vs PR for single-phase grid inverter current control

The current loop of PV inverter with PI controller

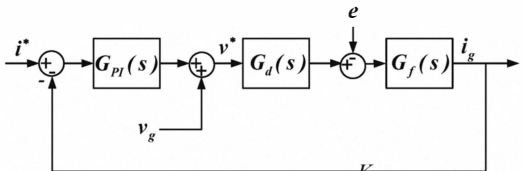

$$\text{PI} = G_{PI}(s) = K_P + \frac{K_I}{s}$$

The current loop of PV inverter with PR controller

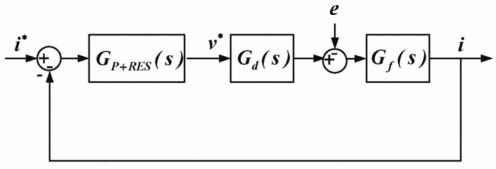

$$\text{PR} = G_c(s) = K_P + K_I \frac{s}{s^2 + \omega_o^2}$$

Inverter $G_d(s) = \dfrac{1}{sT_s + 1}$

Plant $G_f(s) = \dfrac{i_i(s)}{u_i(s)} = \dfrac{1}{L_{fi}s}\dfrac{\left(s^2 + z_{LC}^2\right)}{\left(s^2 + \omega_{res}^2\right)}$ $\quad z_{LC}^2 = \dfrac{1}{L_g C_f}$ $\quad \omega_{res}^2 = \dfrac{\left(L_g + L_i\right)\cdot z_{LC}^{\ 2}}{L_i}$

- No grid voltage feed-forward is required

4561

- GIs tuned to the low harmonics can be used for selective harmonic compensation by cascading the fundamental component GI without involving more transformations

Disturbance rejection comparison

Disturbance rejection (current error ratio disturbance) of the PR+HC, PR and P

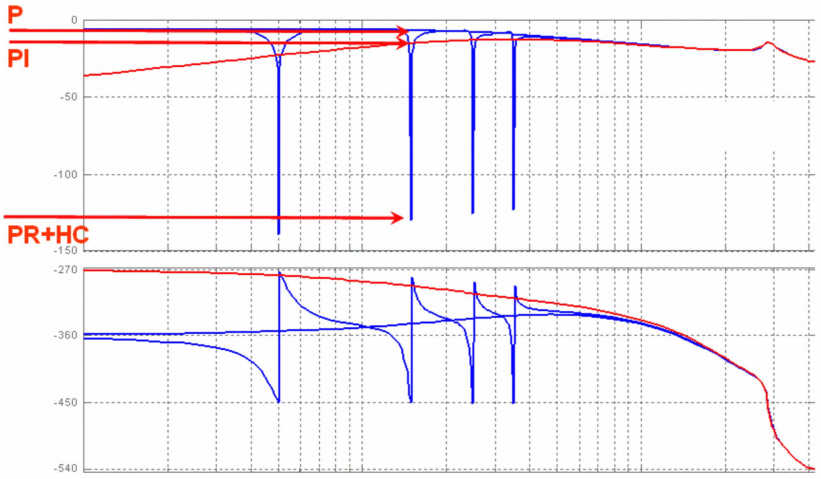

$$\left.\frac{\varepsilon(s)}{u_g(s)}\right|_{i_i^*=0} = \frac{-G_f(s)}{1+G_c(s)\cdot G_d(s)\cdot G_f(s)}$$

- Around the 5th and 7th harmonics the PR attenuation being around 125 dB and the PI attenuation only 8 dB. The PI rejection capability at 5th and 7th harmonic is comparable with that one of a simple proportional controller, the integral action being irrelevant
- PR +HC exhibits high performance harmonic rejections leading to very low current THD!

Experimental results - current harmonics in stationary

PI + Voltage-Feed-Forward (Kp=10, Ti=4Ts) THD = 12%,

PR+HC (Kp=10, Ki=1000, Ki3,5,7=1000) THD = 1.0%.

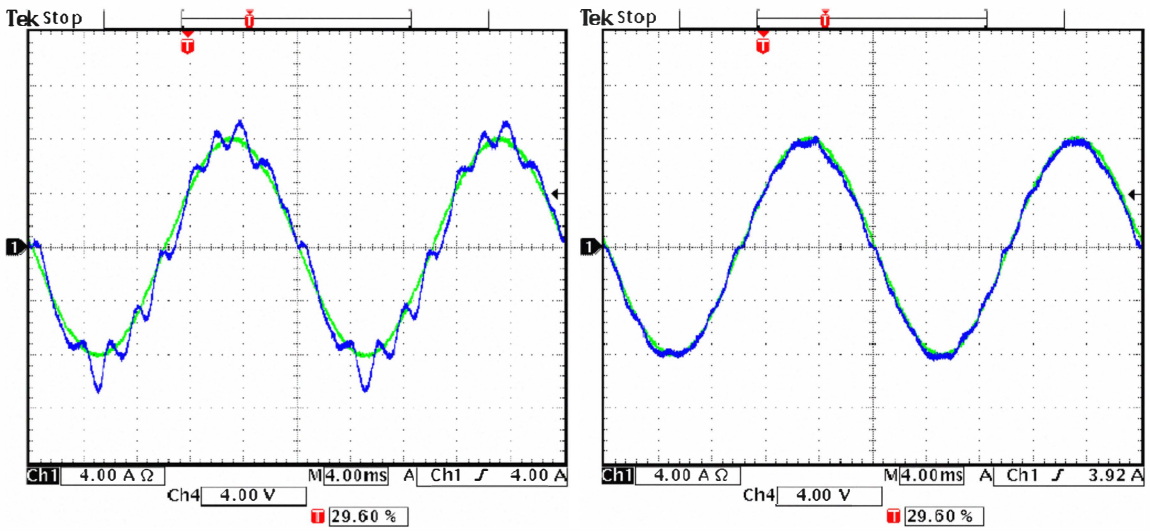

4562

Experimental results - current response at reference step

PI + Voltage-Feed-Forward (Kp=10, Ti=4Ts),
Overshoot = 100%

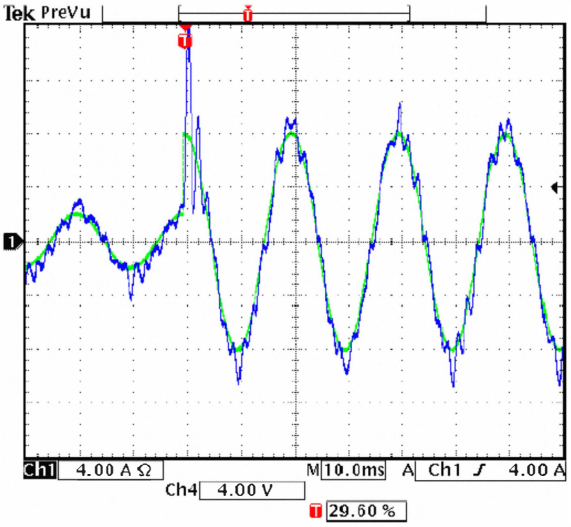

PR+HC (Kp=10, Ki=1000, Ki3,5,7=1000)
Overshoot = 0!

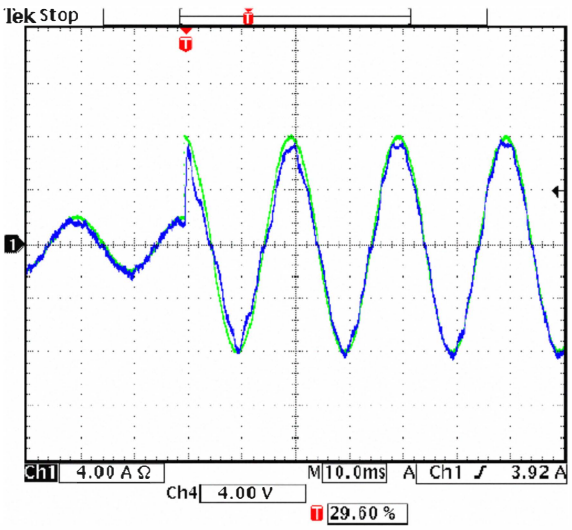

Control Structure - Conclusions

- The most typical control structure is the current controlled voltage source inverter with PWM
- Typically boost dc-dc converter is required
- The MPPT is a necessary feature in order to extract the maximum power from a panel array at any conditions of irradiation and temperature.
- PO and INC are the most used ones. PO+CV is also possible
- According to the topology (dual- or single-stage) the MPPT is implemented in the dc-dc converter or in the dc-ac inverter
- PR current controller better than PI control for sinusoidal references
- PLL is typically required for synchronization
- The Sun-tracking configurations are capable to provide significant increase in the energy production over fixed systems of equivalent characteristics, provided that the availability of the moving parts can be guaranteed and that mutual shading conditions are avoided.
- Key design for sun-tracking are the position and the type of sensor

4563

Grid Monitoring and Synchronization for PV Power Systems

Pedro Rodriguez
Technical University of Catalonia / Aalborg University
prodriguez@ee.upc.edu / pro@iet.aau.dk

Outline

- Grid monitoring
- PLL Basics
- PLL analysis
- Single-phase PLLs using quadrature signals
- PLLs using adaptive filters
- Three-phase PLLs
- Robust three-phase grid synchronization
- Conclusions

4564

Grid Monitoring

A PV inverter shall be designed to deliver power for a specified range of voltages and frequencies

- Monitoring is based on grid connection requirements
- The abnormal utility conditions of concern are voltage and frequency excursions above or below the values stated in the grid codes, and the complete disconnection of the utility, presenting the potential for a distributed resource island.

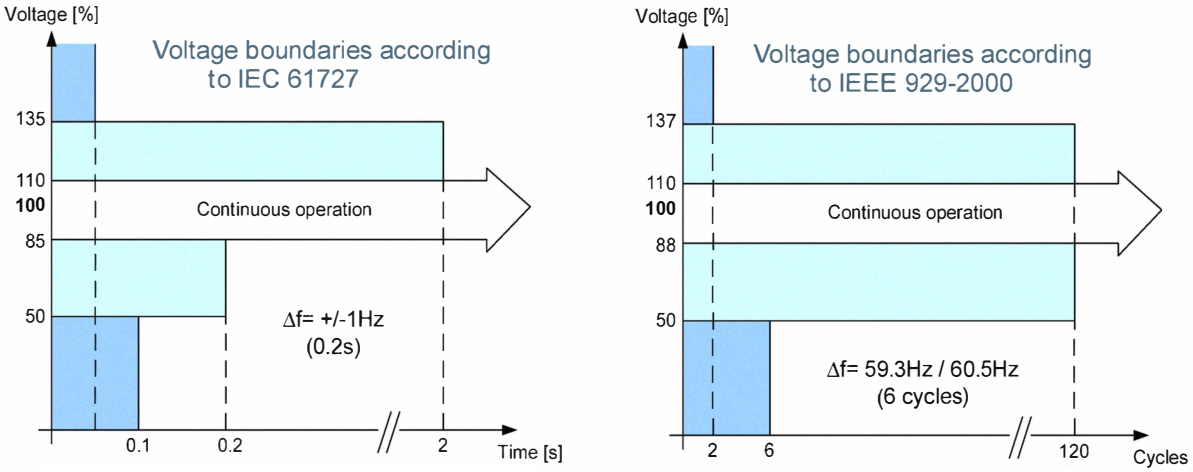

Grid Monitoring

Grid state and limits should be accurately detected

- Test signals are used to evaluate undervoltage, overvoltage, underfrequency, overfrequency, synchronization magnitude difference, synchronization frequency, difference, and synchronization phase difference (IEEE 1547.1-2005).

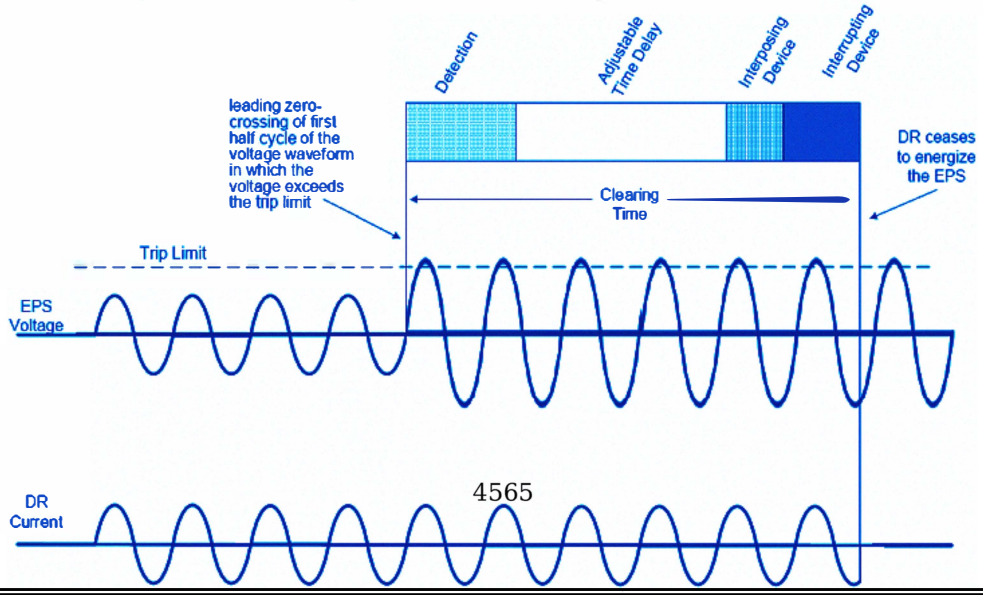

Grid Monitoring

Response of the PV power converter to abnormal grid conditions

- Voltage deviations

IEEE 1547		IEC61727		VDE0126-1-1	
Voltage range (%)	Disconnection time (s)	Voltage range (%)	Disconnection time (s)	Voltage range (%)	Disconnection time (s)
V < 50	0.16	V < 50	0.10	110 ≤ V < 85	0.2
50 ≤ V < 88	2.00	50 ≤ V < 85	2.00		
110 < V < 120	1.00	110 < V < 135	2.00		
V ≥ 120	0.16	V ≥ 135	0.05		

- Frequency deviations

IEEE 1547		IEC61727		VDE0126-1-1	
Frequency range (Hz)	Disconnection time (s)	Frequency range (Hz)	Disconnection time (s)	Frequency range (Hz)	Disconnection time (s)
59.3 < f < 60.5*	0.16	fn-1 < f < fn+1	0.2	47.5 < f < 50.2	0.2

- Reconnection after trip

IEEE 1547	IEC61727
88 < V < 110 [%] AND 59.3 < f < 60.5 [Hz]	85 < V < 110 [%] AND f_n-1 < f < f_n+1 [Hz] AND Min. delay of 3 minutes

Grid Monitoring

Line impedance estimation

- Active and passive detection methods are used for line impedance estimation
- Information from line impedance estimation is used in island mode detection, current control improving, grid faults detection and characterization.

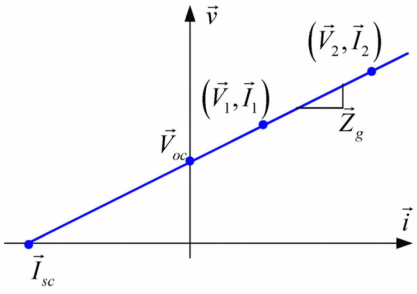

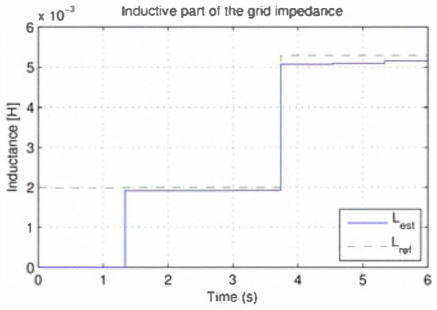

$$\vec{V}_1 = \vec{Z}_g \vec{I}_1 + \vec{V}_g \qquad \vec{V}_2 = \vec{Z}_g \vec{I}_2 + \vec{V}_g$$

$$\vec{Z}_g = \frac{\vec{V}_2 - \vec{V}_1}{\vec{I}_2 - \vec{I}_1}$$

$$R = \frac{(v_{d2} - v_{d1})(i_{d2} - i_{d1}) + (v_{q2} - v_{q1})(i_{q2} - i_{q1})}{(i_{d2} - i_{d1})^2 + (i_{q2} - i_{q1})^2}$$

$$\frac{4566}{\omega L} = \frac{(v_{d2} - v_{d1})(i_{q2} - i_{q1}) - (v_{q2} - v_{q1})(i_{d2} - i_{d1})}{(i_{d2} - i_{d1})^2 + (i_{q2} - i_{q1})^2}$$

Grid Monitoring

High penetration of PV inverter in LV distribution networks

- Line interaction of PV inverters is necessary to regulate the line voltage profile
- Fast and accurate grid monitoring is necessary to regulate the voltage profile in lines with multiple PV inverters.

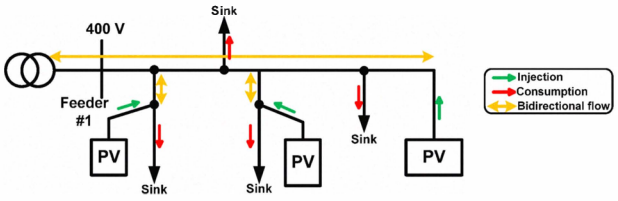

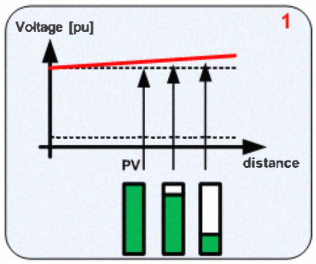

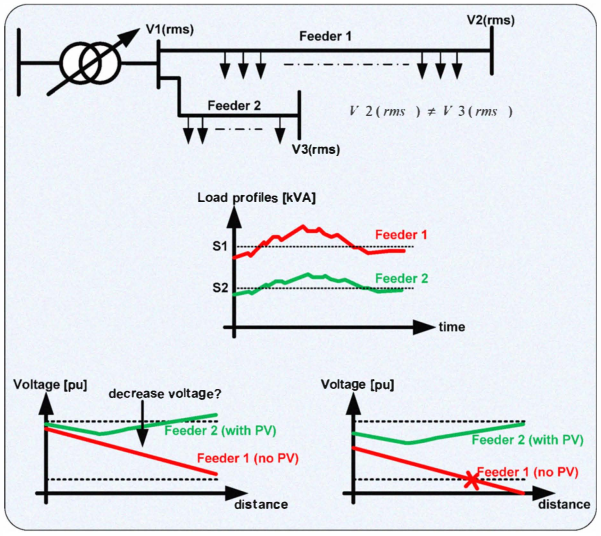

Grid Monitoring

Grid connection of PV inverters

Single-phase inverters up to 500W

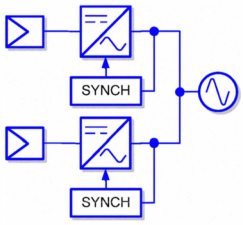

Single-phase inverters up to 1kW to 5kW

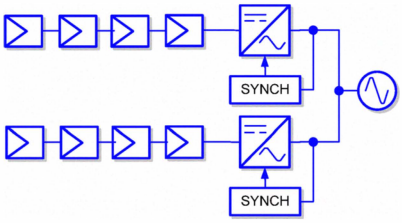

Three-phase inverters from 5kW to 30kW

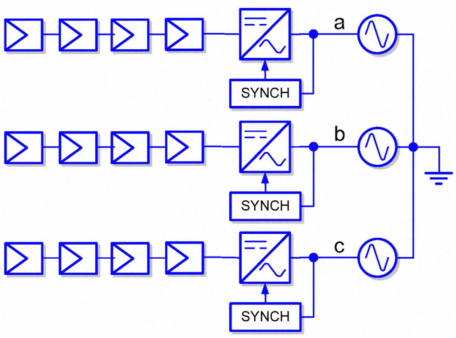

Three-phase inverters higher than 100kW

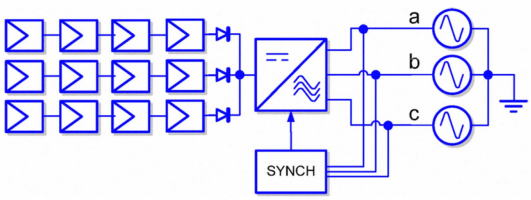

4567

Fourier Analysis [1]

Fourier stated that a generic periodic signal v(t) can be expressed by a sum of the following terms:

$$v(t) = a_0 + \sum_{n=1}^{\infty} \left(a_n \cos(n\omega t) + b_n \sin(n\omega t) \right)$$

where:

$$a_0 = \frac{1}{T} \int_0^T v(t)\, dt,$$

$$a_n = 2\frac{1}{T} \int_0^T v(t) \cos(n\omega t)\, dt = \frac{1}{\pi} \int_{\pi}^{\pi} v(\theta) \cos(n\theta)\, d\theta,$$

$$b_n = 2\frac{1}{T} \int_0^T v(t) \sin(n\omega t)\, dt = \frac{1}{\pi} \int_{\pi}^{\pi} v(\theta) \sin(n\theta)\, d\theta.$$

Adaptive filter based on Fourier series decomposition :

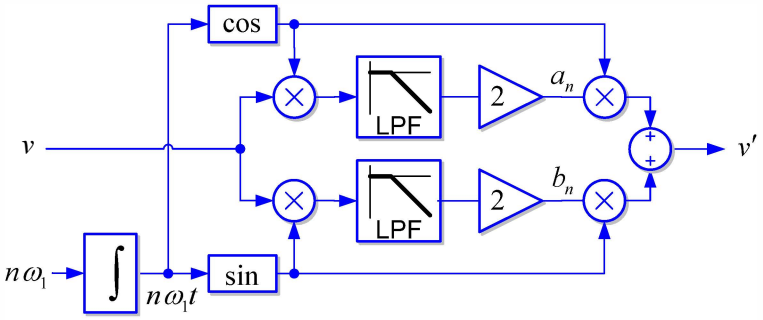

$$\vec{V}_n' = V_n \angle \theta_n \begin{cases} V_n = \sqrt{a_n^2 + b_n^2} \\ \theta_n = \arctan \dfrac{b_n}{a_n} \end{cases}$$

Discrete Fourier Analysis

Complex compact form of Fourier series: $v(t) = \sum_{n=-\infty}^{\infty} c_n e^{jn\omega t}$

Fourier transform: $V(\omega) = \mathcal{F}[v(t)] = \int_{-\infty}^{\infty} v(t) e^{-j\omega t} dt$

Discrete Fourier transform (DFT): $V[n] = \sum_{k=0}^{N-1} v[k] \cdot e^{-j2\pi \frac{k}{N} n}$

Recursive Discrete Fourier transform (RDFT):

$$\left.\begin{aligned} V[n]\big|_{k_S-1} &= \sum_{k=k_S-N}^{k_S-1} v[k] \cdot e^{-j2\pi \frac{k}{N} n} \\ V[n]\big|_{k_S} &= \sum_{k=k_S-N+1}^{k_S} v[k] \cdot e^{-j2\pi \frac{k}{N} n} \end{aligned}\right\} \quad V[n]\big|_{k_S} = V[n]\big|_{k_S-1} + v[k_S] \cdot e^{-j2\pi \frac{k_S}{N} n} - v[k_S - N] \cdot e^{-j2\pi \frac{k_S - N}{N} n} \;\because\; e^{-j2\pi \frac{k_S - N}{N} n} = e^{-j2\pi \frac{k_S}{N} n}$$

$$V[n]\big|_{k_S} = V[n]\big|_{k_S-1} + \left(v[k_S] - v[k_S - N]\right) \cdot e^{-j2\pi \frac{k_S}{N} n}$$

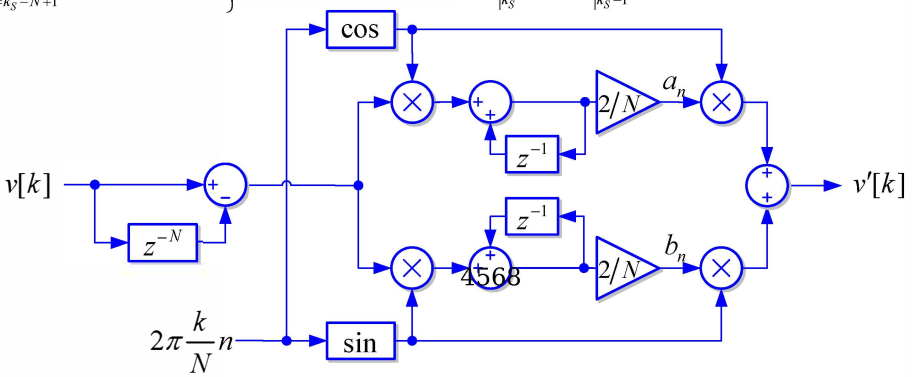

Grid Synchronization

Grid monitoring and synchronization: two close concepts

- Grid synchronization of a power converter is not but a instantaneous monitoring of the state of the grid in which the power converter is connected to.
- Grid synchronization is an adaptive process by means of which an internal reference signal generated by the control algorithm of a grid-connected power converter is brought into line with a particular grid variable, usually the fundamental component of the grid voltage.
- Many biological processes are synchronized to environmental events. Actually, most of us schedule our daily activities phase-locking timing information supplied by a clock.

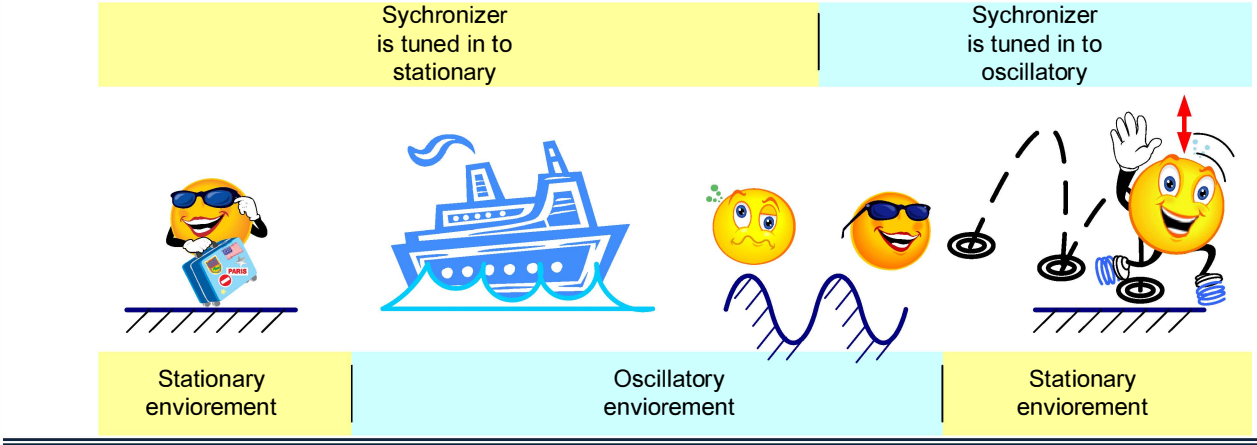

Grid Synchronization

Grid monitoring under abnormal grid conditions: crucial matter

- Under regular operating, phase currents and voltages of a power converter connected to a AC systems will swing back and forth with a steady, uninterrupted rhythm set by the grid voltage.
- Grid synchronization under abnormal grid conditions however is not a crucial matter. Under transient grid faults, it is necessary indentify the grid voltage components of interest and to set a proper control strategy to interact with the grid under such adverse operating conditions.
- Any mistake in synchronization will result in uncontrolled exchange of energy between the power and the grid, which can gives rise to overvoltage, overcurrent, overload, overstress, etc… and finally tripping of protections to disconnect the generator from the grid.

Tutorial on Power Electronics for PV Power Systems Integration, ISIE 2010, 4 July 2010, Bari

PLL basis

Basic idea of synchronization based on a phase-locked loop:

- Phase-locked technology is broadly used in military, aerospace, consumer electronics systems where some kind of feedback is used to synchronize some local periodic event with some recognizable external event
- Many biological processes are synchronized to environmental events. Actually, most of us schedule our daily activities phase-locking timing information supplied by a clock.
- A grid connected power converter should phase-lock its internal oscillator to the grid voltage (or current), i.e., an amplitude and phase coherent internal signal should be generated.

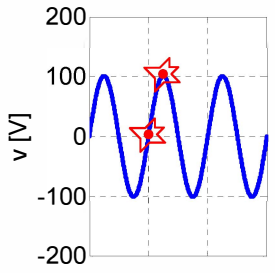

Event based synchronization
(simple, discontinuous, …)

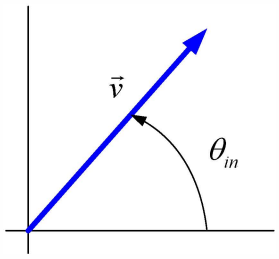

Phase-locked synchronization
(continuous, predictive,…)

PLL basis

Basic blocks:

- Phase Detector (PD). This block generates an output signal proportional to the phase difference between its two input signals. Depending on the type of PD, high frequency ac components appear together the dc phase difference signal.
- Loop Filter (LF). This block exhibits low pass characteristic and filters out the high frequency ac components from the PD output. Typically this is a 1-st order LPF or PI controller.
- Voltage Controlled Oscillator (VCO). This block generates at its output an ac signal whose frequency varies respect a central frequency as a function of the input voltage.

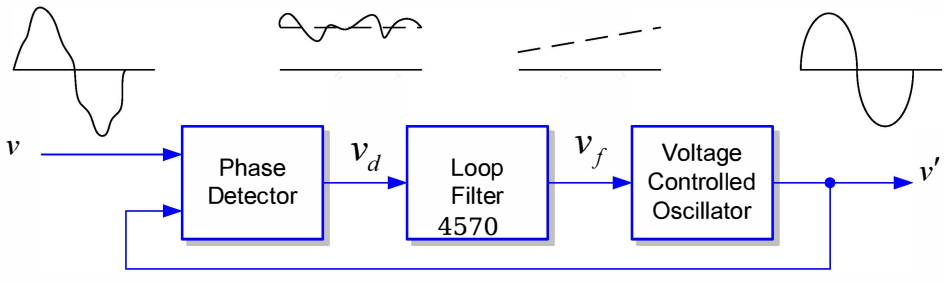

PLL basis

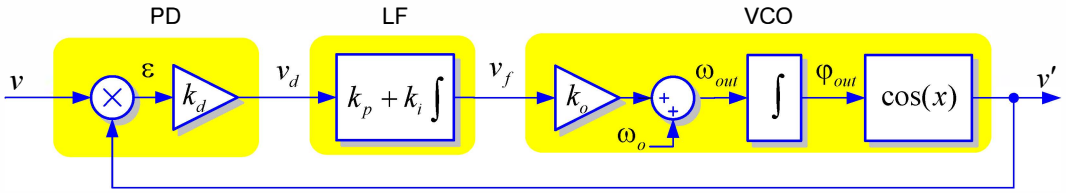

Phase Detector:

Input signal: $v = A\sin\left(\omega_{in}t + \theta_{in}\right)$

VCO output: $v' = \cos\left(\omega_{out}t + \theta_{out}\right)$

Multiplier PD output:

$$v_d = Ak_d \sin\left(\omega_{in}t + \theta_{in}\right)\cos\left(\omega_{out}t + \theta_{out}\right)$$

$$v_d = \frac{Ak_d}{2}\left[\sin\left(\left(\omega_{in} - \omega_{out}\right)t + \left(\theta_{in} - \theta_{out}\right)\right) + \sin\left(\left(\omega_{in} + \omega_{out}\right)t + \left(\theta_{in} + \theta_{out}\right)\right)\right]$$

We are only interested in the 'dc' term between, whereas the term at twice the center frequency should be canceled out by the LF.

$$\overline{v}_d = \frac{Ak_d}{2}\sin\left(\left(\omega_{in} - \omega_{out}\right)t + \left(\theta_{in} - \theta_{out}\right)\right)$$

Let the VCO is tuned with the input frequency, that is $\omega_{in} \approx \omega_{out}$

$$\overline{v}_d = \frac{Ak_d}{2}\sin\left(\theta_{in} - \theta_{out}\right)$$

PLL basis

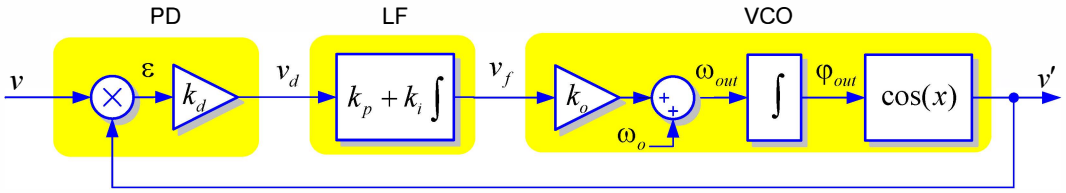

Small signal linearized PD response:

The multiplier PD produces a non-linear phase detection because the sinusoidal function

$$\overline{v}_d = \frac{Ak_d}{2}\sin\left(\theta_{in} - \theta_{out}\right)$$

Let $\theta_{in} \approx \theta_{out}$, so: $\sin\left(\theta_{in} - \theta_{out}\right) \approx \left(\theta_{in} - \theta_{out}\right)$

. Therefore : $\overline{v}_d \approx \frac{Ak_d}{2}\left(\theta_{in} - \theta_{out}\right)$

This equation represents the small signal linearized model of the multiplier PD. Therefore, in the locked state, the multiplier PD represents a zero-order block with gain which is dependent on the input signal amplitude.

Small signal model of the VCO: $\overline{\omega}_{out} = \left(\omega_{out} + \Delta\overline{\omega}_{out}\right) = \left(\omega_o + k_o\overline{v}_f\right) = \omega_{in}$; $\tilde{\omega}_{out} = k_o\tilde{v}_f$

$$\tilde{\theta}_{out}(t) = \int\tilde{\omega}_{out}dt = \int k_o\tilde{v}_f dt$$

Linearized small signal PLL model

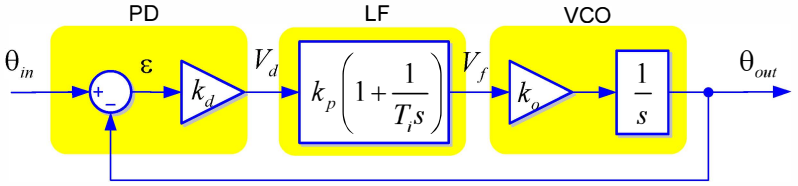

It will be assumed further that K_d=K_o=1 (typically)

$$V_d(s)=\frac{A}{2}\left(\Theta_{in}(s)-\Theta_{out}(s)\right) \qquad V_f(s)=k_p\left(1+\frac{1}{T_i s}\right)V_d(s) \qquad \Theta_{out}(s)=\frac{1}{s}V_f(s)$$

Transfer functions:

Open Loop Phase Transfer Function: $$F_{OL}(s)=\frac{LF(s)}{s}=\frac{K_p\left(1+\frac{1}{T_i s}\right)}{s}=\frac{k_p s+\frac{k_p}{T_i}}{s^2}$$

Closed Loop Phase Transfer Function: (low-pass) $$H_\theta(s)=\frac{\Theta_{out}(s)}{\Theta_{in}(s)}=\frac{LF(s)}{s+LF(s)}=\frac{K_p s+\frac{K_p}{T_i}}{s^2+K_p s+\frac{K_p}{T_i}}$$

Closed Loop Error Transfer Function: (high-pass) $$E_\theta(s)=\frac{V_d(s)}{\Theta_{in}(s)}=1-H_\theta(s)=\frac{s}{s+LP(s)}=\frac{s^2}{s^2+K_p s+\frac{K_p}{T_i}}$$

Linearized small signal PLL model

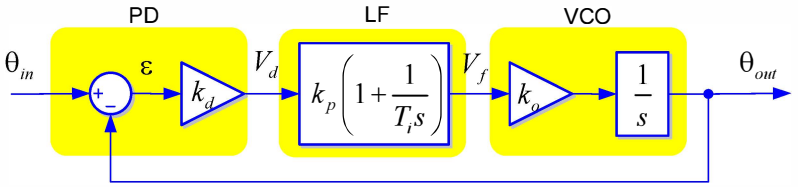

Tuning:

General form of second order transfer functions:

$$H_\theta(s)=\frac{2\zeta\omega_n s+\omega_n^2}{s^2+2\zeta\omega_n s+\omega_n^2} \qquad E_\theta(s)=\frac{s^2}{s^2+2\zeta\omega_n s+\omega_n^2} \qquad \omega_n=\sqrt{\frac{K_p}{T_i}};\quad \xi=\frac{\sqrt{K_p T_i}}{2}$$

Standard specifications for second order systems without zeros as a rough approximation that should give a 5% overshoot at step response

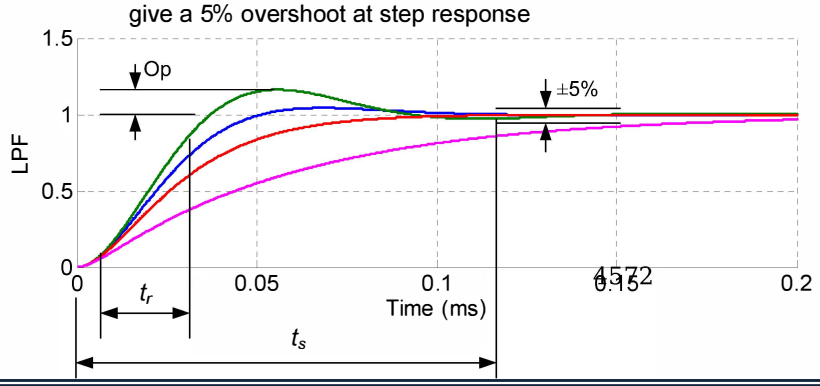

$$\xi=\frac{1}{\sqrt{2}}$$

$$t_s=\frac{4.6}{\xi\omega_n} \quad ; \quad t_r=\frac{1.8}{\omega_n}$$

$$K_p=2\xi\omega_n \; ; \quad T_i=\frac{2\xi}{\omega_n}$$

$$K_p=\frac{9.2}{t_s} \quad ; \quad T_i=\frac{t_s\xi^2}{2.3}$$

Basic PLL model response

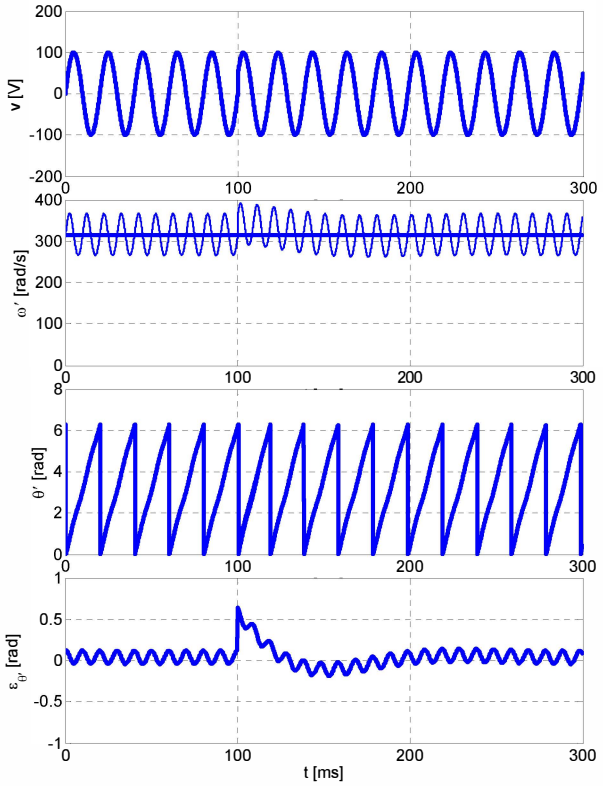

$$\xi = \frac{1}{\sqrt{2}} \quad ; \quad t_s = 100ms$$

$$\xi = \frac{1}{\sqrt{2}} \quad ; \quad \omega_n = 10.34Hz$$

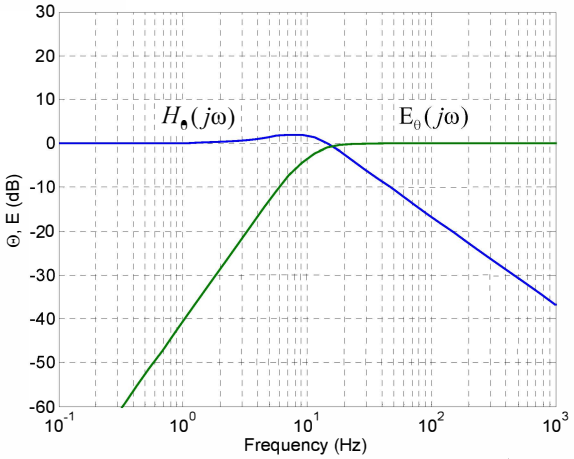

$$\omega_{3dB} = \omega_n \left[1 + 2\xi^2 + \sqrt{\left(1 + 2\xi\right)^2 + 1} \right]^{1/2}$$

$$\xi = \frac{1}{\sqrt{2}} \quad ; \quad \omega_{3dB} = 2.06\omega_n$$

Basic PLL model response

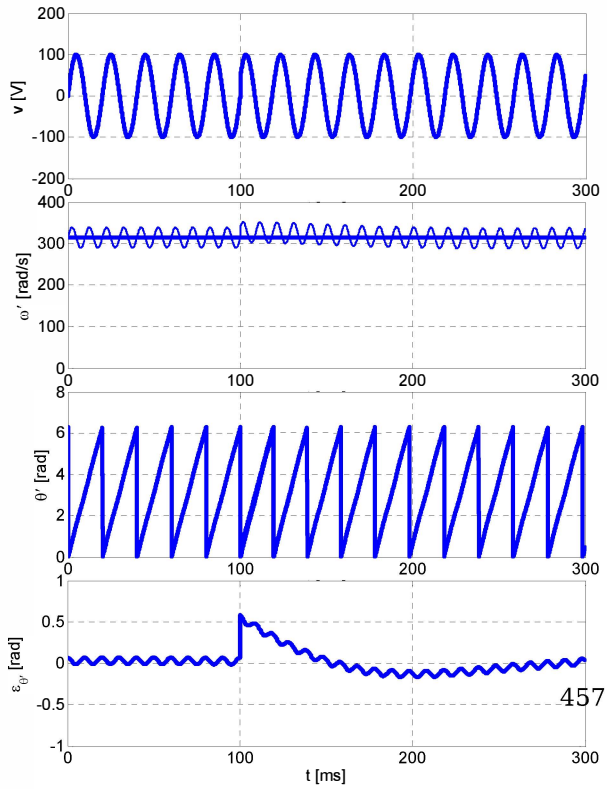

$$\xi = \frac{1}{\sqrt{2}} \quad ; \quad t_s = 200ms$$

$$\xi = \frac{1}{\sqrt{2}} \quad ; \quad \omega_n = 5.17Hz$$

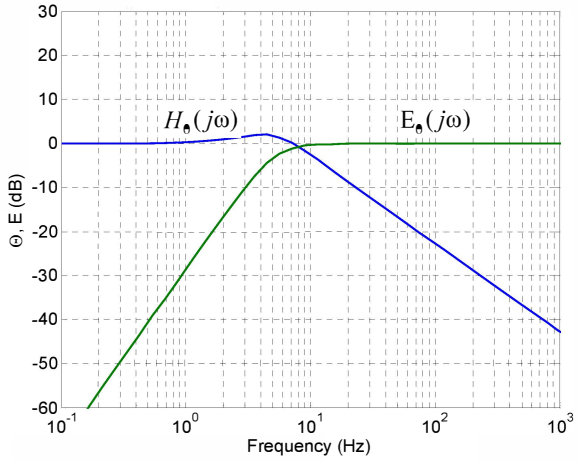

$$\omega_{3dB} = \omega_n \left[1 + 2\xi^2 + \sqrt{\left(1 + 2\xi\right)^2 + 1} \right]^{1/2}$$

$$\xi = \frac{1}{\sqrt{2}} \quad ; \quad \omega_{3dB} = 2.06\omega_n$$

4573

Key parameters of the PLL [2]

- The hold range $\Delta\omega_H$ is the frequency range at which a PLL is able to maintain lock statically.

$$\Delta\omega_H = K_o K_d LF(0)$$

For the PI, *LF(0)*=∞ and the hold range is only limited by the frequency range of the VCO

- The pull-in range $\Delta\omega_P$ is the frequency range at which a PLL will always became locked, but the process can become rather slow. For the PI loop filter this range trends to infinite.

Pull-in time:

$$T_P \approx \frac{\pi^2}{16}\frac{\Delta\omega_{in}^2}{\xi\omega_n^3}$$

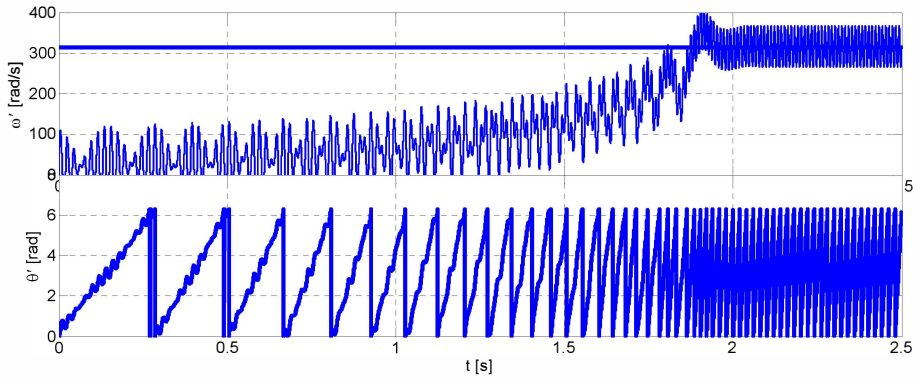

- The lock range $\Delta\omega_L$ is the frequency range within which a PLL locks within one-single beat note between the reference frequency and the output frequency.

$$\Delta\omega_L \approx 2\xi\omega_n \approx 2\xi\sqrt{\frac{k_p}{T_i}} \qquad \text{Lock-in time: } T_L \approx \frac{2\pi}{\omega_n}$$

PLL with orthogonal input signals

Even though input frequency is locked, multiplier PD gives rise to oscillations in the detected phase-angle error signal at twice the input frequency.

LF bandwidth should be limited in order to attenuate oscillations at $\omega_{in}+\omega_{out}$ in the detected phase-angle error signal.

From orthogonal sinusoidal signals we have:

$$V\sin(\omega_{in}+\theta_{in})\cos(\omega_{out}+\theta_{out}) - V\cos(\omega_{in}+\theta_{in})\sin(\omega_{out}+\theta_{out}) = V\sin\left((\omega_{in}-\omega_{out})t+(\theta_{in}-\theta_{out})\right)$$

Assuming operation in the lock rang, i.e., $\omega_{in}=\omega_{out}$: $v_d = V\sin(\theta_{in}-\theta_{out})$

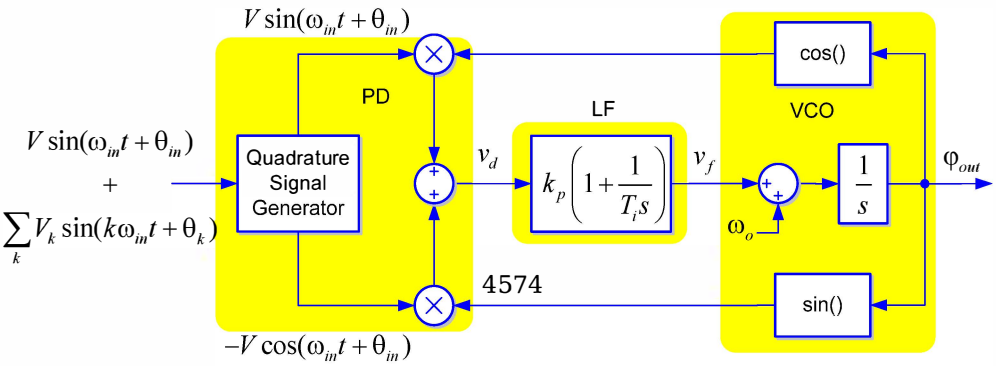

PLL performance

- Specifications: $\hat{V} = 100V \;;\; t_S = 100ms \;;\; \xi = 1/\sqrt{2}$
- Controller parameters: $K_p = \frac{9.2}{t_s} = 92000 \;;\; K_p' = \frac{k_p}{\hat{V}} = 920 \quad ; \quad T_i = \frac{t_s \xi^2}{2.3} = 0.217$
- PLL parameters: $\omega_n = \frac{k_p}{2\xi} = 65.05 \text{ rad/s} \;;\; \omega_{3dB} \approx 2.06\omega_n = 134 \text{ rad/s}$
- Pull-in time: $T_P \approx \frac{\pi^2}{16} \frac{\Delta\omega_{in}^2}{\xi\omega_n^3} = 0.3127\text{s}$

The PD output in the start up is given by: $v_d = V\sin\left(\left(\omega_{in} - \omega_o\right)t + \left(\theta_{in} - \theta_{out}\right)\right) = V\sin\left(\Delta\omega t + \left(\theta_{in} - \theta_{out}\right)\right)$

If LF output was equal zero, the VCO would keep at its central frequency ω_o and the PLL would never pull-in. Actually LF is not zero but a small signal with frequency $\Delta\omega$. Therefore, the VCO output is frequency modulated. Consequently $\Delta\omega$ is not a constant and the VCO is nonharmonically frequency modulated.

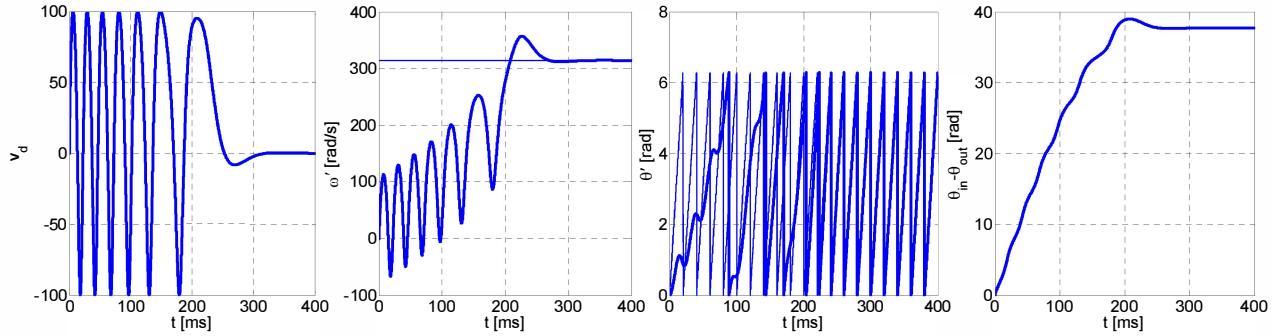

PLL performance

- Lock range and time:

$\Delta\omega_L \approx 2\xi\omega_n = \pm 92 \text{ rad/s}$

$T_L \approx \frac{2\pi}{\omega_n} = 0.096 \text{ s}$

e.g. $\Delta\omega_{in} = -62.83 \text{ rad/s}$

- Pull-out range:

$\Delta\omega_{PO} \approx 1.8\omega_n\left(\xi + 1\right)$

$\approx 199.89 \text{ rad/s}$

Locking inside the pull-out range

e.g. $\Delta\omega_{in} = -188.49 \text{ rad/s}$

Locking outside the pull-out range

e.g. $\Delta\omega_{in} = -219.91 \text{ rad/s}$

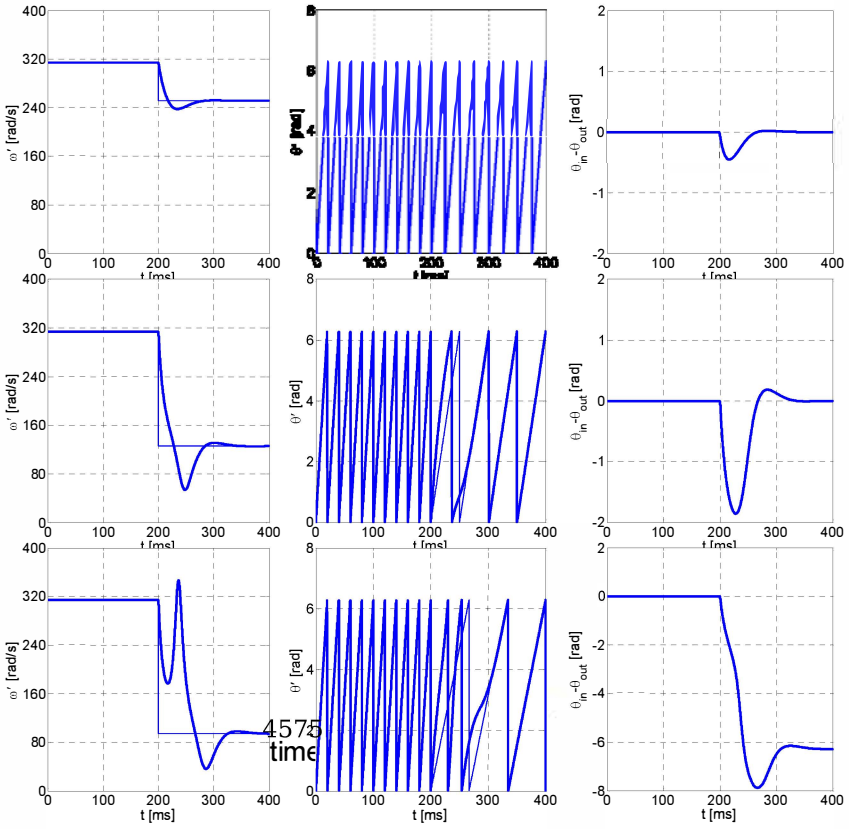

4575
time

Park transformation in the PD

Park transformation:

$$\begin{bmatrix} v_d \\ v_q \end{bmatrix} = \begin{bmatrix} \cos(\varphi_{out}) & \sin(\varphi_{out}) \\ -\sin(\varphi_{out}) & \cos(\varphi_{out}) \end{bmatrix} \begin{bmatrix} v_\alpha \\ v_\beta \end{bmatrix} \qquad \begin{bmatrix} v_\alpha \\ v_\beta \end{bmatrix} = V \begin{bmatrix} \sin(\varphi_{in}) \\ -\cos(\varphi_{in}) \end{bmatrix}$$

$$\begin{bmatrix} v_d \\ v_q \end{bmatrix} = V \begin{bmatrix} \sin(\varphi_{in})\cos(\varphi_{out}) - \cos(\varphi_{in})\sin(\varphi_{out}) \\ -\sin(\varphi_{in})\sin(\varphi_{out}) - \cos(\varphi_{in})\cos(\varphi_{out}) \end{bmatrix} = V \begin{bmatrix} \sin(\varphi_{in} - \varphi_{out}) \\ -\cos(\varphi_{in} - \varphi_{out}) \end{bmatrix}$$

Assuming $\omega_{in}=\omega_{out}$:

$$\begin{bmatrix} v_d \\ v_q \end{bmatrix} = V \begin{bmatrix} \sin(\theta_{in} - \theta_{out}) \\ -\cos(\theta_{in} - \theta_{out}) \end{bmatrix}$$

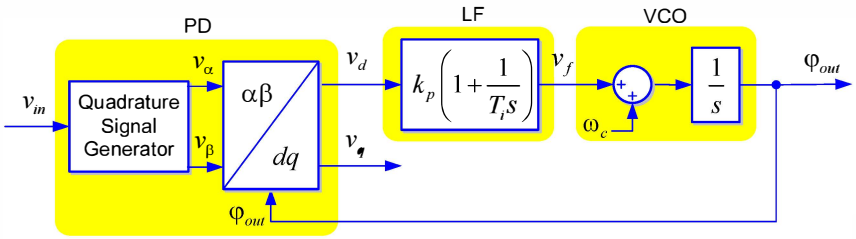

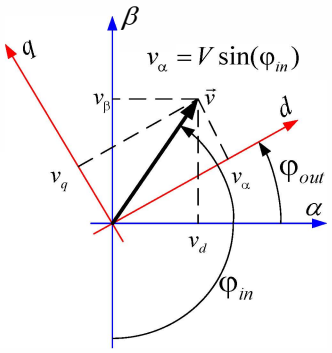

QSG based on transport delay

Transport Delay T/4

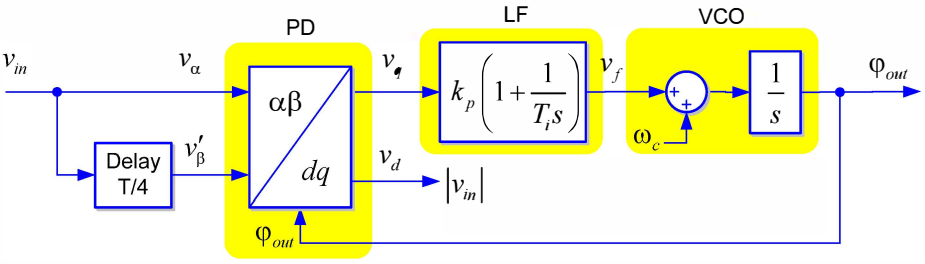

- The transport delay block is easily implemented through the use of a first-in-first-out (FIFO) buffer, with size set to one fourth the number of samples contained in one cycle of the fundamental frequency.
- This method works fine for fixed grid frequency. If the grid frequency is changing with for ex +/-1 Hz, then the PLL will produce an error
- If input voltage consists of several frequency components, orthogonal signals generation will produce errors because each of the components should be delayed one fourth of its fundamental period.

QSG based on Hilbert transform

Hilbert transform [3]

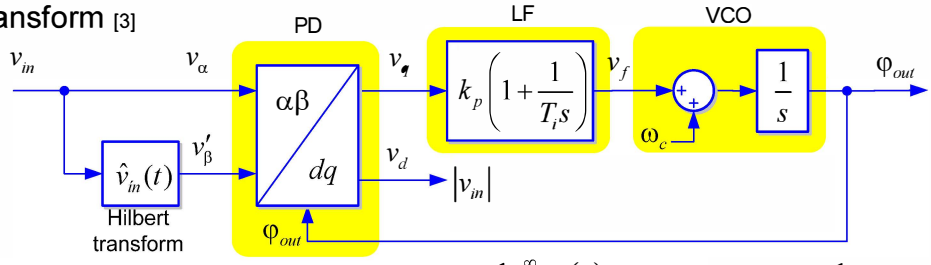

- Time domain Hibert transform: $\hat{g}(t)=\frac{1}{\pi}\int_{-\infty}^{\infty}\frac{g(\tau)}{t-\tau}d\tau \quad \Leftrightarrow \quad \hat{g}(t)=\frac{1}{\pi t}*g(t)$

$$hilbert\left(e^{jkt}\right)=\frac{1}{\pi}\int_{-\infty}^{\infty}\frac{e^{jk\tau}}{t-\tau}d\tau=-je^{jkt}\Big|_{k>0}$$

$$hilbert\left(\sin(kt)\right)=hilbert\left(\frac{e^{jkt}-e^{-jkt}}{2j}\right)=-\frac{e^{jkt}+e^{-jkt}}{2}=-\cos(kt)$$

$$\sin(kt)\rightarrow-\cos(kt)\rightarrow-\sin(kt)\rightarrow\cos(kt)\rightarrow\sin(kt)$$

- Hilbert transform is also called a “quadrature filter”.

Fourier transform: $F\left(\frac{1}{\pi t}\right)=-j\,sign(f)\begin{cases}-j & for \quad f>0\\ +j & for \quad f<0\end{cases}$

QSG based on inverse Park transform

Inverse Park transform [4]

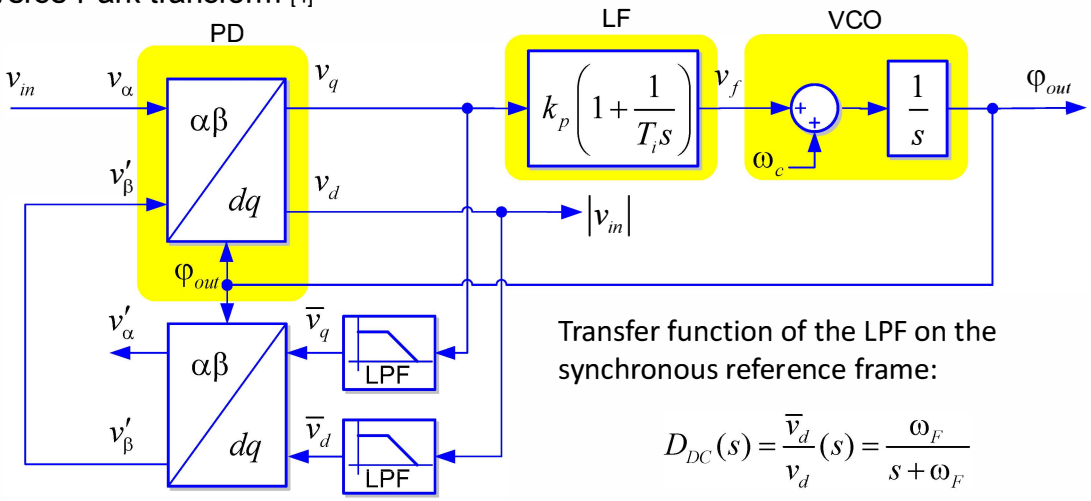

Transfer function of the LPF on the synchronous reference frame:

$$D_{DC}(s)=\frac{\bar{v}_d}{v_d}(s)=\frac{\omega_F}{s+\omega_F}$$

Transfer function of the LPF on the stationary reference frame:

$$B_{AC}(s)=\frac{V_\beta'}{V_\alpha}(s)=\frac{k\omega_o^2}{s^2+sk\omega_o+\omega_o^2}\quad;\quad k=\frac{\omega_f}{\omega_o}$$

$$\left.\begin{aligned}v'_\alpha&=\bar{v}_d\cos(\omega' t)-\bar{v}_q\sin(\omega' t)\\ v'_\beta&=\bar{v}_d\sin(\omega' t)+\bar{v}_q\cos(\omega' t)\end{aligned}\right\}V_\alpha'(s)=\frac{s}{\omega_o}V_\beta'(s)$$

4577

$$A_{AC}(s)=\frac{V_\alpha'}{V_\alpha}(s)=\frac{sk\omega_o}{s^2+sk\omega_o+\omega_o^2}\quad;\quad k=\frac{\omega_f}{\omega_o}$$

F(s) from synchronous to stationary

synchronous reference frame

$$D_{DC}(s) = \frac{\overline{v}_d}{v_d}(s) = \frac{\omega_F}{s + \omega_F}$$

stationary reference frame

$$A_{AC}(s) = \frac{V_\alpha'}{V_\alpha}(s) = \frac{sk\omega_o}{s^2 + sk\omega_o + \omega_o^2}$$

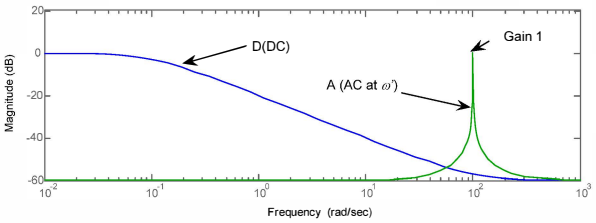

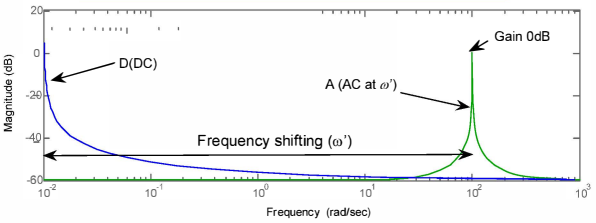

Frequency and time response:

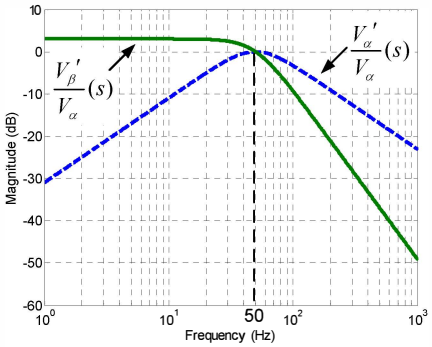

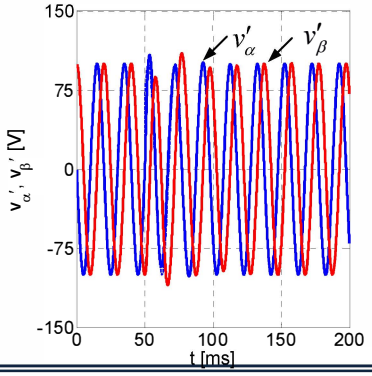

Adaptive Filtering

Adaptive Noise Cancellation [5]

- An adaptive filter is a filter that has the ability of adjust its own parameters automatically according to an optimization algorithm.
- Adactive Noise Cancelling (ANC) is an application of adaptive filtering, in which an auxiliary reference signal n1, correlated to the primary noise signal n0, is adaptively filtered to produce an output signal that is as close a replica as possible of n0. This output signal is subtracted from the primary input. As a result, the primary noise n0 is eliminated by cancellation.
- When the ANC technique is used to cancel out specific frequency components of the input signal, this filtering concept is also called Adaptive Notch Filtering (ANF)

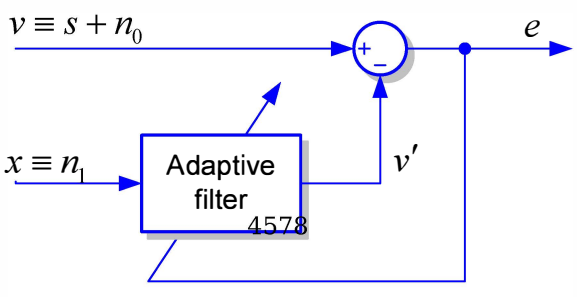

ANC based on the LMS algorithm [6]

The most extended adaptation algorithm used to set the weights of the adaptive filter is the least-mean-squares (LMS) algorithm.

- Reference signal vector: $\mathbf{x}_k = [x_k, x_{k-1}, ..., x_{k-N}]$
- Weights vector: $\mathbf{w}_k = [w_k, w_{k-1}, ..., w_{k-N}]$
- LMS algorithm:

$$v'_k = \mathbf{w}_k^T \cdot \mathbf{x}_k \;;$$
$$e_k = v_k - v'_k \;;$$
$$\mathbf{w}_{k+1} = \mathbf{w}_k + \alpha e_k \mathbf{x}_k$$

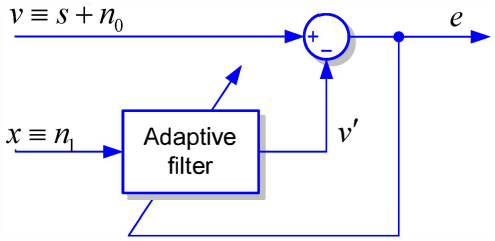

- estimate of the negative gradient: $e_k \cdot \mathbf{x}_k$
- Adaptation gain: α

Schematic representation of a very simple LMS algorithm with only one weight:

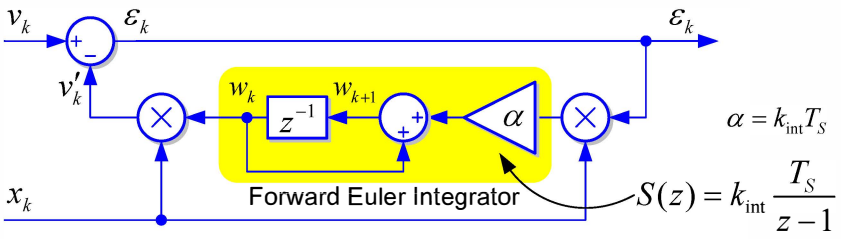

Enhanced PLL (ANF+PLL) [7]

Adaptive Notch Filter + Conventional PLL -> Enhanced PLL

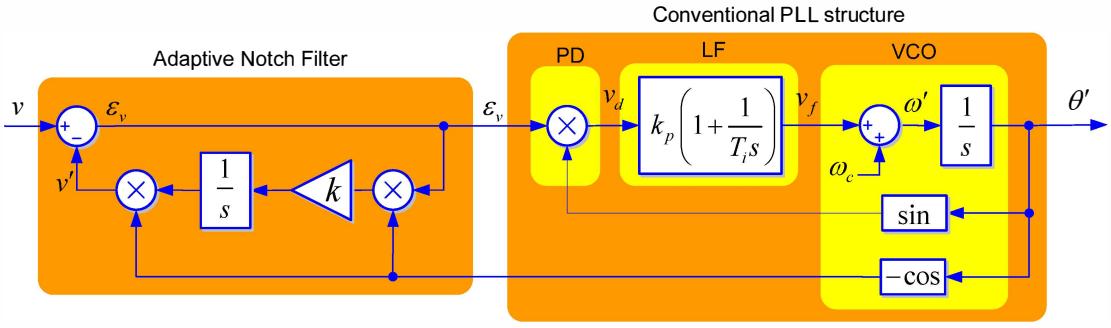

EPLL response:

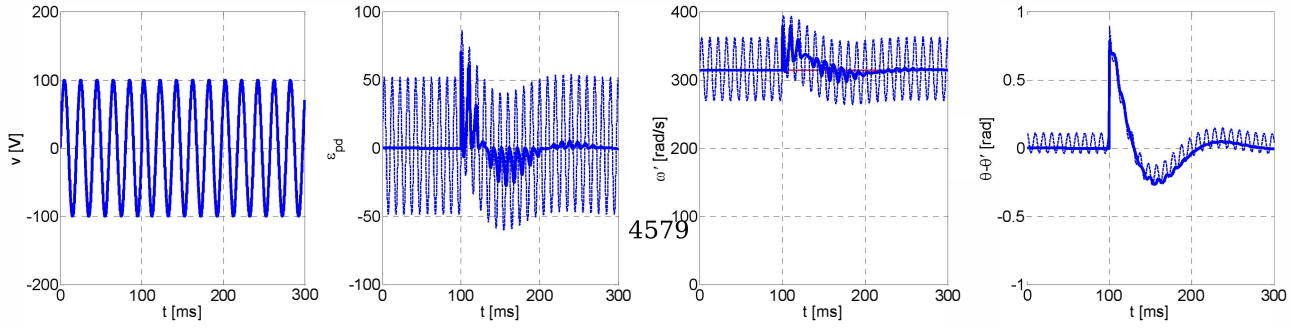

Single Frequency ANC (ANF) with Two Weights

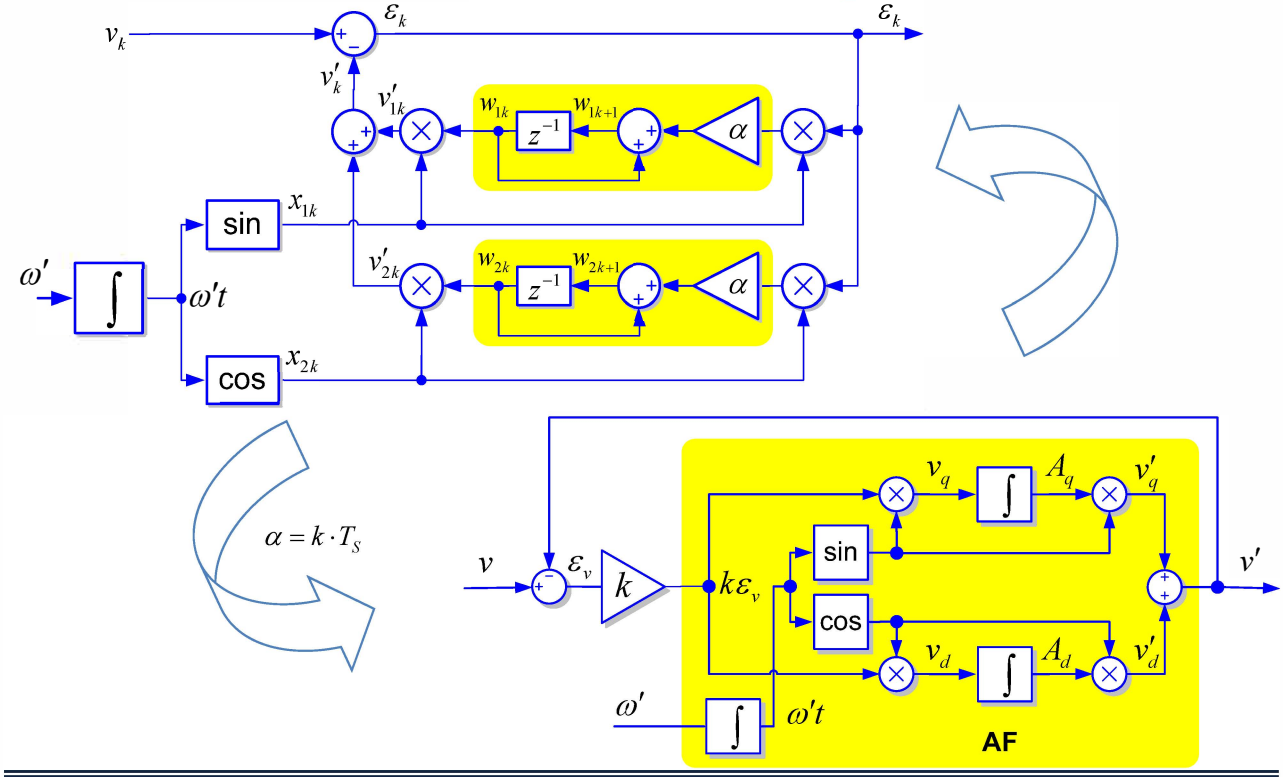

Adaptive Noise Filter

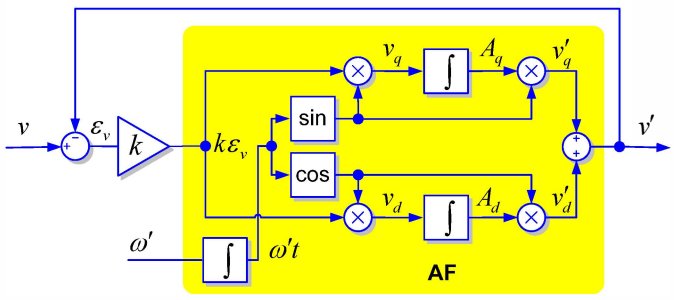

Transfer function of the AF:

$$AF(s) = \frac{v'}{k\varepsilon_v}(s) = \frac{s}{s^2 + \omega'^2}$$

The AF as a resonator with infinite gain for any sinusoid with frequency ω' applied to its input.

Development:

Defining $g = k\varepsilon_v$

$$v_d = g\cos(\omega' t) = \frac{1}{2} g\left[e^{j\omega' t} + e^{-j\omega' t}\right] \qquad v_q = g\sin(\omega' t) = \frac{1}{j2} g\left[e^{j\omega' t} - e^{-j\omega' t}\right]$$

$$A_d(s) = \frac{1}{s} v_d(s) = \frac{1}{2s}\left[g(s + j\omega' t) + g(s - j\omega' t)\right] \qquad A_q(s) = \frac{1}{s} v_q(s) = \frac{1}{j2s}\left[g(s + j\omega' t) - g(s - j\omega' t)\right]$$

$$v'_d(s) = \frac{1}{2}\left[A_d(s + j\omega' t) + A_d(s - j\omega' t)\right] = \frac{1}{4(s + j\omega')}\left[g(s) + g(s + 2j\omega')\right] + \frac{1}{4(s - j\omega')}\left[g(s) + g(s - 2j\omega')\right],$$

$$v'_q(s) = \frac{1}{2j}\left[A_q(s + j\omega' t) - A_q(s - j\omega' t)\right] = \frac{1}{4(s + j\omega')}\left[g(s) - g(s + 2j\omega')\right] + \frac{1}{4(s - j\omega')}\left[g(s) - g(s - 2j\omega')\right].$$

$$v'(s) = v'_d(s) + v'_q(s) = \frac{s}{s^2 + \omega'^2} g(s)$$

The Generalized Integrator [8][9]

The GI is a mathematical concept that stems from the principle that the time-domain convolution product of a function by itself gives rise to the original function multiplied by the time variable.

$$GI(s) = \frac{s}{s^2 + \omega'^2}$$

This transfer function will act as an 'amplitude integrator' for any sinusoid with frequency ω' applied to its input

Resulting adaptive filter:

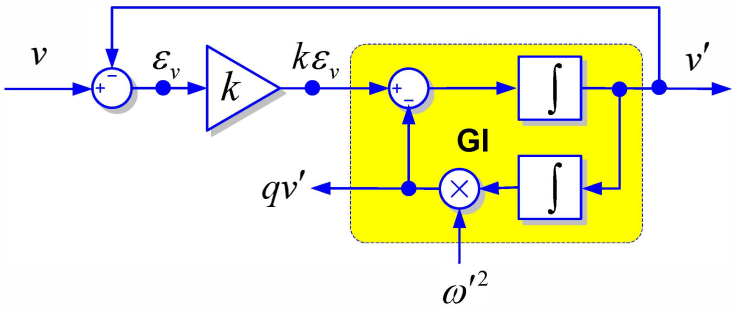

$$D(s) = \frac{v'}{v}(s) = \frac{ks}{s^2 + ks + \omega'^2}$$

$$Q(s) = \frac{qv'}{v}(s) = \frac{k\omega'^2}{s^2 + ks + \omega'^2}$$

v' and qv' signals are in-quadrature. However, the GI is not the most suitable choice to implement a frequency-variable adaptive filter, since both the bandwidth and the static gain of D(s) and Q(s) are not only a function of the gain k, but they also depend on the center frequency of the filter.

Second Order Generalized Integrator (SOGI)[10]

The SOGI, an alternative generalized integrator is proposed to achieve the following transfer function:

$$SOGI(s) = \frac{\omega' s}{s^2 + \omega'^2}$$

Resulting adaptive filter:

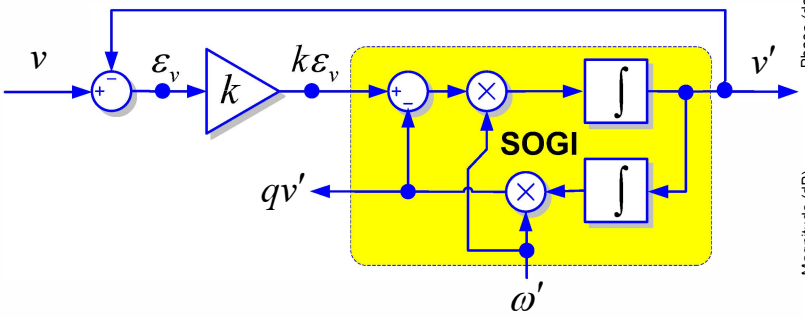

$$D(s) = \frac{v'}{v}(s) = \frac{k\omega' s}{s^2 + k\omega' s + \omega'^2}$$

$$Q(s) = \frac{qv'}{v}(s) = \frac{k\omega'^2}{s^2 + k\omega' s + \omega'^2}$$

$$t_{s(AF)} = \frac{10}{k\omega'}$$

$$\xi = \frac{1}{\sqrt{2}}$$

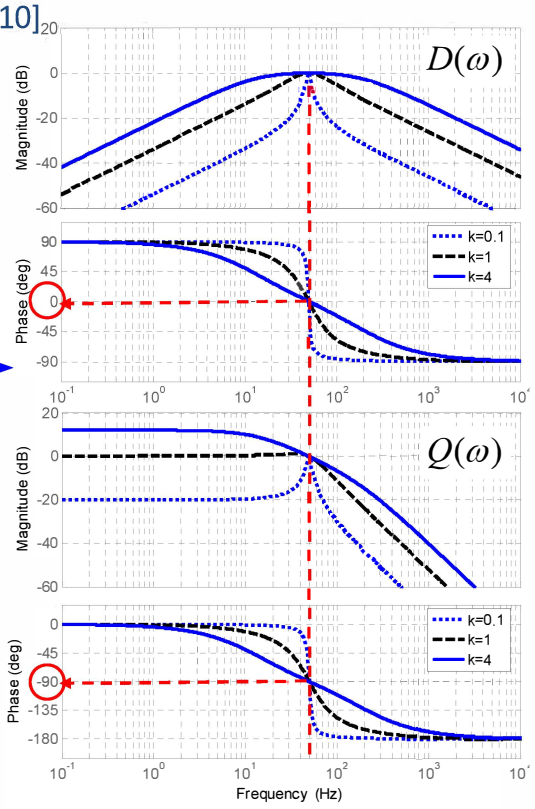

The SOGI-PLL [11]

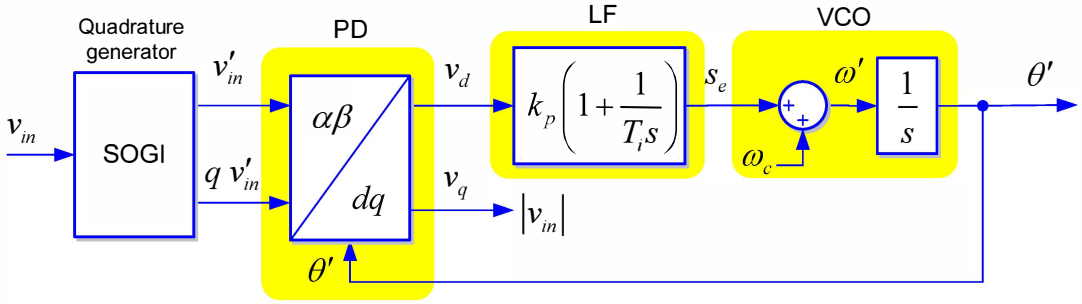

SOGI-PLL response:

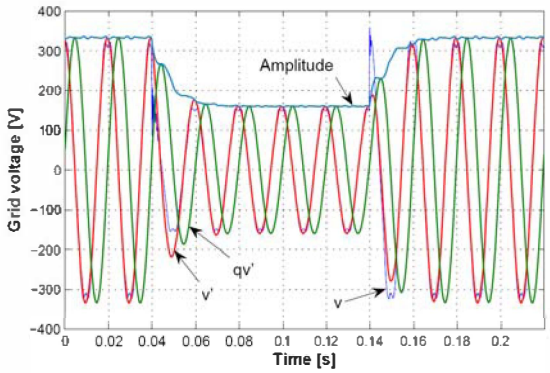

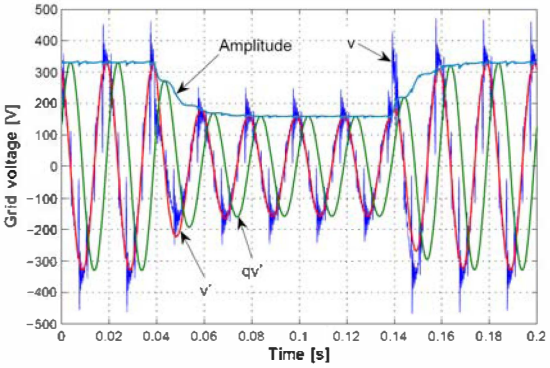

The Frequency-Locked Loop (FLL) [12]

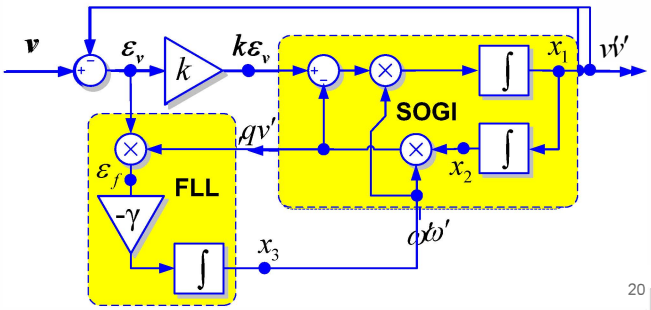

$$D(s)=\frac{v'}{v}(s)=\frac{k\omega' s}{s^2+k\omega' s+\omega'^2}$$

$$Q(s)=\frac{qv'}{v}(s)=\frac{k\omega'^2}{s^2+k\omega' s+\omega'^2}$$

$$E(s)=\frac{\varepsilon_v}{v}(s)=\frac{s^2+\omega'^2}{s^2+k\omega' s+\omega'^2}$$

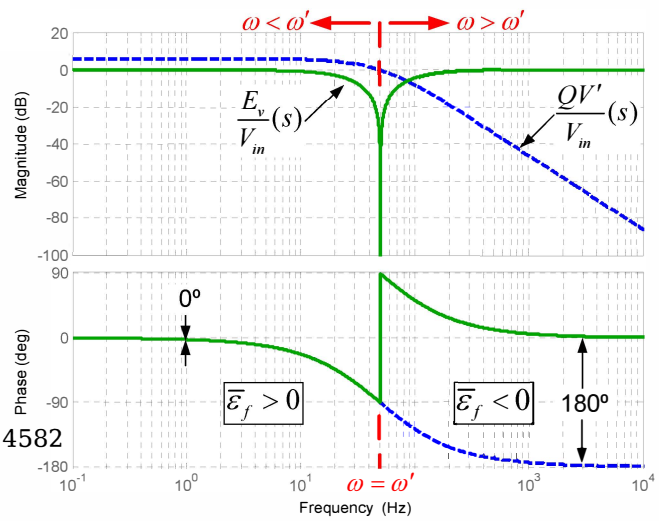

• If a frequency error variable e_f is defined as the product of qv' by e_v, the average value of e_f will be positive when w<w' , zero when w=w' and negative when w>w'.

• An integral controller with a negative gain -g, can be used to make zero the dc component of e_f by shifting the AF resonance frequency w' until matching the input frequency w.

Feedback based linearization of the FLL [13]

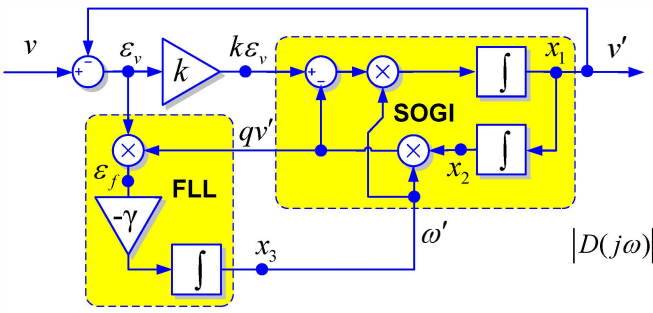

·Steady state response for a sinusoidal input

· $v = V\sin(\omega t + \phi)$ when the FLL is out of tuning

$$\bar{\mathbf{y}}' = \begin{bmatrix} v' \\ qv' \end{bmatrix} = V\left|D(j\omega)\right| \begin{bmatrix} \sin\left(\omega t + \phi + \angle D(j\omega)\right) \\ -\dfrac{\omega'}{\omega}\cos\left(\omega t + \phi + \angle D(j\omega)\right) \end{bmatrix}$$

$$\left|D(j\omega)\right| = \frac{k\omega\omega'}{\sqrt{\left(k\omega\omega'\right)^2 + \left(\omega^2 - \omega'^2\right)^2}} \qquad \angle D(j\omega) = \arctan\frac{\omega'^2 - \omega^2}{k\omega\omega'}$$

State space equations

$$\dot{\mathbf{x}} = \begin{bmatrix} \dot{x}_1 \\ \dot{x}_2 \end{bmatrix} = \mathbf{A}\mathbf{x} + \mathbf{B}v = \begin{bmatrix} -k\omega' & -\omega'^2 \\ 1 & 0 \end{bmatrix}\begin{bmatrix} x_1 \\ x_2 \end{bmatrix} + \begin{bmatrix} k\omega' \\ 0 \end{bmatrix} v$$

$$\mathbf{y} = \begin{bmatrix} v' \\ qv' \end{bmatrix} = \mathbf{C}\mathbf{x} = \begin{bmatrix} 1 & 0 \\ 0 & \omega' \end{bmatrix}\begin{bmatrix} x_1 \\ x_2 \end{bmatrix}$$

$$\dot{\omega}' = -\gamma x_2 \omega'\left(v - x_1\right)$$

$$\dot{\bar{x}}_1 = -\omega^2 \bar{x}_2$$

$$\bar{\varepsilon}_v = \left(v - \bar{x}_1\right) = \frac{1}{k\omega'}\left(\dot{\bar{x}}_1 + \omega'^2 \bar{x}_2\right)$$

$$\bar{\varepsilon}_f = \omega' \bar{x}_2 \bar{\varepsilon}_v = \frac{\bar{x}_2^2}{k}\left(\omega'^2 - \omega^2\right)$$

$$\dot{\omega}' = -\gamma\bar{\varepsilon}_f = \frac{\gamma}{k}\bar{x}_2^2\left(\omega'^2 - \omega^2\right) \approx -2\frac{\gamma}{k}\bar{x}_2^2\left(\omega' - \omega\right)\omega'$$

Feedback based linearization of the FLL [13]

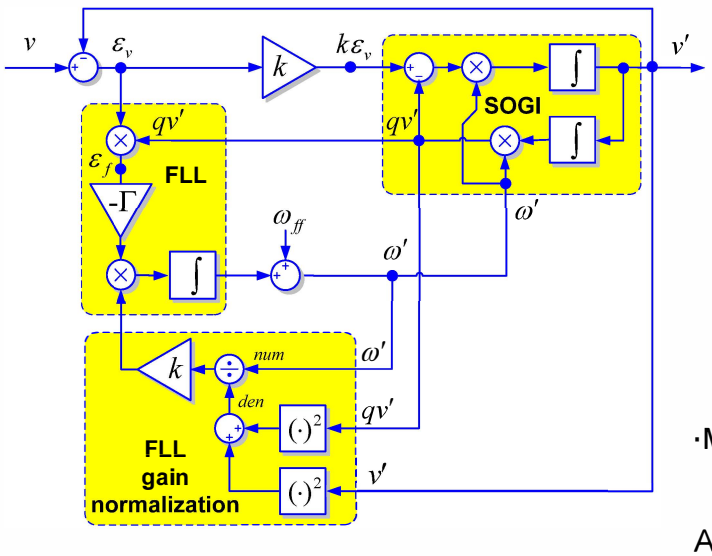

$$\dot{\omega}' = -2\frac{\gamma}{k}\bar{x}_2^2\left(\omega' - \omega\right)\omega'$$

$$\bar{x}_2 = -\frac{V}{\omega}\left|D(j\omega)\right|\cos\left(\omega t + \phi + \angle D(j\omega)\right)$$

$$\bar{x}_2^2 = \frac{V^2}{2\omega^2}\left|D(j\omega)\right|^2\left[1 + \cos\left(2\left(\omega t + \phi + \angle D(j\omega)\right)\right)\right]$$

$$\dot{\bar{\omega}}' = -\frac{\gamma V^2}{k\omega'}\left(\bar{\omega}' - \omega\right)$$

·Making $\gamma = \dfrac{k\omega'}{V^2}\Gamma$ results that $\dot{\bar{\omega}}' = -\Gamma\left(\bar{\omega}' - \omega\right)$

Averaged FLL dynamics

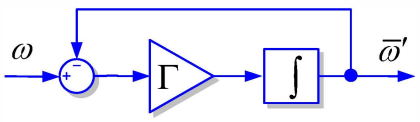

4583

$$\frac{\bar{\omega}'}{\omega} = \frac{\Gamma}{s + \Gamma}$$

$$t_{s(FLL)} \approx \frac{5}{\Gamma}$$

Feedback based linearization of the FLL [13]

SOGI-FLL response:

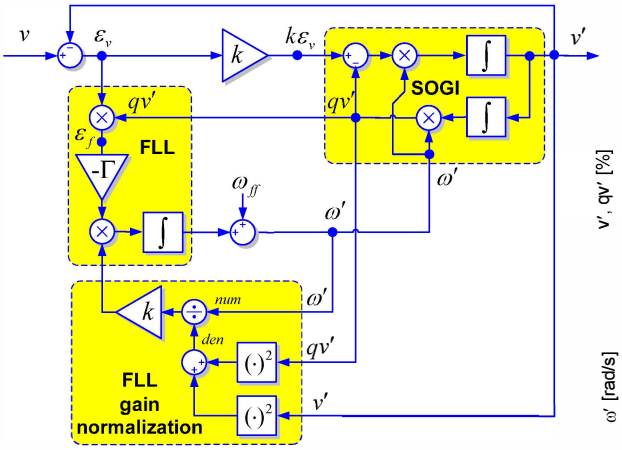

$$t_{s(AF)} = \frac{10}{k\omega'};\ \xi = \frac{1}{\sqrt{2}} \qquad t_{s(FLL)} \approx \frac{5}{\Gamma} \qquad t_{S(FLL)} \geq 2 \cdot t_{S(AF)}$$

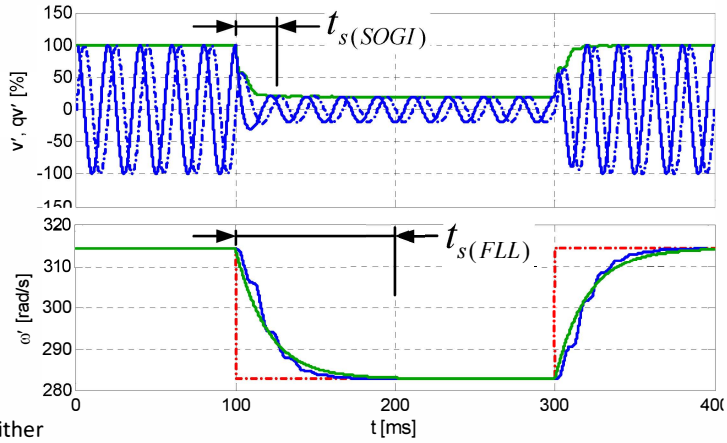

- Does not need any trigonometric function since neither synchronous reference frame nor voltage controlled oscillator are used in its algorithm.
- Is frequency-adaptive by using a perfectly controlled FLL and not a PLL.
- Is highly robust in front of transient events since grid frequency is more stable than voltage phase-angle.
- Attenuates high-order harmonics of the grid voltage.
- Entails light computational burden, using only five integrators for detection of both sequence components.

Three-phase voltage characterization

Distorted and unbalanced three-phase voltage vector

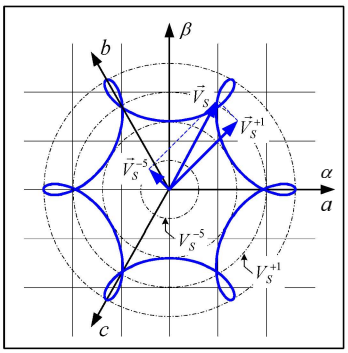

$$|\mathbf{v}_S| = \sqrt{\left(V_S^{+1}\right)^2 + \left(V_S^{n}\right)^2 + 2V_S^{+1}V_S^{n}\cos\left[(n-1)\omega t\right]}$$

$$\theta = \omega t + \tan^{-1}\left\{\frac{V_S^{n}\sin\left[(n-1)\omega t\right]}{V_S^{+1} + V_S^{n}\cos\left[(n-1)\omega t\right]}\right\}$$

Neither constant amplitude nor rotation speed

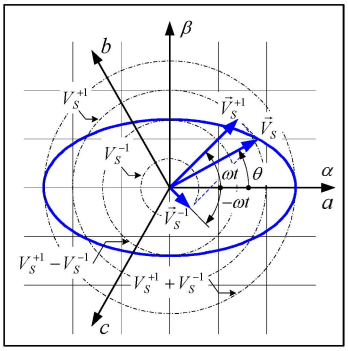

$$|\mathbf{v}_S| = \sqrt{(V_S^{+1})^2 + (V_S^{-1})^2 + 2V_S^{+1}V_S^{-1}\cos(-2\omega t + \phi^{-1})}$$

$$\theta = \omega t + \tan^{-1}\left(\frac{V_S^{-1}\sin(-2\omega t + \phi^{-1})}{V_S^{+1} + V_S^{-1}\cos(-2\omega t + \phi^{-1})}\right)$$

Conventional Synchronous Reference Frame PLL [14]

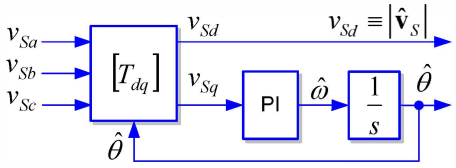

$$\mathbf{v}_{S_{(dq)}} = \begin{bmatrix} v_{Sd} \\ v_{Sq} \end{bmatrix} = V_S^{+1} \begin{bmatrix} \cos(\omega t - \hat{\theta}) \\ \sin(\omega t - \hat{\theta}) \end{bmatrix} + V_S^{-1} \begin{bmatrix} \cos(-\omega t + \phi^{-1} - \hat{\theta}) \\ \sin(-\omega t + \phi^{-1} - \hat{\theta}) \end{bmatrix}$$

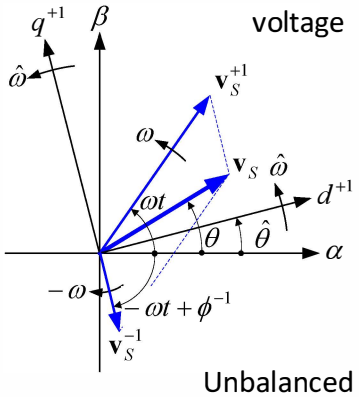

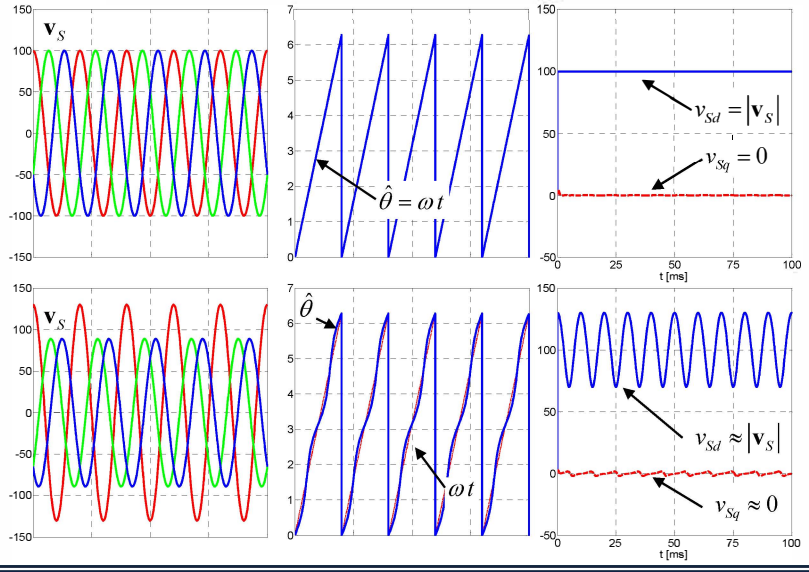

Conventional Synchronous Reference Frame PLL [14]

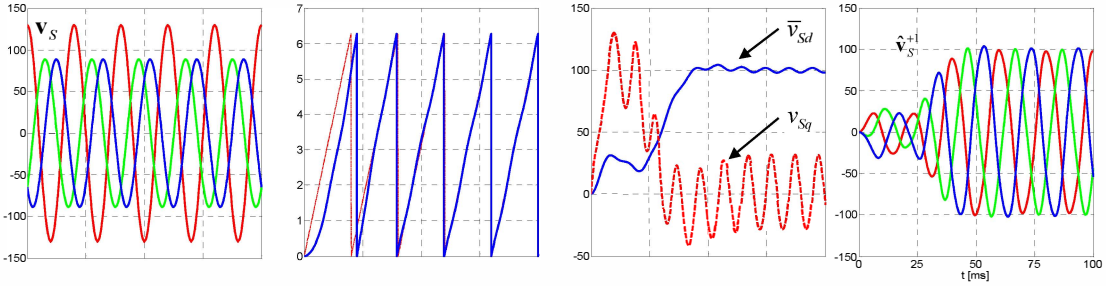

Setting a low PLL bandwidth and using a low-pass filter it is possible to obtain a reasonable approximation of the positive sequence voltage but the dynamic is too slow.

Other filtering strategies can be used to cancel out the double frequency oscillation keeping high locking dynamics [5], e.g., decoupling cells, repetitive controller based on a DFT algorithm, move average filters, Kalman filters, etc.

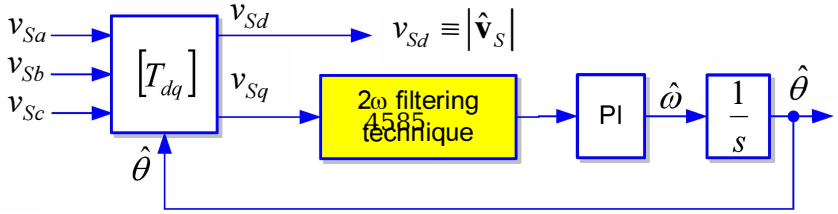

Decoupled Double SRF-PLL [15]

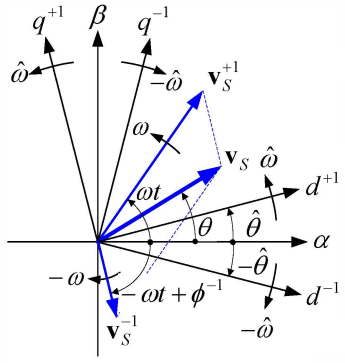

$$\mathbf{v}_{S\,(dq^{+1})} = \begin{bmatrix} v_{Sd^{+1}} \\ v_{Sq^{+1}} \end{bmatrix} = \left[T_{dq^{+1}}\right] \cdot \mathbf{v}_{S\,(\alpha\beta)} = V_S^{+1} \begin{bmatrix} \cos(\omega t - \hat{\theta}) \\ \sin(\omega t - \hat{\theta}) \end{bmatrix} + V_S^{-1} \begin{bmatrix} \cos(-\omega t + \phi^{-1} - \hat{\theta}) \\ \sin(-\omega t + \phi^{-1} - \hat{\theta}) \end{bmatrix}$$

$$\mathbf{v}_{S\,(dq^{-1})} = \begin{bmatrix} v_{Sd^{-1}} \\ v_{Sq^{-1}} \end{bmatrix} = \left[T_{dq^{-1}}\right] \cdot \mathbf{v}_{S\,(\alpha\beta)} = V_S^{+1} \begin{bmatrix} \cos(\omega t + \hat{\theta}) \\ \sin(\omega t + \hat{\theta}) \end{bmatrix} + V_S^{-1} \begin{bmatrix} \cos(-\omega t + \phi^{-1} + \hat{\theta}) \\ \sin(-\omega t + \phi^{-1} + \hat{\theta}) \end{bmatrix}$$

Near of synchronization: $\theta' \approx \omega t$

$$\mathbf{v}_{S\,(dq^{+1})} \approx V_S^{+1} \begin{bmatrix} 1 \\ \omega t - \hat{\theta} \end{bmatrix} + V_S^{-1} \begin{bmatrix} \cos(-2\omega t + \phi^{-1}) \\ \sin(-2\omega t + \phi^{-1}) \end{bmatrix}$$

$$\mathbf{v}_{S\,(dq^{-1})} \approx V_S^{+1} \begin{bmatrix} \cos(2\omega t) \\ \sin(2\omega t) \end{bmatrix} + V_S^{-1} \begin{bmatrix} \cos(\phi^{-1}) \\ \sin(\phi^{-1}) \end{bmatrix}$$

This terms act as interferences on the SRF dq^n rotating at $n\omega$ frequency and viceversa

Generic decoupling cell:

$$\begin{bmatrix} v_{Sd^n} \\ v_{Sq^n} \end{bmatrix} = \begin{bmatrix} V_S^n \cos(\phi^n) \\ V_S^n \sin(\phi^n) \end{bmatrix} + V_S^m \cos(\phi^m) \begin{bmatrix} \cos((n-m)\omega t) \\ -\sin((n-m)\omega t) \end{bmatrix} + V_S^m \sin(\phi^m) \begin{bmatrix} \sin((n-m)\omega t) \\ \cos((n-m)\omega t) \end{bmatrix}$$

$$\begin{bmatrix} v_{Sd^m} \\ v_{Sq^m} \end{bmatrix} = \begin{bmatrix} V_S^m \cos(\phi^m) \\ V_S^m \sin(\phi^m) \end{bmatrix} + V_S^n \cos(\phi^n) \begin{bmatrix} \cos((n-m)\omega t) \\ \sin((n-m)\omega t) \end{bmatrix} + V_S^n \sin(\phi^n) \begin{bmatrix} -\sin((n-m)\omega t) \\ \cos((n-m)\omega t) \end{bmatrix}.$$

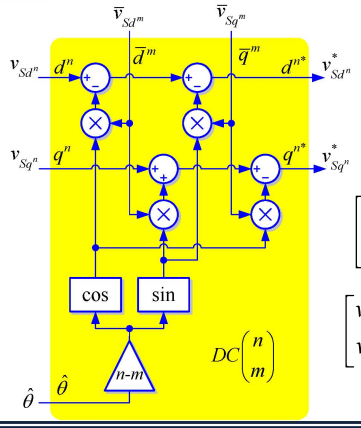

Decoupled Double SRF-PLL [15]

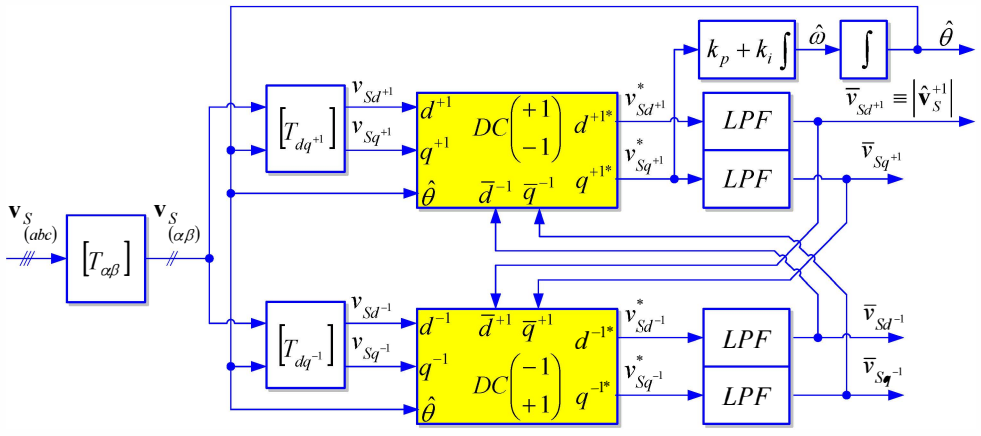

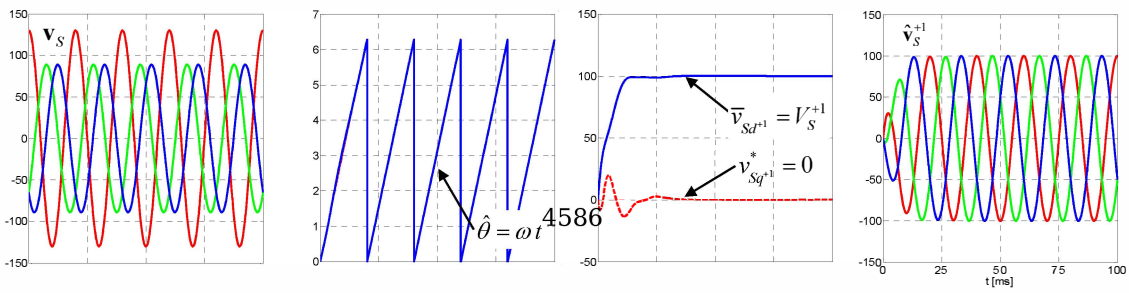

Decoupled Double SRF-PLL [15]

Sag (dip) type C ($\vec{V} = 0{,}6\angle -20^\circ \quad \vec{F} = 0{,}9\angle -10^\circ$

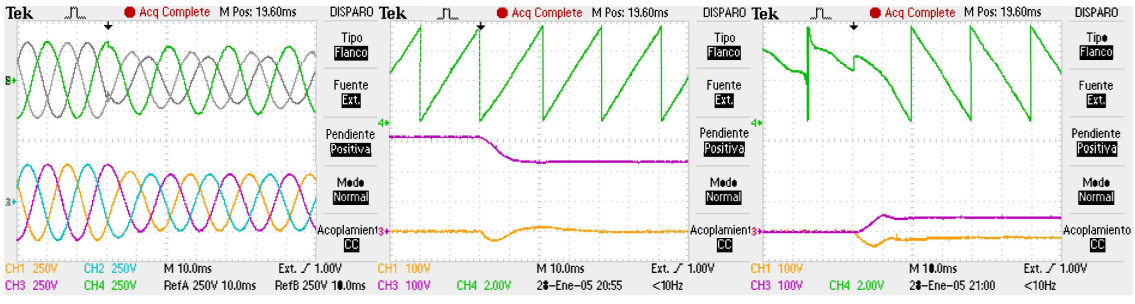

Sag (dip) type D ($\vec{V} = 0{,}6\angle -20^\circ \quad \vec{F} = 0{,}9\angle -10^\circ$

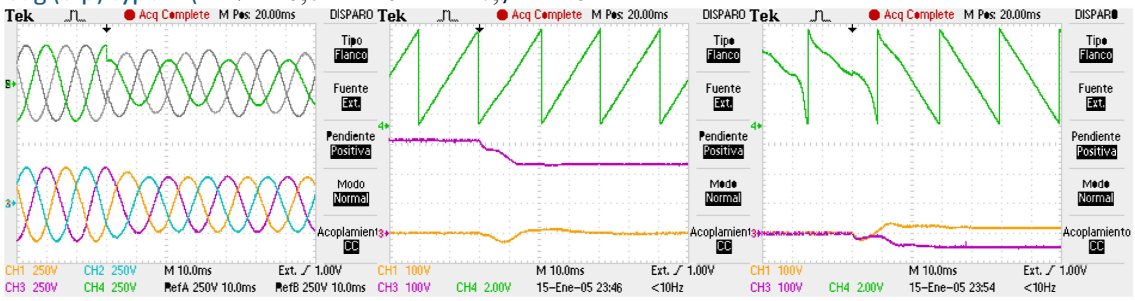

Three-phase voltage components

Instantaneous symetrical components

$$\mathbf{v}^+_{abc} = \begin{bmatrix} v^+_a & v^+_b & v^+_c \end{bmatrix}^T = [T_+]\mathbf{v}_{abc} \qquad [T_+] = \frac{1}{3}\begin{bmatrix} 1 & a & a^2 \\ a^2 & 1 & a \\ a & a^2 & 1 \end{bmatrix}$$

$$\mathbf{v}^-_{abc} = \begin{bmatrix} v^-_a & v^-_b & v^-_c \end{bmatrix}^T = [T_-]\mathbf{v}_{abc} \qquad [T_-] = \frac{1}{3}\begin{bmatrix} 1 & a^2 & a \\ a & 1 & a^2 \\ a^2 & a & 1 \end{bmatrix}$$

Fortescue operator

$$a = e^{j\frac{2\pi}{3}} = -1/2 + e^{j\frac{\pi}{2}}\sqrt{3}/2$$

Symmetrical components are expressed as a function of the *j* operator

$$\begin{bmatrix} v^+_a \\ v^+_c \end{bmatrix} = \begin{bmatrix} \frac{1}{3} & -\frac{1}{6} - j\frac{1}{2\sqrt{3}} & -\frac{1}{6} + j\frac{1}{2\sqrt{3}} \\ -\frac{1}{6} - j\frac{1}{2\sqrt{3}} & -\frac{1}{6} + j\frac{1}{2\sqrt{3}} & \frac{1}{3} \end{bmatrix} \begin{bmatrix} v_a \\ v_b \\ v_c \end{bmatrix} \qquad v^+_b = -v^+_a - v^+_c$$

Symmetrical components can be also calculated on the $\alpha\beta$ domain

$$\mathbf{v}_{\alpha\beta} = [T_{\alpha\beta}]\mathbf{v}_{abc} \;;\; [T_{\alpha\beta}] = \sqrt{\frac{2}{3}}\begin{bmatrix} 1 & -\frac{1}{2} & -\frac{1}{2} \\ 0 & \frac{\sqrt{3}}{2} & -\frac{\sqrt{3}}{2} \end{bmatrix}$$

$$\mathbf{v}^+_{\alpha\beta} = [T_{\alpha\beta}]\mathbf{v}^+_{abc} = [T_{\alpha\beta}][T_+]\mathbf{v}_{abc} = [T_{\alpha\beta}][T_+][T_{\alpha\beta}]^T\mathbf{v}_{\alpha\beta} = \frac{1}{2}\begin{bmatrix} 1 & -q \\ q & 1 \end{bmatrix}\mathbf{v}_{\alpha\beta},$$

$$\mathbf{v}^-_{\alpha\beta} = [T_{\alpha\beta}]\mathbf{v}^-_{abc} = [T_{\alpha\beta}][T_-]\mathbf{v}_{abc} = [T_{\alpha\beta}][T_-][T_{\alpha\beta}]^T\mathbf{v}_{\alpha\beta} = \frac{1}{2}\begin{bmatrix} 1 & q \\ -q & 1 \end{bmatrix}\mathbf{v}_{\alpha\beta},$$

Quadrature operator

$$q = e^{-j\frac{\pi}{2}}$$

PLL with a Dual SOGI (DSOGI-PLL)

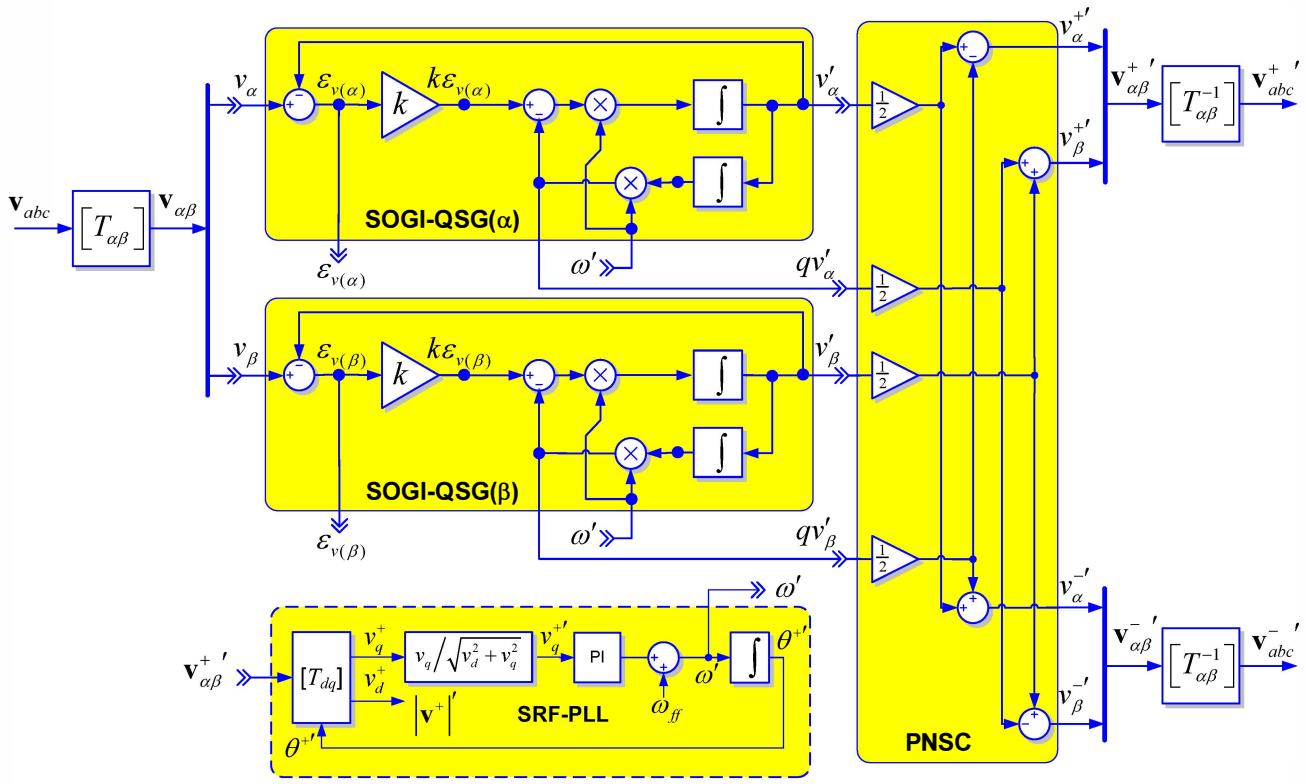

FLL with a Dual SOGI (DSOGI-FLL) [16]

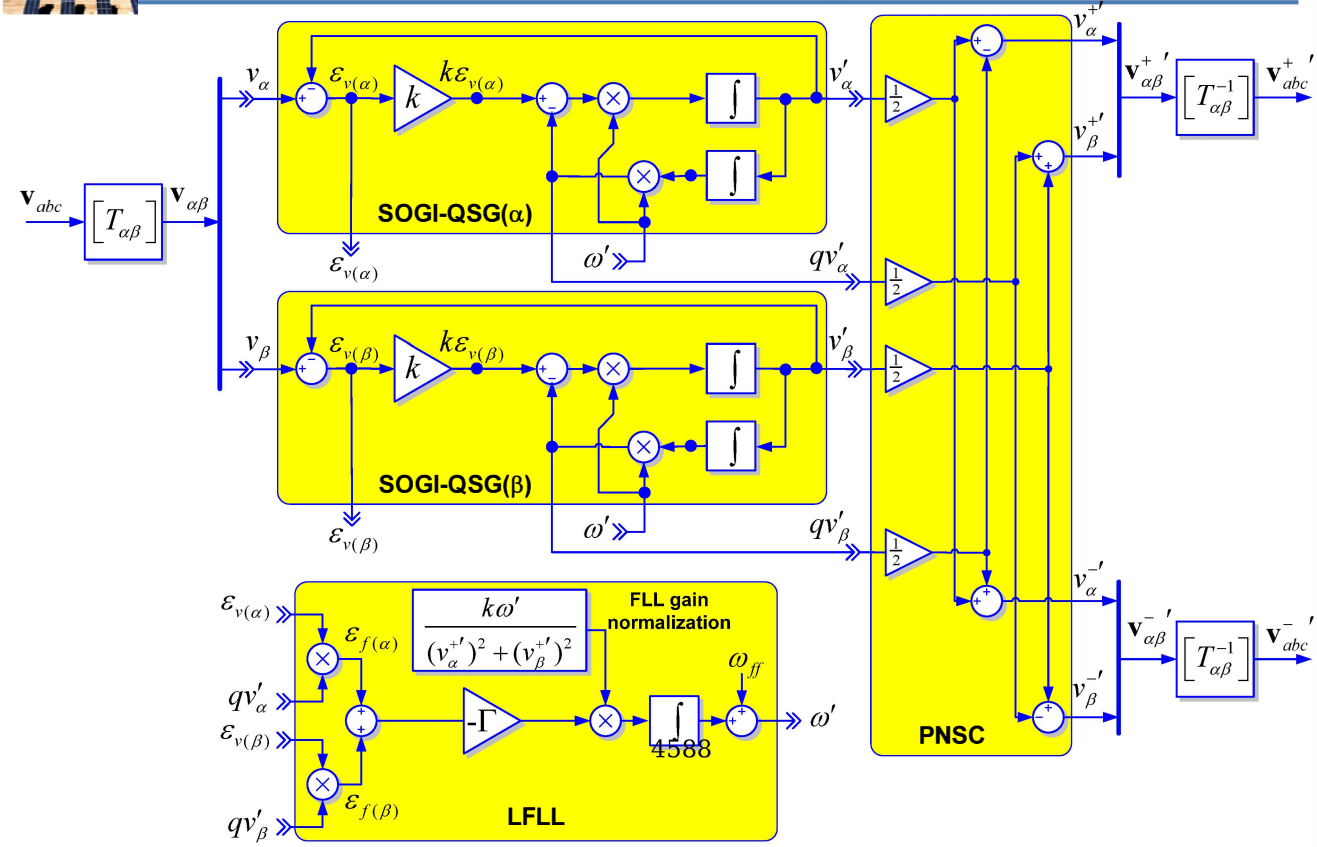

FLL with a Dual SOGI (DSOGI-FLL)

DSOGI-FLL

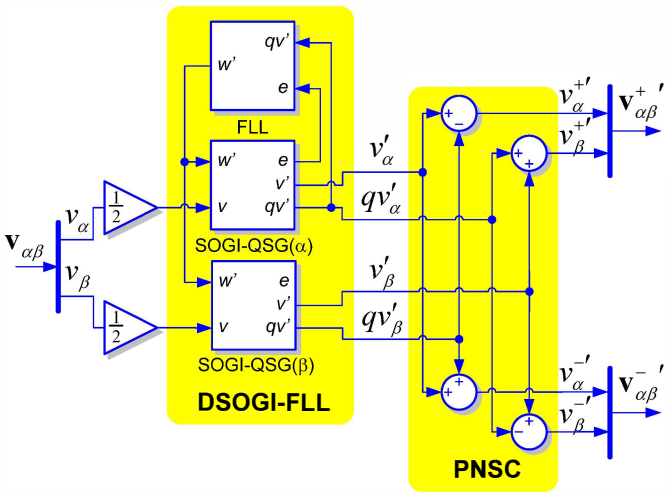

- The SOGI-FLL does not use any phase-angle for synchronizing with the input signal and is provides a set of orthogonal signals *v-qv*.
- ISC method is used on the αβ domain
- Both SOGIs work at the same frequency, therefore only one FLL is necessary
- DSOGI-FLL is a method extremely simple and effective for synchronizing in single-phase and three-phase systems.
- It depends on one of the most stable grid variables, the grid frequency.

FLL with a Dual SOGI (DSOGI-FLL)

DSOGI-FLL response:

Voltage sag

Frequency variation

Voltage distortion

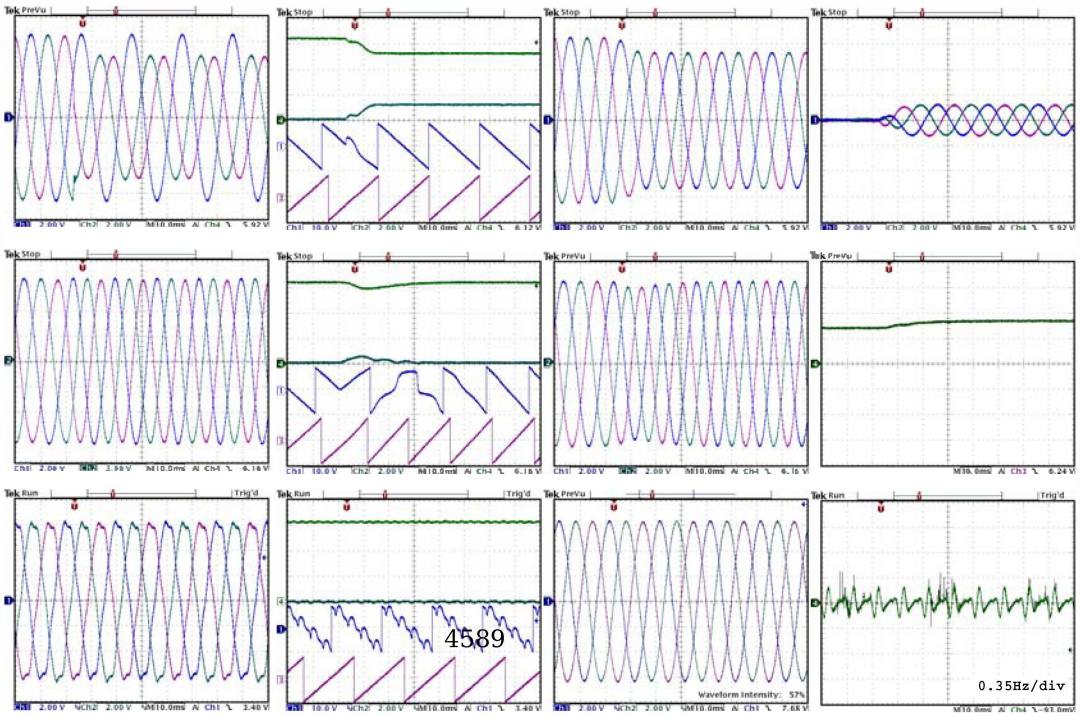

Conclussions

- Grid monitoring is performed by grid-converters to determine connection conditions and to support grid services
- The multiplier PD of a conventional single-phase PLL should be improved to synchronize with ac electrical networks.
- Quadrature-signal generation is an effective technique to implement single-phase PLLs
- Adaptive filters allow implementing advanced grid synchronization systems
- The FLL makes possible to design frequency adaptive filters for grid synchronization.
- In three-phase systems, grid synchronization, estimating the instantaneous positive and negative sequence components, is essential to ride through transient faults
- Conventional SRF-PLL is not the most suitable technique for synchronizing unbalanced grid voltages
- The DDSRF-PLL makes possible a good synchornization during unbalanced conditions by decoupling axis signals on the positive- and negative-reference frames.
- The DSOGI-FLL is a very effective and stable solution for grid monitoring and synchronization under generic grid operating conditions.

Grid Synchronization

References

[1] Transnational College of Lex Tokyo, Y. Sakakibara, A. Gleason, "Who Is Fourier?: A Mathematical Adventure", Language Research Foundation, April 1995. ISBN-10: 0964350408.

[2] R. E. Best, "Phase_locked Loops: Design, Simulation, and Applications". ISBN-0071412018, New York: McGraw-Hill Professional, 5th edition, 2003.

[3] M. Saitou, N. Matsui, T. Shimizu, "A Control Strategy of Single-phase Active Filter Using a Novel d-q Transformation" in Proc. Industry Applications Conference 2003 (IAS'03), Vol. 2, Oct. 2003, pp.1222 – 1227.

[4] Silva, S.M.; Lopes, B.M.; Filho, B.J.C.; Campana, R.P.; Bosventura, W.C. "Performance evaluation of PLL algorithms for single-phase grid-connected systems", in Proc. Industry Applications Conference 2004 (IAS'04), Vol. 4, Oct. 2004 Page(s):2259 – 2263

[5] Haykin, Simon S. Adaptive Filter Theory. Upper Saddle River, N.J.: Prentice Hall, 2002.

[6] B. Widrow, J.R., Jr. Glover, J.M. McCool, J. Kaunitz, C.S. Williams, R.H. Hearn, J.R. Zeidler, Jr. Eugene Dong, R.C. Goodlin, "Adaptive noise cancelling: Principles and applications," Proceedings of the IEEE , vol.63, no.12, pp. 1692-1716, Dec. 1975.

[7] M. Karimi-Ghartemani and M.R. Iravani, "A Nonlinear Adaptive Filter for Online Signal Analysis in Power Systems: Applications," IEEE Trans. On Power Delivery, vol. 17, no. 2, April 2002 Page(s):617 – 622

[8] Yuan, X., Merk, W., Stemmler, H., and Allmeling, J., "Stationary frame generalized integrators for current control of active power filters with zero steady-state error for current harmonics of concern under unbalanced and distorted operating conditions," IEEE Trans. Ind. Appl., vol. 38, no.2, pp. 523–532, Mar./Apr. 2002.

[9] K. de Brabandere, T. Loix, K. Engelen, B. Bolsens, J. Van den Keybus, J. Driesen, and R. Belmans, "Design and Operation of a Phase-Locked Loop with Kalman Estimator-Based Filter for Single-Phase Applications," in Proc. IEEE Ind. Electron. Conf. (IECON'06), Nov. 2006, pp. 525-530.

[10] P. Rodriguez, R. Teodorescu, I. Candela, A.V. Timbus, M. Liserre, and F. Blaabjerg, "New Positive-sequence Voltage Detector for Grid Synchronization of Power Converters under Faulty Grid Conditions," in Proc. IEEE Power Electron. Spec. Conf. (PESC'06), Jun. 2006, pp. 1-7.

[11] Ciubotaru, M, Teodorescu, R., Blaabjerg, F., "A New Single-Phase PLL Structure Based on Second Order Generalized Integrator" – Proceedings of International Conference on Power for Specialists Conference, PESC'06, Korea, 11-12 June 2006 Page(s):1 - 6 vol.4

[12] P. Rodríguez, A. Luna, M. Ciobotaru, R. Teodorescu, and F. Blaabjerg, "Advanced Grid Synchronization System for Power Converters under Unbalanced and Distorted Operating Conditions," in Proc. IEEE Int. Conf. on Ind. Electron. (IECON'06), Paris, 6-10 Nov. 2006.

[13] P. Rodriguez, A. Luna, I Candela, R. Teodorescu, F. Blaabjerg, "Grid synchronization of power converters using multiple second order generalized integrators," Industrial Electronics, 2008. IECON 2008. 34th Annual Conference of IEEE , vol., no., pp.755-760, 10-13 Nov. 2008

[14] Se-Kyo Chung - "A phase tracking system for three phase utility interface inverters" Power Electronics, IEEE Transactions on Volume 15, Issue 3, May 2000 Page(s):431 - 438

[15] P. Rodríguez, J. Pou, J. Bergas, J.I. Candela, R. Burgos and D. Boroyevich, "Decoupled Double Synchronous Reference Frame PLL for Power Converters Control," Power Electronics, IEEE Transactions on, Vol.22, Iss.2, March 2007, Pages:584-592

[16] P. Rodriguez, A. Luna, J.I. Candela, R. Rosas, R. Teodorescu, F. Blaabjerg, "Multi-Resonant Frequency-Locked Loop for Grid Synchronization of Power Converters Under Distorted Grid Conditions," IEEE Trans. on Ind. Electron., vol.PP, no.99, pp.1-1, Apr. 2010.

4590

Grid requirements for PV Systems

Marco Liserre
Politecnico di Bari
liserre@poliba.it

Outline

- Grid requirements
- Islanding
- Passive AI methods
- Active AI methods

4591

International Regulations

Grid connection requirements

- *IEEE 1547-2003 Standard for Interconnecting Distributed Resources with Electric Power Systems*
- *IEEE 1547.1- 2005 Standard for Conformance Tests Procedures for Equipment Interconnecting Distributed Resources with Electric Power Systems*
- *IEEE 929-2000, Recommended Practice for Utility Interface of Photovoltaic (PV) Systems – incorporated in IEEE 1547*
- *UL 1741, Standard for Inverters, Converters, and Controllers for Use in Independent Power Systems - elaborated by Underwriters Laboratories Inc. – compatibilzed with IEEE 1547*
- *IEC61727 [6] Photovoltaic (PV) systems - Characteristics of the utility interface - December 2004*
- *IEC 62116 Ed.1 2005: Testing procedure of islanding prevention measures for utility interactive photovoltaic inverter (describes the tests for IEC 61727) – approved in 2007*
- *VDE0126-1-1 2006 Automatic disconnection device between a generator and the public low-voltage grid" – Safety issues- applied on German Market*

EMC

- *IEC 61000-3-2, Ed. 3.0 – "Electromagnetic compatibility (EMC) –Part 3-2: Limits –Limits for harmonic current emissions (equipment input current ≤16 A per phase)", ISBN 2-8318-8353-9, November 2005*
- *EN 61000-3-3, Ed. 1.2 —"Electromagnetic compatibility (EMC) –Part 3-3: Limits – Limitation of voltage changes, voltage fluctuations and flicker in public low-voltage supply systems, for equipment with rated current ≤16 A per phase and not subject to conditional connection", ISBN 2-8318-8209-5, November 2005*
- *IEC 61000-3-12, Ed. 1 – "Electromagnetic compatibility (EMC)–Part 3-12:Limits – Limits for harmonic currents produced by equipment connected to public low-voltage systems with input current >16 A and ≤75 A per phase", November 2004*
- *IEC 61000-3-11, Ed. 1 —" Electromagnetic compatibility (EMC) – Part 3-11: Limits – Limitation of voltage changes, voltage fluctuations and flicker in public low-voltage supply systems – Equipment with rated current ≤75 A and subject to conditional connection" , August 2000Standard EN 50160 – "Voltage Characteristics of Public Distribution System", CENELEC: European Committee for Electrotechnical Standardization, Brussels, Belgium, November 1999*

Utility Voltage Quality

- *Standard EN 50160 – "Voltage Characteristics of Public Distribution System", CENELEC: European Committee for Electrotechnical Standardization, Brussels, Belgium, November 1999 .*

Public Voltage Quality – EN50160

- ***voltage unbalance for three phase inverters. Max unbalance is 3%***
- ***voltage amplitude variations: max +/-10%***
- ***frequency variations: max +/-1%***
- ***voltage dips: duration < 1 sec, deep < 60%***
- ***voltage harmonic levels. Max voltage THD is 8%***

Odd harmonics				Even harmonics	
Not multiple of 3		Multiple of 3			
Order *h*	Relative voltage (%)	Order *h*	Relative voltage (%)	Order *h*	Relative voltage (%)
5	6	3	5	2	2
7	5	9	1.5	4	1
11	3.5	15	0.5	6..24	0.5
13	3	21	0.5		
17	2				
19	1.5				
23	1.5				
25	1.5				

4592

Response to abnormal grid conditions

- ***Voltage deviations***

IEEE 1547		IEC61727		VDE0126-1-1	
Voltage range (%)	Disconnection time (s)	Voltage range (%)	Disconnection time (s)	Voltage range (%)	Disconnection time (s)
V < 50	0.16	V < 50	0.10	110 ≤ V < 85	0.2
50 ≤ V < 88	2.00	50 ≤ V < 85	2.00		
110 < V < 120	1.00	110 < V < 135	2.00		
V ≥ 120	0.16	V≥ 135	0.05		

Obs. The purpose of the allowed time delay is to ride through short-term disturbances to avoid excessive nuisance tripping

- ***Frequency deviations***

IEEE 1547		IEC61727		VDE0126-1-1	
Frequency range (Hz)	Disconnection time (s)	Frequency range (Hz)	Disconnection time (s)	Frequency range (Hz)	Disconnection time (s)
59.3 < f < 60.5*	0.16	fn-1 < f < fn+1	0.2	47.5 < f < 50.2	0.2

* for systems with power < 30 kW the lower limit can be adjusted in order to allow participation in the frequency control

Obs. The VDE0126-1-1 allow much lower frequency limit and thus frequency adaptive synchronization is required.

- ***Reconnection after trip***

IEEE 1547	IEC61727	VDE0126-1-1
88 < V < 110 [%] AND 59.3 < f < 60.5 [Hz]	85 < V < 110 [%] AND fn-1 < f < fn+1 [Hz] AND Min. delay of 3 minutes	N/A

Power Quality

- ***DC Current Injection***

IEEE 1574	IEC61727	VDE0126-1-1
Idc < 0.5 [%] of the rated RMS current	Idc < 1 [%] of the rated RMS current	Idc < 1A Max Trip Time 0.2 s

Obs. For IEEE 1574 and IEC61727 the dc component of the current should be measured by using harmonic analysis (FFT) and there is no maximum trip time condition

- ***Current harmonics***

IEEE 1547 and IEC 61727						
Individual harmonic order (odd)*	h < 11	11 ≤ h < 17	17 ≤ h < 23	23 ≤ h < 35	35 ≤ h	Total harmonic distortion THD (%)
(%)	4.0	2.0	1.5	0.6	0.3	5.0

Obs. The test voltage for IEEE1574/IEC61727 should be produced by an electronic power source with a voltage THD < 2.5% (typically ideal sources)

IEC 61000-3-2 for class A equipments apply also

Odd harmonics		Even harmonics	
Order *h*	Current (A)	Order *h*	Current (A)
3	2.30	2	1.08
5	1.14	4	0.43
7	0.77	6	0.30
9	0.40	8 ≤ *h* ≤ 40	0.23 x 8/*h*
11	0.33		
13	0.21		
13 ≤ *h* ≤ 39	0.15 x 15/*h*		

4593

Obs. The current limits in IEC61000-3-2 are given in amperes and are in general higher than the ones in IEC61727. For equipments with a higher current than 16 A but lower than 75A another similar standard IEEE 61000 3-12 [12] applies

Power Quality

- ***Average Power Factor***

- ***Only in IEC61727 it is stated that the PV inverter shall have an average lagging power factor greater than 0,9 when the output is greater than 50%. Most PV inverters designed for utility-interconnected service operate close to unity power factor.***
- ***In IEEE1574 as this a general standard that should allow also distributed generation of reactive power there is no requirement for the power factor***
- ***No power factor requirements are mentioned in VDE0126-1-1***
- ***Obs. Usually the power factor requirement for PV inverters should be interpreted now as a requirement to operate at quasi-unity power factor without the possibility of regulating the voltage by exchanging reactive power with the grid. For high power PV installations connected directly to the distribution level local grid requirements apply as they may participate in the grid control. For low power installations it is also expected that in the near future the utilities will allow them to exchange reactive power but new regulations are still expected.***

Draft German Grid Code

Generating Plants in Low Voltage Networks

Forum Netztechnik / Netzbetrieb im VDE (FNN)

1. Voltage Rise

Maximum allowed voltage change is calculated in terms of short circuit power of PCC:

$$\Delta u_{max} = k_{max} \frac{S_{Emax}}{S_{kV}} \leq 3\%$$

Skv is network short circuit power at PCC

SEmax is maximum generating power at PCC

2. Harmonics

Allowable harmonic limits based on network short circuit power at PCC

Valid for both <16A and >16A

Harmonic number	Allowable, based harmonic current $i_{\nu,\mu\ zul}$ in A/MVA
3	3
5	1,5
7	1
9	0,7
11	0,5
13	0,4
17	0,3
19	0,25
23	0,2
25	0,15
$25 < \nu < 40$ [1]	$0{,}15 \times 25/\nu$
even	$1{,}5/\nu$
$\mu < 40$	$1{,}5/\nu$
$\mu,\nu > 40$ [2]	$4{,}5/\nu$

Forum Netztechnik / Netzbetrieb im VDE (FNN)

Draft German Grid Code

Generating Plants in Low Voltage Networks

Forum Netztechnik / Netzbetrieb im VDE (FNN)

3. Unbalance

Maximum 4.6-kVA unbalance is allowed between three phases
Max. single-phase connection power is 10 kVA
If S >30 kVA, then only three-phase connection is allowed

L 1	L 2	L 3	Unsymmetrie	Allowed?
4,6 kVA	0	0	4,6 kVA	Yes
4,6 kVA	2,5 kVA	0	4,6 kVA	Yes
10 kVA	6 kVA	8 kVA	4 kVA	Yes
10 kVA	5 kVA	3 kVA	**7 kVA**	No
10 kVA	7 kVA	**11 kVA**	4 kVA	No
10 kVA	**10 kVA**	**11 kVA**	1 kVA	No
50 kVA (3-phase ac)			0	Yes

4. Max. allowable Short-circuit current

Roughly, For synchronous generators: $I_{sc}=8xI_{rated}$

For asynchronous generators: $I_{sc}=6xI_{rated}$

For inverters: $I_{sc}=I_{rated}$

Forum Netztechnik / Netzbetrieb im VDE (FNN)

Draft German Grid Code

Generating Plants in Low Voltage Networks

Forum Netztechnik / Netzbetrieb im VDE (FNN)

5. Active Power Limitation

- Typical output power reduction steps: 100%, 60%, 30%, 0%
- Generation plants must be able to implement any set-point given by network operator
- No information about P-f relation is given in draft at that moment

6. Reactive Power Control

Generating plant must be able to produce reactive power in any PCC point:

From cos(φ)=0.9 (under-excited) to cos(φ)=0.9 (over-excited)

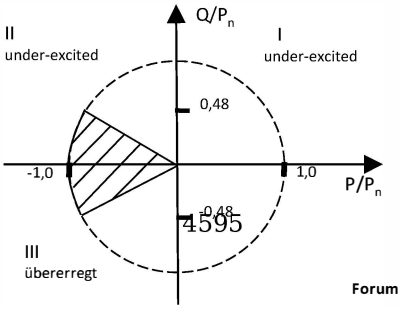

Forum Netztechnik / Netzbetrieb im VDE (FNN)

6. Reactive Power Control (cont.)

Reactive power control methods:

- Fixed power factor
- Fixed reactive power (Qfixed)
- Set power factor in terms of active power (given by network operator)

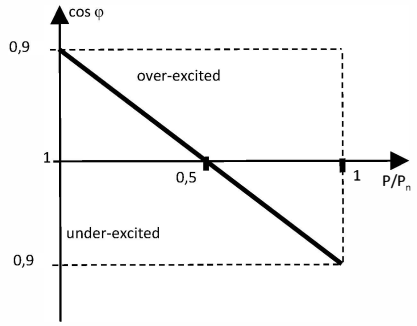

must adjust itself within 10sec!

Draft German Grid Code
Generating Plants in Low Voltage Networks
Forum Netztechnik / Netzbetrieb im VDE (FNN)

7. Disconnection from network

- Over-voltage, under-voltage, over-frequency and under-frequency

Protective function	*Protective relay settings*	
Under-voltage protection U<	0,8 U_n	< 100 ms
Over-voltage protection U>	1,1 U_n	< 100 ms
Over-voltage protection U>>	1,15 U_n	< 100 ms
Under-frequency protection f<	47,5 Hz	< 100 ms
Over-frequency protection f>	50,2 Hz	< 100 ms

- 10-min moving average for over-voltage monitoring
- Fault ride-through is not featured in draft code for LV network

4596

Draft Spanish Grid Code O.P.12.2 (2008)

- applies for new wind or PV plants bigger than 10MW installed after January 1st 2011
- requires LVRT down to 0V
- requires for first time a voltage controller for defining the reactive power support during voltages outside the normal range
- recommends for future the possible requirement of inertia emulation and power oscillation damping (POD), two features that requires some active power storage that remind very much the synchronous generator technology

Annex of O.P. 12.2 Restricted to the technical requirements of wind power and photovoltaic facilities (Draft), by Red Electrica in October 2008 www.ree.es (translated in English by Spanish Wind Association AEE www.aeolica.es).

Draft Spanish Grid Code O.P.12.2 (2008)

VRT

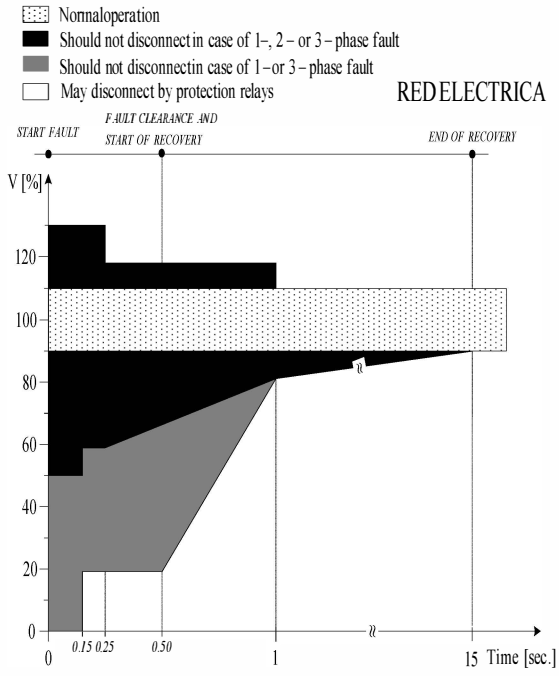

•No disconnection is allowed within the black area for 1- 2- and 3-phase faults.

•No disconnection is allowed within the grey area for 1- and 3-phase faults.

•No disconnection is allowed for 1 sec. for 1.15 p.u. level and 250 ms for 1.3 sec.

•During the whole transient regime, the facility must be able to inject to the grid at least the nominal apparent current.

•The facility might not consume active and reactive power at the grid connection point during both, fault duration and the duration of voltage recovery following fault clearance.

4597

Annex of O.P. 12.2 Restricted to the technical requirements of wind power and photovoltaic facilities (Draft), by Red Electrica in October 2008 www.ree.es (translated in English by Spanish Wind Association AEE www.aeolica.es).

Draft Spanish Grid Code - MV

Reactive Current Injection – Implemented as Voltage Controller

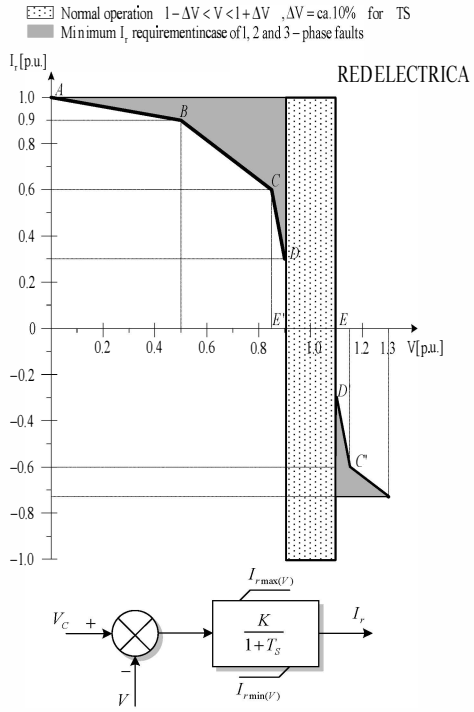

- enabled for any voltage outside the normal range.
- during the fault, the plant should inject/absorb *positive sequence* reactive currents based on the action of the voltage controller with minimum saturation levels defined by the polygonal curve ABCDE. In case of overvoltage, the saturation levels are mirrored but for voltages higher than1.3 p.u., disconnection is required by protection relays.
- These levels should be implemented as saturation levels for the voltage controller that runs in both normal and faulty operation.
- Once the fault is cleared, the voltage controller will keep be enabled for at least 30 sec. after voltage level reenter the normal operation range. Afterwards, the voltage controller will be disabled and the reactive power requirements for normal operation will apply

Annex of O.P. 12.2 Restricted to the technical requirements of wind power and photovoltaic facilities (Draft), by Red Electrica in October 2008 www.ree.es (translated in English by Spanish Wind Association AEE www.aeolica.es).

Draft Spanish Grid Code - MV

Active Current Injection – Implemented as Voltage Controller

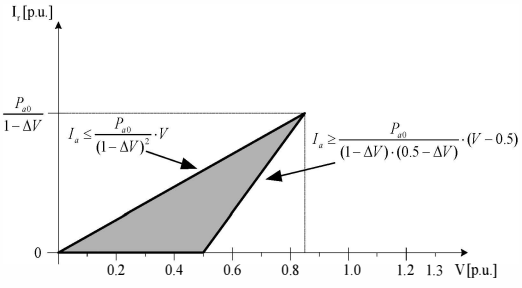

Resuming Active power

The voltage dependent active current control previous mentioned ensures that after the fault clearance without disconnection, the active power level prior to disturbance will be restored smoothly within **250 ms**.

- During faults, the plant should limit the active current within the grey area (excluding the active current increments/reductions due to frequency control or, if applicable inertia emulation).
- The active current limitation is a function of Pao, the active power that the facility was generating prior to the disturbance and voltage level
- For voltage levels lower than 0.5 the active current can be reduced to zero
- Any possible violation of these active current limits must be corrected before 40 ms.
- In case of current saturation, reactive current limitation given by voltage controller saturation has priority over active current limitation.
- The gain of the active current controller should ensure dynamic response (90% rise) in less than 40 ms for V< 0.85 and 250 ms for V > 0.85

Annex of O.P. 12.2 Restricted to the technical requirements of wind power and photovoltaic facilities (Draft), by Red Electrica in October 2008 www.ree.es (translated in English by Spanish Wind Association AEE www.aeolica.es).

Draft Spanish Grid Code - MV

Future "recommended" functions – Inertia Emulation

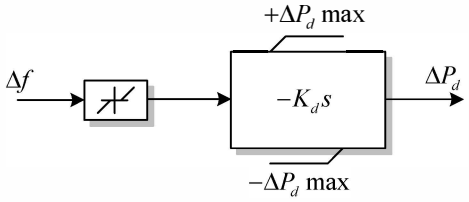

- Implemented as PD controller with Δf as input
- The gain K_d should be adjustable between 0 and 15 sec., and the response time should be such that in 50ms the active power should increase at least by Δ P = 5% .
- In order to be able to generate the required saturation levels, **energy storage** of any technology is required able to inject or absorb at least **10%** active power for at least **2 sec**.
- The deadband of frequency variation will be limited to 10 mHz.
- The IE should be disabled for voltages lower than 0.85 p.u.

Annex of O.P. 12.2 Restricted to the technical requirements of wind power and photovoltaic facilities (Draft), by Red Electrica in October 2008 www.ree.es (translated in English by Spanish Wind Association AEE www.aeolica.es).

Draft Spanish Grid Code - MV

Future "recommended" functions – Power Oscillation Damping (POD)

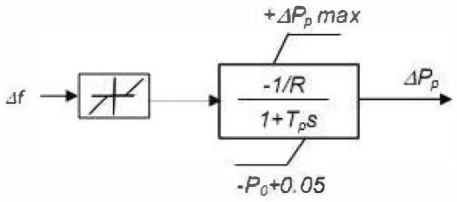

$$R = -\frac{\Delta f / f_{base}}{\Delta P_p / M_{base}}$$

- Another feature "borrowed" from SG technology (Power System Stabilizer - PSS)
- increase or decrease the output power in such a way to reduce the power oscillations in the low frequency range (0.15 – 2.0 Hz) (undamped modes)
- The POD can be implemented by "sharing" the existing power-frequency regulator.
- The POD can "share" the energy storage used for IE.
- The deadband of frequency variation will be limited to 10 mHz.
- The POD should be disabled for voltages lower than 0.85 p.u.

4599

Annex of O.P. 12.2 Restricted to the technical requirements of wind power and photovoltaic facilities (Draft), by Red Electrica in October 2008 www.ree.es (translated in English by Spanish Wind Association AEE www.aeolica.es).

Islanding Definition

- ***What is islanding?***

Islanding for grid connected PV systems takes place when the PV inverter does not disconnect very short time after the grid is tripped, i.e. it is continuing to operate with local load. In the typical case of residential electrical system co-supplied by a roof-top PV system, the grid disconnection can occur as a result of a local equipment failure detected by the ground fault protection, or of an intentional disconnection of the line for servicing. In both situations if the PV inverter does not disconnect the following consequences can occur:

- ***Retripping the line or connected equipment damaging due to of out-of-phase closure***
- ***Safety hazard for utility line workers that assume de-energized lines during islanding***

In order to avoid these serious consequences safety measures called anti-islanding (AI) requirements have been issued and embodied in standards

Anti-Islanding Requirements – IEEE 1574

In IEEE 1574 the requirement is that after an unintentional islanding where the distributed resources (DR) continues to energize a portion of the power system (island) through the PCC, the DR shall detect the islanding and cease to energize the area within 2 seconds.

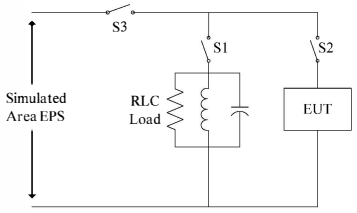

NOTES
1 – Switch S1 may be replaced with individual switches on each of the RLC load components
2 – Unless the EUT has a unity output p.f., the receiver power component of the EUT is considered to be a part of the islanding load circuit in the figure.

Adjustable RLC load should be connected in parallel between the PV inverter and the grid. The resonant LC circuit should be adjusted to resonate at the rated grid frequency and to have a quality factor of 1 or in other words the reactive power generated by [VAR] should equal the reactive power absorbed by [VAR] and should equal the power dissipated in [W]

The parameters of the RLC load should be fine tuned until the grid current through S3 should be lower than 2% of the rated value on a steady-state base. In this balanced condition, the S3 should be open and the time before disconnection should be measured and should be lower than 2 seconds.

The UL 1741 standard in US has been harmonized with AI req stated in IEEE 1547

Anti-Islanding Requirements – IEC52116

In IEC 62116-2006 similar AI requirements as the IEEE1547 is proposed. The test can also be utilized by other inverter interconnected DER. In the normative reference IEC 61727-2004 the ratings of the system valid in this standard has a rating of 10 kVA or less, the standard is though subject to revision. The test circuit is the same as in the IEEE1547.1test (Figure 4.1) power balance is required before the island detection test. The requirement for passing the test contains more test cases but the conditions for confirming island detection do not have a significant deviation compared to the IEEE1547.1 test.

The inverter is tested at three levels of output power (A 100-105%, B 50-66% and C 25-33% of inverters output power). Case A is tested under maximum allowable inverter input power, case C at minimum allowable inverter output power if > 33 %.

The voltage at the input of the inverter also has specific conditions (see [8]). All conditions are to be tested at no deviation in real and reactive load power consumption then for condition A in a step of 5% both real and reactive power iterated deviation from -10% to 10% from operating output power of inverter.

Condition B and C are evaluated by deviate the reactive load in an interval of ±5 % in a step of 1 % of inverter output power.

The maximum trip time is the same as in IEEE 1547.1 standards 2 s.

In IEC61727, there is no specific description of the anti-islanding requirements. Instead reference to IEC62116 is done.

Anti-Islanding Requirements – VDE-0126-1

The VDE0126-1-1 allows the compliance with one of the following anti-islanding methods:

A. Impedance measurement

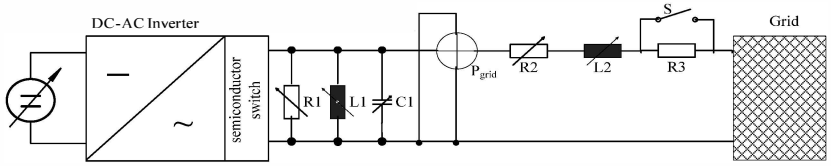

B. Disconnection detection with RLC resonant load

The test circuit is the same with the one from IEEE1547.1 depicted in Fig. 4.1 and the test conditions are that the RLC resonant circuit parameters should be calculated for a quality factor of using (4.1)

With balanced power the inverter should disconnect after the disconnection of S2 in maximum 5 seconds for the following power levels: 25%, 50% and 100%.

C. Voltage monitoring

For three-phase PV inverters a passive anti-islanding method is accepted by monitoring all three phases voltage with respect to the neutral. This method is conditioned by having individual current control in each of the three phases.

Finding an software based anti-islanding method has been a very challenging task resulting in a large number of research work and publications

Standards overview

In this chapter an overview of the most relevant standards related to the grid connection requirements of PV inverters is given.
High efforts are done by the international standard bodies in order to "harmonize" the grid requirements for PV inverters worldwide.
Recently the IEEE1574 standard has done a big step in the direction of issuing a standard that includes grid requirements not only for PV inverters but for all distributed resources under 10 MVA.
Underwriters Laboratories in US has revised this year the UL 1471 by accepting the grid requirements of IEEE1574 and also IEC62116 was revised to harmonize with the requirements of IEEE1574 in the anti-islanding requirements.
Even the very specific German standard VDE0126-1-1 was revised in 2006 where the grid impedance measurement has become optional and an alternative requirement very similar to IEEE1574 was included. All these positive actions needs to be followed by adoption in different countries that still use their own local regulations.
The most relevant conditions from these standards are highlighted in order to envisage the impact on the control strategies. For designing purposes, the readers are strongly recommended to access the complete texts of the standards and deal with all the related details.
For large MW PV parks, grid-connection requirements are inlined with wind power connected to either distribution or transmission levels.

Overview of AI Methods

There main approaches can be employed for islanding detection:

- Grid-resident detection
- External switched capacitor detection
- Inverter-resident detection

4602

Overview of AI Methods

Grid-resident methods require either a communication system through the power line or a external switched capacitor at the PCC in order to detect the islanding condition accurately, which increases the system complexity and its economical costs.

External Switched Capacitor (ESC) Detection is based on the concept that an external capacitor periodical switched on in parallel with the grid would produce a zero-crossing delay proportional with the grid impedance

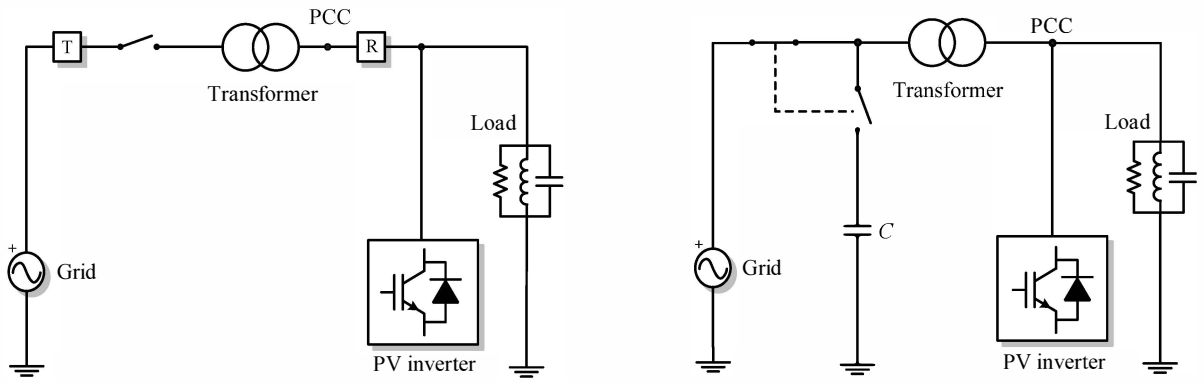

Overview of AI Methods

Inverter-resident detection

It relies exclusively on *software implementation* inside the PV inverter control platform and can use:

- *Passive methods.*
- *Active methods*
- *Mixed methods*

4603

Overview of AI Methods

The passive methods are based on the detection of a change of a power system parameter (typically voltage, frequency, phase or harmonics) caused by the power mismatch after the loss of grid. Passive methods have non-zero NDZ and are typically combined with active methods to improve the reliability.

The active methods generate a disturbance in the PCC in order to force a change of a power system parameter that can be detectable by the passive meth- ods. With active methods, the NDZ can be significantly reduced; however they have the potential to affect power quality and to generate instability in the grid especially if more inverters are connected in parallel.

Non Detection Zone - NDZ

The reliability of islanding detection methods can be represented by the non- detection zone (NDZ) defined in the power mismatch space (versus) at the point of common coupling (PCC) where the islanding is not detectable and the potential for parasitic trips.

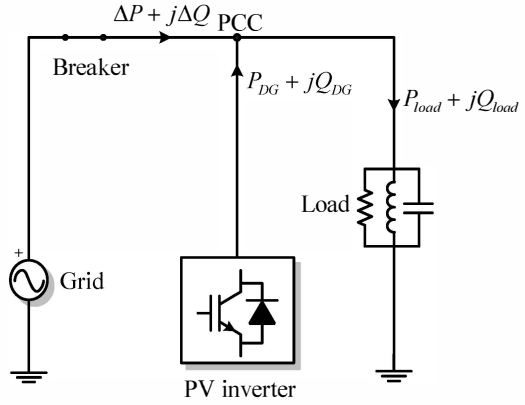

4604

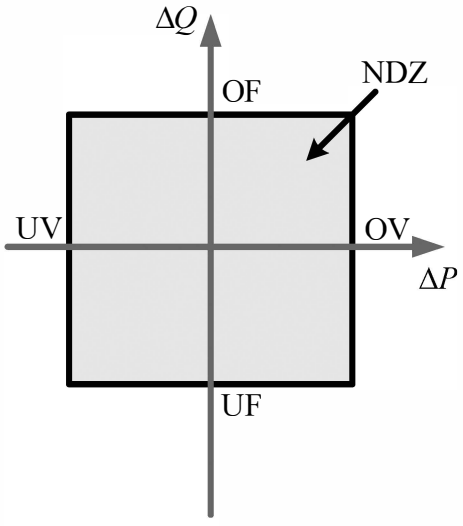

Passive methods (UOF-OUV detection)

Voltage and frequency monitoring is typically used in order to trip the inverter in case of Over Under Voltage or Over Under Frequency. The worst case for islanding detection is represented by a condition of balance of the active and reactive power in which there is no change in amplitude and frequency.

Strengths

- low cost option

Weaknesses

- Large NDZ

NDZ

The minimum values for and that would hit the OUF or OUV can be determined analytically as:

$$q\cdot\left(1-\left(\frac{f}{f_{\min}}\right)^2\right)\le\frac{\Delta Q}{P_{DG}}\le q\cdot\left(1-\left(\frac{f}{f_{\max}}\right)^2\right) \qquad \left(\frac{V}{V_{\max}}\right)^2-1\le\frac{\Delta P}{P_{DG}}\le\left(\frac{V}{V_{\min}}\right)^2-1$$

Thus the NDZ can be precisely determined but in most cases this method is considered to be insufficient as anti-islanding protection complying with the PV standards

Passive methods (Phase Jump detection)

This method observes the phase difference between the inverter terminal voltage and its output current that typically occurs during islanding due to reactive power mismatch. The phase can change much faster than the frequency, so much faster island detection is theoretically possible.

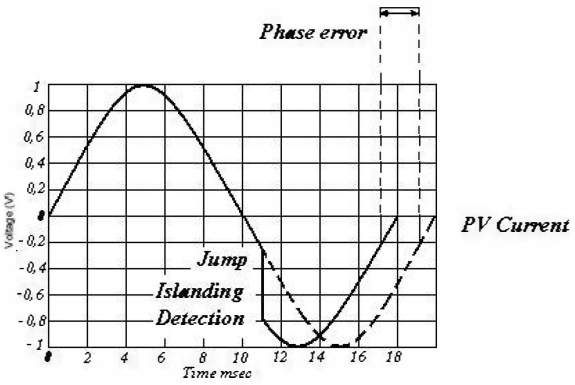

Strengths

- Fast Detection
- Easy to implement (using Zero-Croos detection)

Weaknesses

- Noise susceptibility

NDZ

A load with a zero phase angle at the utility frequency will not produce a phase error when the utility is disconnected

Passive methods (Harmonic detection)

This method, based on the use of the Kalman filter estimation of the 3rd, 5th and 7th harmonic variation exploits the natural sensitivity to disturbances of a grid voltage sensorless control to highlight islanding condition.

The algorithm evaluate not the absolute value of the grid voltage harmonics but the variation of the spectrum power density (energy).

Resonant HC are used for detection

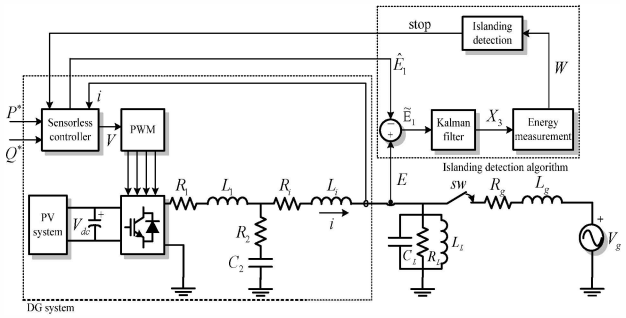

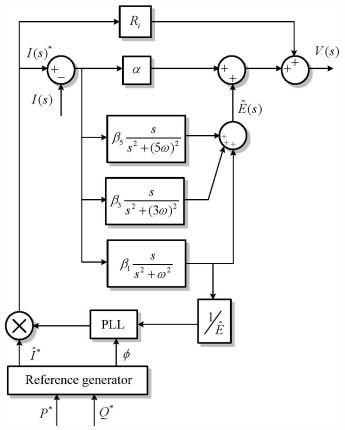

•Liserre, M.; Pigazo, A.; Dell'Aquila, A.; Moreno, V.M., "An Anti-Islanding Method for Single-Phase Inverters Based on a Grid Voltage Sensorless Control," Industrial Electronics, IEEE Transactions on ,vol.53, no.5, pp.1418-1426, Oct. 2006.

Passive methods evaluation

The reliability of passive methods is limited as there will always be a non-zero NDZ for small power unbalance. Thus passive methods are often combined with active methods.

Method	NDZ	Trip time (power balance)
OUV	-17 %≤ΔP≤24 %	Not applicable
OUF	-5%≤ΔQ≤5%	Not applicable
PJD	-5%≤ΔQ≤5%	Not applicable
HM	Absent	It can be less than 200 ms

4606

F. De Mango, M. Liserre, A. Dell'Aquila and A. Pigazo, "Overview of anti-islanding algorithms for PV systems. Part I: Passive methods," in Proc. of *12th International Power Electronics and Motion Conference*, pp. 1878-1883. August 2006

Active methods

The active methods are based on the generation of small perturbations at the output of the PV inverter generating small changes in one of the power system parameter (frequency, phase, harmonics, etc..).

The most commonly used techniques are based on:

- Frequency drift
- Voltage drift
- Grid impedance estimation
- Phase injection

Active methods (Frequency drift Methods)

Active Frequency Drift (AFD)

When disconnected from the utility, the frequency of PCC is forced to drift up or down, augmenting the "natural" frequency drift caused by the system seeking the load's resonant frequency.

$$cf = \frac{2T_z}{T} = \frac{\delta f}{f + \delta f} \quad ; \delta f = 0.5 - 1.5 Hz$$

$$i_i = \sqrt{2} I \sin\left[2\pi\left(f + \delta f\right)\right] t$$

$$\theta_{AFD} = \pi f T_z = \frac{\pi \delta f}{f + \delta f}$$

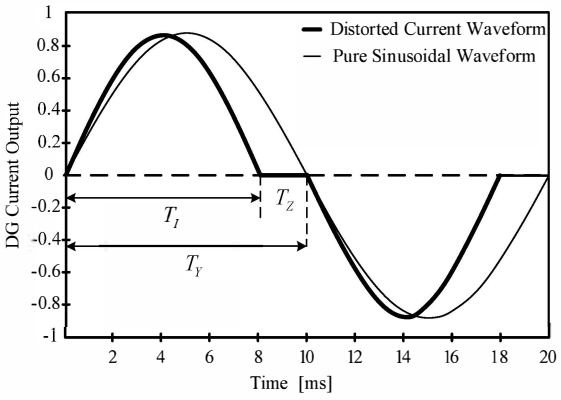

NDZ depends on Q

•Ropp, M.E.; Begovic, M.; Rohatgi, A., "Analysis and performance assessment of the active frequency drift method of islanding prevention," IEEE Transaction on Energy Conversion, vol.14, no.3, pp.810-816, Sep 1999.

Active methods (Frequency drift Methods)

Slip-Mode Frequency Shift (SMS)

A *positive feedback is* applied to the phase of PCC voltage to destabilize the inverter by changing the short-term frequency. If the utility is tripped and the frequency of PCC voltage is distorted, the inverter phase response curve increases the phase error and hence, causes instability in the frequency. This instability further amplifies the perturbation of the frequency of PCC voltage and the frequency is eventually driven away until it hits OUF protection.

$$i_i = \sqrt{2} I \sin\left(2\pi f t + \theta_{SMS}\right)$$

$$\theta_{SMS} = \theta_m \sin\left(\frac{\pi}{2}\right)\frac{f_i - f}{f_m - f}$$

$$NDZ(Q) = 0 \quad if: \frac{\theta_m}{f_m - f} \geq \frac{12Q}{\pi^2}$$

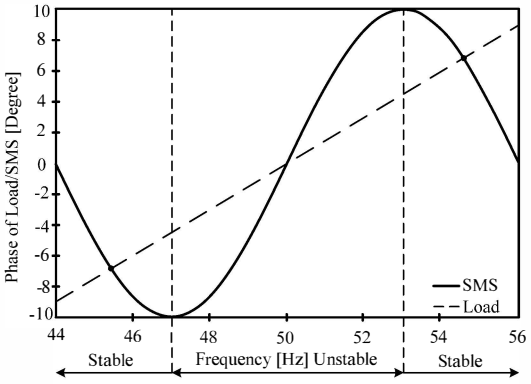

•W.Bower, M.Ropp: "Evaluation of Islanding Detection Methods for Utility-Interactive Inverters in Photovoltaic Systems",Sandia National Labs., Albuquerque, NM, SANDIA Report SAND2002-3591 Nov. 2002 (online ordering: http//www.doe.gov/bridge).

Active methods (Frequency drift Methods)

Sandia Frequency Shift (SFS) also called Active Frequency Drift with Positive Feedback (AFDPF) is an extension of the AFD method, and is another method that utilizes positive feedback. In this method, it is the frequency of voltage at PCC to which the positive feedback is applied. To implement the positive feedback, the "chopping fraction" from AFD is made to be a function of the error in the line frequency

$$cf = cf_0 + k(f - f_n)$$

NDZ can be reduced to 0 for

$$Q < 4.8$$
$$cf_0 = 0.05$$
$$k = 0.01$$

•Lopes, L.A.C.; Huili Sun, "Performance assessment of active frequency drifting islanding detection methods," Energy Conversion, IEEE Transaction on, vol.21, no.1, pp. 171-180, March 2006.

Active methods (Frequency drift Methods)

Active Frequency Drift with Pulsating Chopping Factor (AFDPCF) is an improved SFS method is reported where the chopping factor instead of depending on a gain, has an alternating pulse shape leading to faster frequency drift during islanding.

Actually the frequency is pushed to increase in one period and then to decrease in the second period. The positive and negative value of the chopping factor can be set using analytical calculation by imposing a certain grid current THD as required by standards. Thus, complying with power quality standard can be guaranteed. Also the potential for parallel operation is higher than the previous AFD base method.

$$cf = \begin{cases} cf_{\max} & \text{if } Tcfmax\_on \\ cf_{\max} & \text{if } Tcfmin\_on \\ 0 & \text{otherwise} \end{cases}$$

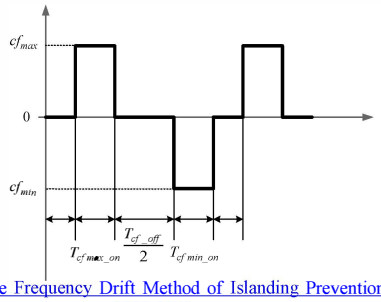

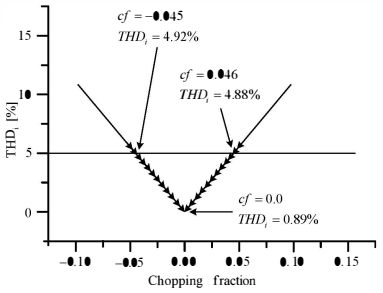

•Jung, Y.; Choi, J.; Yu, B.; So, J.; Yu, G., "A Novel Active Frequency Drift Method of Islanding Prevention for the grid-connected Photovoltaic Inverter," Power Electronics Specialists Conference, 2005. PESC '05. IEEE 36th , vol., no., pp.1915-1921, 2005.

Active methods (Frequency drift Methods)

GE Frequency Shift (GEFS) is another frequency drift AI method based on positive feedback like SFS. Here the reactive current reference is augmented with a positive feedback derived from the frequency estimation with proper filtering and gain in order to maintain the stability. Increasing the reactive current reference will lead to higher reactive power which in case of islanding on RLC load will further increase the frequency so the frequency is quickly pushed outside the OUF limits.

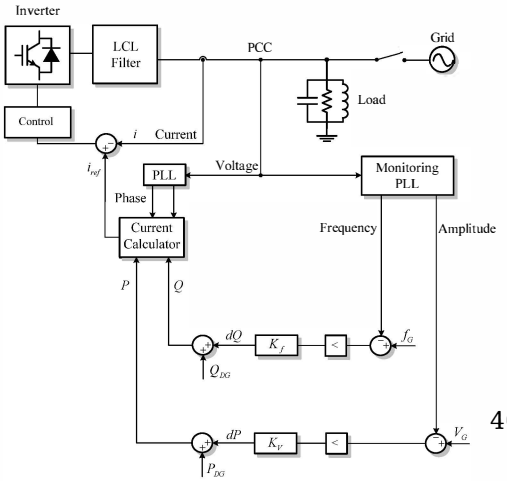

4609

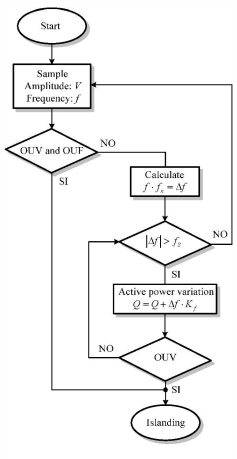

•Ye, Z.; Walling, R.; Garces, L.; Zhou, R.; Li, L.; Wang, T. "Study and Development of Anti-Islanding Control for Grid-Connected Inverters" NREL/SR-560-36243. Golden, CO: National Renewable Energy Laboratory. May 2004.

Active methods (Frequency drift Methods)

Reactive power Variation (RPV) The concept here is to add a harmonic disturbation signal (typically low frequency) in the reference of the reactive current . In the presence of the grid, this disturbance will try to modulate the voltage frequency with the disturbing one but will not be able due to the stiff character. In islanding situation, the voltage will depend linearly with the current and the frequency variations will be present and can be detected

For ex 1 Hz – 1% harmonic current is added to the reactive current reference with very reliable detection not-sensitive to the grid impedance. A frequency deviation detector is used to count the half periods between zero crossing that deviates from the rated frequency. After a predetermined count the trip signal is generated. Shorter detection times can be obtained by increasing the frequency of the harmonic current if desired but keeping low its amplitude.

•G. Hernandez-Gonzalez; R. Iravani, "Current injection for active islanding detection of electronically-interfaced distributed resources," IEEE Trans. on Power Delivery, vol.21, no.3, pp.1698-1705, July 2006.

Active methods (Voltage Drift Methods)

Sandia Voltage Shift (SVS) is an islanding detection method which uses positive feedback in the amplitude of the grid voltage. If there is a decrease in the amplitude of PCC voltage (usually it is the RMS value that is measured in practice), the PV inverter reduces its current output and thus its power output. If the utility is connected, there is little or no effect when the power is reduced. When the utility is absent and there is a reduction of the voltage in PCC. This reduction leads to a further reduction in PV inverter output current, leading to an eventual reduction in voltage that can be detected by the UVP.

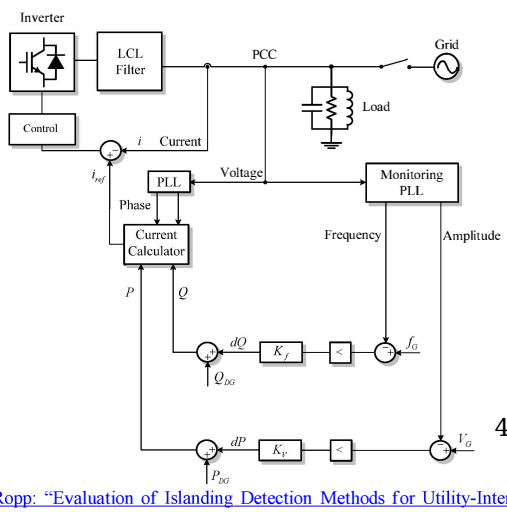

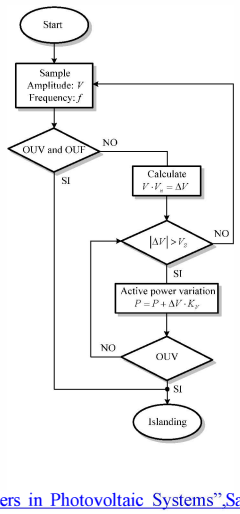

•W.Bower, M.Ropp: "Evaluation of Islanding Detection Methods for Utility-Interactive Inverters in Photovoltaic Systems",Sandia National Labs., Albuquerque, NM, SANDIA Report SAND2002-3591 Nov. 2002 (online ordering: http//www.doe.gov/bridge).

Active methods (Grid impedance estimation)

The concept is that a certain disturbance, such as harmonic injection or variation are used to estimate the grid impedance based on the response of the grid.

- *Harmonic Injection (HI)*
- *Grid Impedance Estimation by Active Reactive Power Variation (GIE-ARPV)*

Active methods (Grid impedance estimation)

Harmonic Injection (HI) is based on injection of *non-characteristic* harmonic current (ex 75Hz, 400, 500 Hz) and extraction of the resultant voltage harmonic which is dependent on the grid impedance at that frequency.

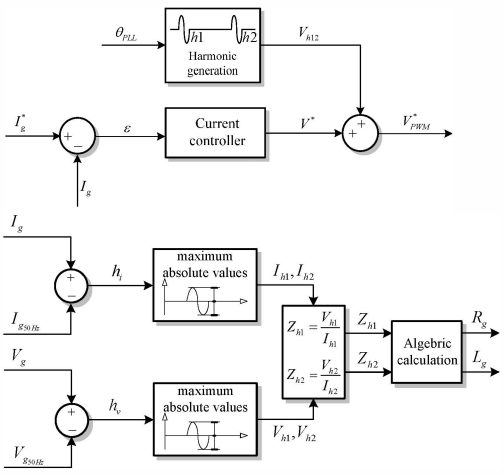

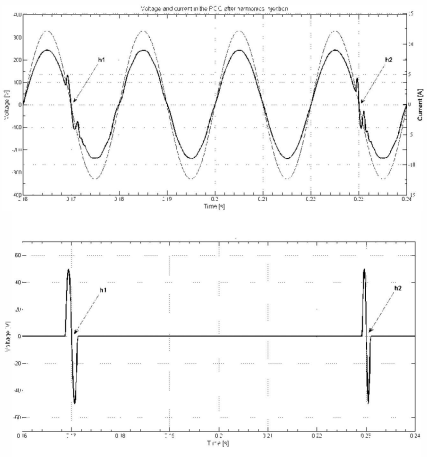

4611

•Ciobotaru, Mihai; Teodorescu, Remus; Blaabjerg, Frede, "On-line grid impedance estimation based on harmonic injection for grid-connected PV inverter," Industrial Electronics, 2007. ISIE 2007. IEEE International Symposium on , vol., no., pp.2437-2442, 4-7 June 2007.

Active methods (Grid impedance estimation)

Grid Impedance Estimation by Active & Reactive Power Variation (GIE-ARPV)

This method is based on the fact that the grid impedance can be calculated by using 2 stationary working points and solving the Voltage Kirchhoff Law.

Usually small pulse variations of P are used to determine the resistive part and small Q variations to determine the inductive part of the grid impedance

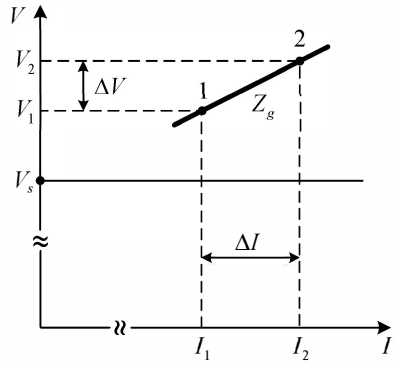

$$\begin{cases} R_g = \dfrac{\Delta V_d \cdot \Delta I_d + \Delta V_q \cdot \Delta I_q}{\Delta I_d^2 + \Delta I_q^2} \\ L_g = \dfrac{\Delta V_q \cdot \Delta I_d - \Delta V_d \cdot \Delta I_q}{\left[\Delta I_d^2 + \Delta I_q^2\right] \cdot \omega} \end{cases}$$

In PV plants applications, P is continuosly changed and in close future Q too!

•Ciobotaru, M.; Teodorescu, R.; Rodriguez, P.; Timbus, A.; Blaabjerg, F., "Online grid impedance estimation for single-phase grid-connected systems using PQ variations," Power Electronics Specialists Conference, 2007. PESC 2007. IEEE , vol., no., pp.2306-2312, 17-21 June 2007.

Active methods (PLL based islanding detention)

This method takes advantage of the existing PLL structure responsible for the synchronization of the inverter output current with the grid voltage and is based on the deliberately alteration of the derived angle of the inverter current angle .A feedback signal is then extracted from the voltage at the PCC (namely from) as a consequence of the injected signal The signal injection can be done with either positive or negative sign

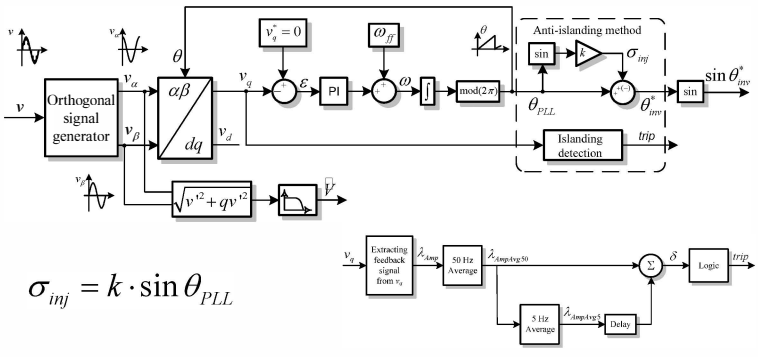

$$\sigma_{inj} = k \cdot \sin\theta_{PLL}$$

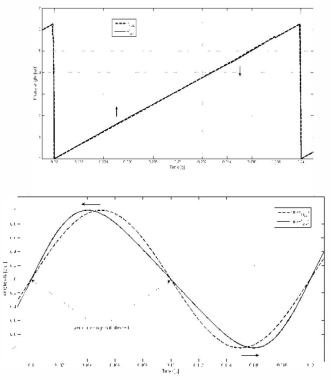

4612

•Ciobotaru, M.; Agelidis, V.; Teodorescu, R., "Accurate and less-disturbing active anti-islanding method based on PLL for grid-connected PV Inverters," Power Electronics Specialists Conference, 2008. PESC 2008. IEEE , vol., no., pp.4569-4576, 15-19 June 2008.

Mixed methods

Overcomes the limitations of both active and passive techniques

Takes the advantage of both active and passive techniques

Passive method is used to detect islanding first. In case of no clear discrimination perturbation will be injected

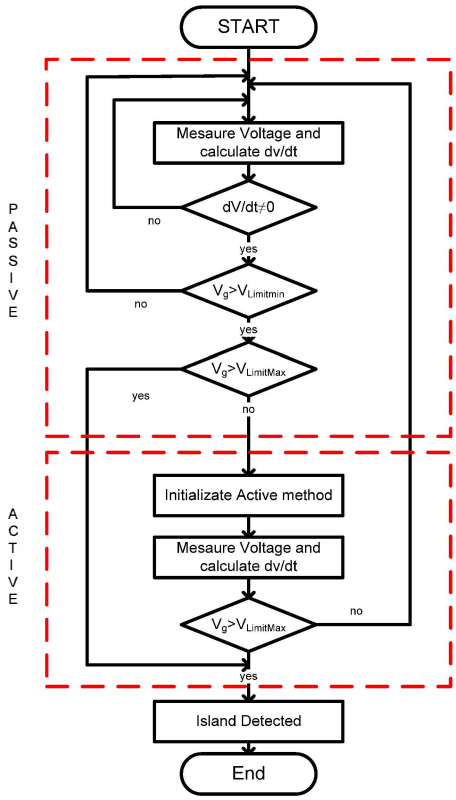

Conclusion

AI active method	Reliability	Maintaining Power Quality	Suitability for parallel inverter operation	Potential for standardization
Active Frequency Drift - AFD	Medium as it is not able to eliminate the NDZ	Low as it introduces low harmonics	Low as it can not handle concurrent detections	Low. More likely for the AFD with positive feedback
Slip Mode Frequency Shift – SMS	Medium as it is not able to eliminate the NDZ	Medium as PF is affected but no harmonics are injected	Low as it can not handle concurrent detections	Low
Sandia Frequency Shift (SFS+SVS)	High it can eliminate NDZ but it is susceptible for parasitic trips	Medium – with continuously drifting the PQ can be affected	Medium. It can work with parallel inverters but PQ can be affected.	Medium. More likely for the improved AFDPCF or GEFS
Active Frequency Drift with Pulsating Chopping Factor AFDPCF	Medium High – usually it leads to longer detection times as AFDPF but stability is controlled	High – it introduces harmonics but THD can be controlled	High, but limited in case one inverter is increasing frequency while another is decreasing it	High – as both stability and THD degradation can be controlled
General Electric Frequency Shift – GEFS	Very High – as NDZ can be eliminated and stability can be controlled.	Very High – practically no influence on THD	High but not unlimited. According to GE more research is needed	High as no degradation of THD is made

•Petrone, G.; Spagnuolo, G.; Teodorescu, R.; Veerachary, M.; Vitelli, M., "Reliability Issues in Photovoltaic Power Processing Systems," Industrial Electronics, IEEE Transactions on , vol.55, no.7, pp.2569-2580, July 2008.

Conclusion

AI active method	Reliability	Maintaining Power Quality	Suitability for parallel inverter operation	Potential for standardization
Reactive Power Variation - RPV	Moderately High – It can eliminate NDZ	High as no harmonics are injected, only the PF can be slightly reduced	Low as frequency changes at PCC can be also caused by other inverters	Low due to low suitability for parallel operation
Grid Impedance Estimation – Harmonic Injection GIE-HI	High as NDZ can be eliminated. There is potential for parasitic trip depending on grid impedance	Medium – depending on time between injections	Low – readings can be influenced during parallel injection	Low as ENS has softened now the requirements and accept IEEE1547 as alternative
Grid Impedance Estimation – External Capacitor Switching –- ESC	High- It can eliminate NDZ	Low – It introduces low harmonics	Low for inverter level implementation. It can be implemented as one unit for a group of inverters	Low – as for inverter level can not compete with software anti-islanding methods
Grid Communication (GC)	Very High – as long as communication is good. It does not depend on PQ mismatch	High (no influence on PQ)	Very High – just as it is dependant on communication reliability	Moderately High – on long terms due to cost issues

•Petrone, G., Spagnuolo, G., Teodorescu, R., Veerachary, M., Vitelli, M., "Reliability Issues in Photovoltaic Power Processing Systems," Industrial Electronics, IEEE Transactions on , vol.55, no.7, pp.2569-2580, July 2008.

Standards Overview

References

[1] Dugan, R.C.; Key, T.S.; Ball, G.J., "Distributed resources standards," Industry Applications Magazine, IEEE , vol.12, no.1, pp. 27-34, Jan.-Feb. 2006

[2] IEEE Std 929-2000 – "IEEE Recommended Practice for Utility Interface of Photovoltaic (PV) Systems,", ISBN 0-7381-1934-2 SH94811, April 2000.

[3] UL standard 1741, "Inverters, Converters, and controllers for Use in Independent Power Systems", Underwriters Laboratories Inc. US, 2001

[4] IEEE Std 1547-2003 – "Standard for Interconnecting Distributed Resources with Electric Power Systems," ISBN 0-7381-3720-0 SH95144, IEEE, June 2003

[5] IEEE Std 1547.1-2005 – "Standard Conformance Test Procedures for Equipment Interconnecting Distributed Resources with Electric Power Systems" ISBN 0-7381-4736-2 SH95346, IEEE, July 2005

[6] IEC 61727 Ed.2 – "Photovoltaic (PV) Systems - Characteristics of the Utility Interface", December, 2004

[7] IEC 62116 CDV Ed. 1 – "Test procedure of islanding prevention measures for utility-interconnected photovoltaic inverters", IEC 82/402/CD:2005

[8] VDE V 0126-1-1 "Automatic disconnection device between a generator and the public low-voltage grid",VDE Verlag, Doc nr. 0126003, 2006

[9] IEC 61000-3-2, Ed. 3.0 – "Electromagnetic compatibility (EMC) –Part 3-2: Limits –Limits for harmonic current emissions (equipment input current ≤16 A per phase)", ISBN 2-8318-8353-9, November 2005

[10] EN 61000-3-3, Ed. 1.2 —"Electromagnetic compatibility (EMC) –Part 3-3: Limits – Limitation of voltage changes, voltage fluctuations and flicker in public low-voltage supply systems, for equipment with rated current ≤16 A per phase and not subject to conditional connection", ISBN 2-8318-8209-5, November 2005

[11] Standard EN 50160 – "Voltage Characteristics of Public Distribution System", CENELEC: European Committee for Electrotechnical Standardization, Brussels, Belgium, November 1999 .

[12] IEC 61000-3-12, Ed. 1 – "Electromagnetic compatibility (EMC) –Part 3-12:Limits – Limits for harmonic currents produced by equipment connected to public low-voltage systems with input current >16 A and ≤75 A per phase" , November 2004

[13] IEC 61000-3-11, Ed. 1 —" Electromagnetic compatibility (EMC) – Part 3-11: Limits – Limitation of voltage changes, voltage fluctuations and flicker in public low-voltage supply systems – Equipment with rated current ≤75 A and subject to conditional connection" , August 2000